University of Szeged
Department of Pharmaceutical Technology
Head: Prof. Dr. Piroska Szabó-Révész Ph.D., Ds.C.

Ph.D Thesis

Modelling of the postcompressional properties of direct-compressed scored tablets with the use of artificial neural networks

by
Tamás Sovány
pharmacist

Supervisor
Prof. Dr. Klára Pintye-Hódi

Szeged
2010

Publications related to the thesis

I. **T. Sovány**, P. Kása jr., K. Pintye-Hódi.: *Comparison of halving of tablets prepared with eccentric and rotary tablet press* AAPS PharmSciTech, 10 (2009) 430-436

II. **T. Sovány**, P. Kása jr., K. Vakli, K. Pintye-Hódi.: *X-ray computed microtomography for the determination of the realtionships between structure and breaking of scored tablets* X ray Spectrometry 38 (2009) 505-509

III. **T. Sovány**, P. Kása jr., K. Pintye-Hódi.: *Modeling of subdivision of scored tablets with the application of artificial neural networks* Journal of Pharmaceutical Sciences (2010) 905-915

Other publications

I. Kása P., **Sovány T.**, Hódi K.: *Pelletek formulálásának optimálása mesterséges neurális hálózatok segítségével*, Acta Pharmaceutica Hungarica 77. 116-122. 2007.

II. **T. Sovány**, K. Nikowitz, G. Regdon jr., P. Kása jr., K. Pintye-Hódi: *Raman spectroscopic investigation of film thickness* Polymer Testing, 28 (2009) 770-772

Presentations

I. Kása Péter, **Sovány Tamás**, Pintyéné Hódi Klára, Szabóné Révész Piroska Diltiazem-klorid tartalmú pelletek formulálása mesterséges neuráli hálózat segítségével XIII. Congressus Pharmaceuticus Hungaricus Budapest, Magyarország 2006. május 25-27.

II. Kása Péter, **Sovány Tamás**, Pintyéné Hódi Klára, Szabóné Révész Piroska Mesterséges neurális hálózattal támogatott diltiazem-klorid tartalmú pelletek formulálása Gyógyszerkutatási Szimpózium 2006 Debrecen, Magyarország 2006. november 24-25.

III. **Sovány Tamás** Mesterséges neurális hálózatok alkalmazása granulátumok formulaoptimalizálásában Magyar Tudomány Ünnepe 2007 Szeged, Magyarország 2007. november 6.

IV. **Sovány Tamás**, ifj. Kása Péter, Pintyéné Hódi Klára Pelletformulálás optimalizálása mesterséges neurális hálózatokkal Gyógyszerkutatási Szimpózium 2007 Szeged, Magyarország 2007. november 9-10.

V. **T. Sovány**, P. Kása jr., K. Pintye-Hódi Dividability of tablets prepared by direct compressed binary powder mixtures 6th World Meeting on Pharmaceutics, Biopharmaceutics and Pharmaceutical Technology Barcelona, Spanyolország 2008. április 7-10.

VI. **Sovány Tamás**, ifj. Kása Péter, Pintyéné Hódi Klára Direkt préseléssel készült tabletták felezhetőségének vizsgálata mesterséges neurális hálózatokkal Műszaki Kémiai Napok ’08 Veszprém, Magyarország 2008. április 22-24.

VII. **T. Sovány**, P. Kása jr., K. Pintye-Hódi Comparison of halving of tablets prepared by eccentric and rotary tablet press 7th Central European Symposium on Pharmaceutical Technology and Biodelivery Systems Ljubljana, Szlovénia 2008. szeptember 18-20.

VIII. **Sovány Tamás**, ifj. Kása Péter, Pintyéné Hódi Klára Excenteres és rotációs gépen készült tabletták felezhetőségének összehasonlítása „Gyógyszer az Ezredfordulón VII.” Továbbképző Konferencia Sopron, Magyarország 2008. szeptember 25-27.

IX. **Sovány Tamás**, ifj. Kása Péter, Hódi Klára Préselési ciklusban kifejtett préserő hatása a tabletták textúrájára és tulajdonságaira Műszaki Kémiai Napok ’09 Veszprém, Magyarország 2009. április 21-23.

X. **Sovány Tamás** Excenteres és rotációs gépen készült tabletták oszthatóságának összehasonlítása IX. Clauder Ottó Emlékverseny Budapest, Magyarország 2009. április 23-24.

XI. **Tamás Sovány**, Ilija Ilic, Kitti Papós, PéterKása jr., Stane Srcic, Klára Pintye-Hódi The role of surface free energy and plasticity of the materials in tablet formulation 1st World Conference on Physico-Chemical Methods in Drug Discovery and Development Rovinj, Horvátország 2009. szeptember 27. - október 2.

XII. Péter Kása jr., **Tamás Sovány**, Stane Srcic, Endre Horváth, Zoltán Kónya, Imre Kiricsi, Klára Pintye-Hódi Preparation and investigation of biayer tablets

containing theophylline combined titanate nanotubes 1st World Conference on Physico-Chemical Methods in Drug Discovery and Development Rovinj, Horvátország 2009. szeptember 27. - október 2.

XIII. **Sovány Tamás**, Ilija Ilic, Papós Kitti, ifj. Kása Péter, Stane Srcic, Hódi Klára A felületi szabadenergia és a plaszticitás szerepe tablettaformulálás során XIV. Congressus Pharmaceuticus Hungaricus Budapest, Magyarország 2009. november. 13-15.

XIV. Márta Venczel, Gabriella Újhelyi, **Tamás Sovány**, Klára Pintye-Hódi Flow Through Dissolution - a Useful Tool from Discovery Phase to Preclinical Development XIV. Congressus Pharmaceuticus Hungaricus Budapest, Magyarország 2009. november. 13-15.

XV. ifj. Kása Péter, **Sovány Tamás**, Stane Srcic, Horváth Endre, Kónya Zoltán, Kiricsi Imre, Hódi Klára Kétrétegű tabletták előállítása és vizsgálata teofillin tartalmú titán nanocsövekből XIV. Congressus Pharmaceuticus Hungaricus Budapest, Magyarország 2009. november. 13-15.

XVI. P. Kása jr., **T. Sovány**, S. Srcic, E. Horváth, Z. Kónya, I. Kiricsi, K. Pintye-Hódi Formulation and investigation of biayer tablets containing theophylline combined titanate nanotubes 7th World Meeting on Pharmaceutics, Biopharmaceutics and Pharmaceutical Technology Valletta, Málta 2010. március 8-11.

XVII. **T. Sovány**, P. Kása jr., K. Pintye-Hódi Teaching problems of artificial neural networks in the modelling of properties of tablets 7th World Meeting on Pharmaceutics, Biopharmaceutics and Pharmaceutical Technology Valletta, Málta 2010. március 8-11.

Table of contents

1. Introduction

Tablets are the most common dosage form, accounting for over 65% of marketed medicines. The simplicity of usage and the great variability in size, shape, colour and flavour can enhance the patient's compliance. Moreover, the many possibilities to prolong or modify the drug dissolution can enhance the therapeutic effect of this dosage form. However, the claim for personalized therapy or application of the medicine in paediatrics necessitates the production of different doses or the possibility of subdivision. The subdivision of tablets for the ensurance of dose flexibility may be an easier and cheaper solution from the aspect of production. However, to ensure the appropriate mechanical properties and dividability of tablets to guarantee consequent dosing is a difficult problem, which is influenced by many parameters of the applied materials or mixtures, or the settings of the instruments. The size and shape of the particles [1-5], the surface free energy [6,7] and plasticity of the materials [8,9], or the differences in the compression mechanisms of the tablet presses [10] all have a significant influence on the postcompressional properties of tablets.

For an understanding of these multifactorial effects, a deep investigation of the interactions between the applied materials and equipment, and of the effect of the parameters of the production method is necessary. The developments in computer science, the speed of difficult calculations, and the data-mining methods, such as factorial design or artificial neural networks (ANNs), now permit the *in silico* modelling of these problems, and the prediction of the probable parameters of the products.

2. Aims

Despite its considerable difficulty, its increasing importance in paediatrics and the ever stricter requirements of the drug authorities, the subdivision of scored tablets is a poorly studied field. Only a few investigations of the production of scored tablets from technological aspects are to be found in the literature [11-13]. Most of the articles deal with scored tablets from a clinical point of view. The results show that, although there are studies which concludes that tablets with score lines can be split safely [14], most patients have problems with the breaking of the marketed products [15-17]. Some of these problems can be corrected through appropriate training of the patients [13,17-20] and

scored tablets have their therapeutic and economic advantages [21], but the improvement of breakability remains important, as this in the only way to ensure the uniformity of dosing [19,22,23], especially in the case of modified release dosage forms [24].

The aims of my studies were as follows:
Primary aim: The *in silico* modelling of the compression of scored tablets, for prediction of the postcompressional properties, and especially the subdivision of the products, with the help of ANNs.
Secondary aims: The determination of the best predictable neural model necessitated a better understanding of the effects of material behaviour, and the settings of the tablet presses.
The relationship between the structure and the breaking properties of tablets also formed an important part of the study.

3. Literature survey

3.1. Tablets

Tablets are usually prepared by compressing uniform volumes of particles or particle aggregates produced by granulation methods. In the manufacture of tablets, means are taken to ensure that they possess a suitable mechanical strength so as to avoid crumbling or breaking on handling or subsequent processing. Chewable tablets are prepared to ensure that they are easily crushed by chewing [25]. There are different types of tablets: tablets for oral use, sublingual tablets, swelling tablets, retard tablets, coated tablets, swimming tablets, intestinosolvent tablets, injectable tablets, implantable tablets and vaginal tablets. The world “tablet” comes from the Latin word “tabuletta” (little table), which was used for different solid dosage forms. Tablets are nowadays often made by compression, and most of them are cylinder-shaped, so the name “compressi”, used also by the Ph. Eur. appears better [26]. Tablets have many advantages, such as relatively simple, economic and exact production, controllable dosing, the simple protection of active pharmaceutical ingredients (APIs) from environmental circumstances or gastric fluid, long lasting stability, or comfortable and easy use. Most APIs can be processed into tablets, as can liquid materials with the use of absorbents. Furthermore, controlled drug release can also be achieved. As the source of the name shows, tablets have long been known as a dosage form. However,

the modern and widely used compressed form acquired significant importance in the middle of the 19th century, when William Brockedon developed his manual tablet press in 1843. 30 years later, in 1874, J. A. McFerran constructed the first rotary tablet press. The development of the presses continued in 1876, when Young introduced the first automatic working tablet press and in 1878 Robert Fuller started tablet preparation. In 1896, the first coated tablet press was introduced, and in 1900 the compression roll was developed for rotary machines by Killian [26].

3.2. Material characterization

As mentioned above, numerous physicochemical properties can influence the behaviour of materials during compression. The crystal characteristics, and the size and shape of the particles have a significant influence on the flow properties and rearrangement profile of the materials [27]. Furthermore, the specific surface area and size of the different crystalline planes also markedly affect the surface characteristics [28-31]. These effects increase with decrease of the particle size because of the increasing specific surface, and the surface characteristics will be more and more important [32]. The surface characteristics are of considerable importance in the particle-particle and particle-equipment interactions [28,33], and exert the influence on the behaviour of the materials in the different pharmaceutical processes, such as granulation [34-37], coating [38,39], and tabletting, where the interparticulate binding forces [40] and the friction on the die wall [41,42] are strongly related to the surface properties of the applied materials. These properties can be modified or improved through the mechanical processing of the raw materials, such as the mixing [43], grinding [28,43] or coating of the crystals [44,45].

There are many possibilities to determine the surface characteristics of materials. The oldest methods are based on the measurement of the wettability of the materials in different liquids [46,47]. The surface free energy of a solid material can be calculated on the basis of the Young equation, after measurement of the contact angles of liquids with known surface tensions on the surface of the solid (see Section 4.2.1). However, a knowledge of the full surface free energy is usually not enough, because the behaviour of materials during processing [28] or application [48-50] of the dosage form is mainly determined only by the dispersive or polar component of the surface free energy. The polarity index, which gives a good description of the behaviour of a material in response to water, was first used by Zografi and Tam [51]. Two basic methods of contact angle measurements are the sessile

drop and the Wilhelmy-plate methods. These methods have many advantages, such as fast and easy measurement, good reproducibility, small product requirement, etc. [52]. However, there is a considerable drawback: the methods require the preprocessing of the analysed materials into comprimates, as need flat surfaces for exact measurements. Other drawbacks are that these methods are time-dependent, and also depend on the moisture content, porosity and surface roughness of the test sample [53,54]. Some of these problems can be solved by presaturation of the sample with the test liquid [53]. Critical evaluation of these methods has indicated that the preprocessing can modify the surface characteristics of the sample, so that the result will be unrealistic. The fixing of the test material onto the surface of a glass carrier will provide more realistic data [55]. However, the resulting rough surface makes exact measurements more difficult. Some research has proved that despite the unrealistic results, the measurements with the different contact angle methods provide tendencies comparable with inverse gas chromatography (IGC) [55,56]. Moreover, Planišek et al. suggest that, when total nonpolar liquids are applied for the determination of the dispersive component of surface free energy, the results will be the same with contact angle measurements and IGC [57]. This is important because although IGC measurements require no preprocessing [58] and give realistic data, the measurement is much longer and more difficult. Nevertheless, IGC could be very effective in the exploration of batch to batch variations [59,60] or polymorphic forms [61], despite a critical assessment that most of the literature reports use a simplification in the calculation of the surface energy, which causes difficulties in the detection of interindividual differences [62]. All of the above-mentioned methods have the drawback that only the bulk of the materials can be characterized, and no information can be obtained on to the different regions of the materials or tablets. These smaller regions can be studied with different probes of atomic force microscopy (AFM) [63], or can be derived by molecular modelling [64,65]. This latter method also provides a possibility for predictions of the probable behaviour of the materials, even in the phase of molecular design.

The surface free energy can also be related to the deformability of the applied materials, because the moisture content of the material has a significant effect on the compressibility [33]. The moisture content will act on the strength of interparticulate bonding, and also on the ratio of plastic/elastic deformations [66]. The plasticity or elasticity of materials, which can be calculated from the force-displacement diagrams on an instrumented tablet press will basically determine the tablet hardness and capping phenomenon [67,68]. However, besides these properties, many characteristics of materials have considerable effects on the postcompressional properties of tablets, such as the degree of crystallinity (amorphous

materials have better compressibility) [69-71], crystal structure and habit [2, 72-75], or the size and shape of the particles [4,76]. There are different methods to assess these effects, and to describe the behaviour of materials during compression. The simplest methods may be the displaying of the tablet porosity (compactibility) or tablet tensile strength (tablettability) against the compression force [77-79]. Tablet tensile strength can be calculated from the geometric parameters and breaking hardness of the tablets and allows the comparison of tablets with different geometries. The relationship was described for round tablets by Fell and Newton [80], and then also for differently shaped tablets [81,82]. Nevertheless, the above-mentioned functions could have value for the prediction of postcompressional properties of tablets, though they can not provide any information about the exact mechanism of powder densification. Many of different equations have been proposed to describe these processes [83], and all of them provide more or less information about the mechanism of powder densification. Perhaps the most important among them is the Heckel equation, which was devised to describe the densification of metal powders in 1961 [84,85]. This is the most frequently applied equation in the literature [86-101], but since it was developed for metals, which mostly exhibit plastic behaviour, it has been criticized when used for pharmaceuticals [102,103]. One of the greatest problems with this equation is that it works with density values, and the results depend on the exactness of the density measurements [104]. The measurement of the density of the materials is strongly affected by the moisture content, [104-106]. An additional problem is that, because of the curvature of the function, the equation does not fit well at lower densities; this problem can be solved by hyperbolic curve fitting [97]. Some papers offer solutions to the problems of the Heckel equation [99,107,108], whereas others recommend the use of other powder densification equations [98,100]; the Walker [109], Adams [98] or Kawakita-Lüdde [110] equations usually fit much better for pharmaceutical powders [99,100]. However, Denny states that the Kawakita model can be used only for a limited number of materials as compared with the Heckel plot [101].

3.3. Compression process and tablet texture

All of the above-mentioned properties have significant effects on the postcompressional properties of the tablets. Nevertheless, the mechanism of the compression (determined by the process settings) and the postcompressional changes have the same importance. The applied compression force naturally determines the hardness of the tablets, but extent of

breaking in the densification of the material [111], also influences the postcompressional changes/relaxation in the tablet parameters [112]. The speed of tabletting [113,114] and the type of the tablet press [10,115] likewise exert considerable effects on the tablet properties. In the case of rotary presses, the tilting of the punches (especially at higher compression forces) causes changes in the densification of the particles, which can result in significant differences in tablet texture [116]. The shape and curvature of the punches have also similar effects [117,118], which will determine the force distribution and breaking of the tablet, which may be the most important property of scored tablets.

The packaging and deformation of the particles [119,120], the density and pore distribution [121-123] and the general tablet texture can be studied very well, by means of computer microtomography [124-126]. The method is based on the same principles as medical tomography [127]; a fully three-dimensional picture of the sample can be reconstructed from the X-ray slices with appropriate software applications [128-130]. The analysis is non-destructive, so it is comparable with other destructive methods in order to full information about the mechanical properties or dissolution of the tablets. Moreover, the method can be used for chemical mapping, film thickness and integrity measurements, or contamination and counterfeit screening [131].

3.4. Artificial neural networks (ANNs)

In the middle of the 1940s, scientists turned to a new research field, with the aim of understanding and modelling the mechanism of the learning and memory formation of the human brain, with the help of different mathematical algorithms. These studies were developed into artificial intelligence researches. ANN models mimic the structure and function of the human brain; they are adaptive, self-organizing and fault-tolerant. These principles make them able to accommodate to different problems, and hence ANNs are able to “learn”. Thanks to these properties, ANNs demonstrate a slightly superior ability to predict unseen data. Their combination with other systems, such as neurofuzzy logic, had the added advantage of generating rule sets representing the cause–effect relationships contained in the experimental data [132]. In recent decades, many articles have been devoted to their usefulness in pharmaceutical process modelling [133-139]. They can be utilized in a wide range of design of solid dosage forms for the optimization [140] and scaling-up of granulation processes [141], and the optimization of tablet formulae [142,143] or film coating systems [144]. ANNs demonstrate considerable advances over

traditional statistical analysis methods [145,146], and great ability to model non-linear problems. These advances can be utilized in the design of controlled release systems [140,142,147-151], the modelling of in vitro-in vivo correlation data [152], or the evaluation of certain analytical results [146,153,154].

In general, ANNs are built up from nodes, connected with weights. Two main ANN types can be distinguished. Supervised ANNs have strongly hierarchical structures; the nodes are regulated in layers (Fig. 1).

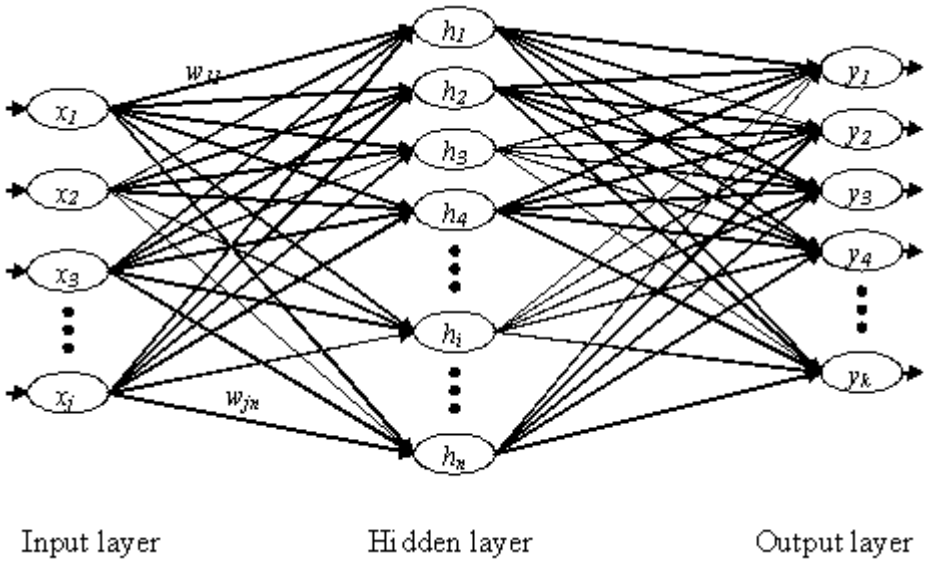

Figure 1. General structure of supervised ANNs

The teaching of supervised ANNs is based on the changes in the weights of the connections, whereas unsupervised ANNs have no hierarchical structure, and the number and positions of the neurons are not determined preliminarily. During the training phase, the neurons are regulated into groups, and the information is based not only on the connections between the groups, but also on the distances between the groups, i.e. a topological map. The operation of supervised ANNs is simpler and less chaotic than in the case of unsupervised ANNs, so the use of these types is much widespread. The most frequently used types of ANNs are radial basis function (RBF), generalized regression neural networks (GRNN) and multilayer perceptrons (MLP). However, it is a scientific principle that, if the data give a good fit, then the simplest model should always be chosen, which results in simpler data analysis. The simplest, one-layer ANN model is the linear one, where the input and output neurons are directly connected, without any hidden layer. This structure gives an NxM matrix with an Nx1 bias vector. The learning is based on the

singular value decomposition (SVD) algorithm [155,156]. In these studies, a similar model was used as comparative standard of the predictive force of different ANNs.

Nevertheless, multilayer ANNs are more advanced and in most cases give much better predictions. In the RBF networks, the input neurons are connected with the neurons of the radial layer. These neurons are associated with a Gaussian activation function, and carry out the clustering of data via sub-sampling or the K-means method [157]. Their number generally corresponds to the number of output neurons. The processed data are usually subjected to a linear transformation via the SVD algorithm. The networks are able to handle either classification or regression problems. However, the appropriate classification of the data comes up against many difficulties [158].

Bayesian neural networks have similar structures to those of RBF, but have two hidden layers and are divided into two groups. probabilistic neural networks (PNN) are specified for classification, while GRNNs, reported by Specht in 1991 [159], handle regression problems. The radial layer has the same function as in the RBF network, but the number of neurons usually corresponds to the number of training cases. The second layer is the pattern layer, which calculates the weighted sum of the vectors from the radial neurons [160]. The number of neurons in the pattern layer is always the number of outputs + 1. The drawback of the above-mentioned two types of ANNs is the defined structure, and the fact that extrapolation is not possible because of the Gaussian activation.

In contrast, the MLP, which is based on the one-layer perceptron model of Kohonen et al. [161], and which was evaluated by Rumelheart et al. in 1986 [162], is probably the most popular type of ANNs, as it is freely variable. It can handle one or more hidden layers with linear, hyperbolic tangent or logistic activation functions. Thanks to its popularity, numerous learning algorithms (back-propagation, conjugate gradient descent, quasi-Newton, etc.) have been developed for the MLP [163,164]. Its high variability allows the MLP to offer probably the most powerful models, but finding the optimum structure of the ANN is somewhat difficult. The Kolomorogov theorem specifies that one layer is sufficient for the modelling of most problems. However, determination of the number of neurons in this hidden layer is a difficult problem [165]. A number of recommendations are available in the literature for determination of the number of hidden neurons, such as the number of neurons being the number of inputs + 1, or the number of hidden neurons being half of the sum of the numbers of input and output neurons. However, these recommendations do not calculate with the difficulty of the applied training set. The equations developed by Jadid et al. and by Carpenter for determination of the maximum number of hidden neurons [166] take these settings also into account. Nevertheless, the

number is still usually determined via trials. A further problem that the behaviour of networks with the same structure can be different during the training phase, depending on the slope of the applied activation function [167]. Nevertheless, after appropriate settings, these systems can handle many types of optimization of drug formulations [168].

4. Materials and methods

4.1. Materials

Drotaverine HCl is a yellow, fine, adhesive powder, which is well soluble in water. This antispasmodic API developed in Hungary, is frequently used in the treatment of gastrointestinal or menstruation spasms. It has tabular structured crystals (Fig. 2), with good compression behaviour. However, its high surface free energy and the high tendency to adhesion cause serious problems during compression. These problems are usually solved by preliminary granulation of the material.

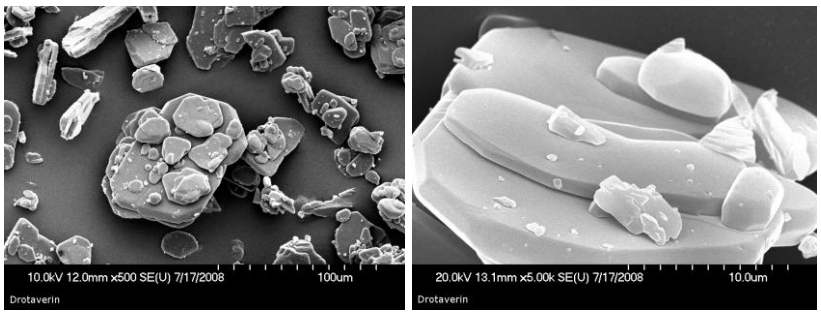

Figure 2. SEM pictures of Drotaverine HCl

Microcrystalline cellulose (Vivapur 102, J. Rettenmeier & Söhne, Germany) is a binder material widely used in the field of direct compression.

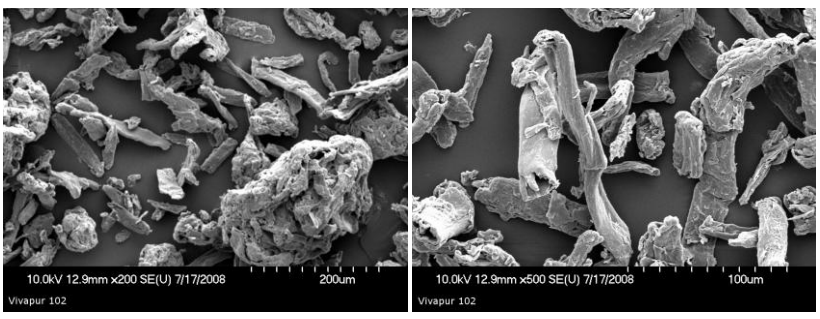

Figure 3. SEM pictures of microcrystalline cellulose

Despite its anisometric particles (Fig. 3), it has acceptable flow properties, and the deformability and plasticity of the particles result in very strong interparticulate binding after compression.

Spray-dried mannitol (Pearlitol SD 200, Roquette Pharma, France) is a white, crystalline powder which mainly contains α-mannitol. The particles have an almost isometric structure (Fig. 4), which usually contains holes, because of its spray-drying production. Its relatively low surface free energy and excellent plasticity makes it an ideal excipient for direct compressible formulations.

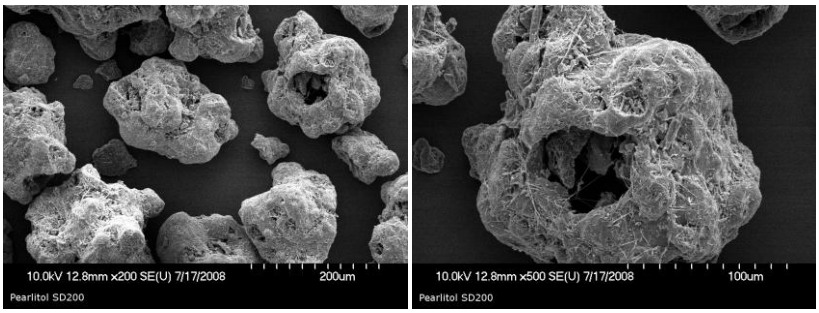

Figure 4. SEM pictures of spray-dried mannitol

Agglomerated α-lactose monohydrate (Tablettose 70, Meggle Pharma, Germany) is a white crystalline powder developed as a filler material for direct compression. It has good flow properties, but its agglomerates (Fig. 5) break during compression.

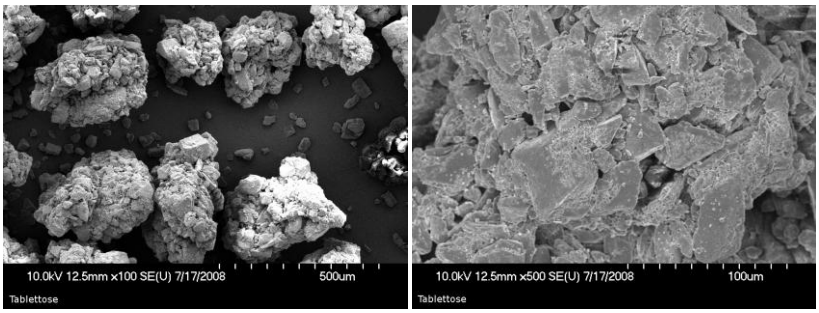

Figure 5. SEM pictures of agglomerated lactose

After the breaking, the material shows brittle behaviour and strong sticking to die and punches. Despite these disadvantageous properties, its use in Drotaverine-containing formulations is recommended in view of certain technological aspects.

Magnesium stearate (Ph. Eur.) is a white powder which, due to its low surface free energy, is widely used as an antiadhesive material and lubricant to facilitate the preparation of solid dosage forms.

4.2. Methods

4.2.1. Material characterization

The flow properties of the materials and mixtures were determined with a PharmaTest PTG-1 powder rheological tester (Pharma Test Appartebau, Germany), with the use of stainless steel and teflon funnels. The orifices in both cases are 10 mm in diameter. The flow time for 100 ml material, the angle of repose and the bulk density were measured.

The compaction behaviour of the materials was tested with an Engelsmann stampfvolumeter (JRS Pharma, Germany). From the bulk and tapped density data, the Hausner factor and the Carr index were calculated and evaluated by the categories described by Wells [169].

The particle size distribution and the shape of the powders was examined were a Laborlux S light microscope and a Quantimet 500 MC image-analysing system (Leica Cambridge Ltd., UK), based on the measurement of 1000 randomly selected, individual particles. The length, breadth, area and perimeter were measured and the convex perimeter and roundness of particles were calculated with the software after appropriate calibration.

A scanning electron microscope (Hitachi 2400 S, Japan) was used to study the morphological properties of crystals, and a Polaron sputter apparatus (Polaron, UK) was applied to induce electric conductivity on the surface of the samples.

The surface free energy of materials was determined with a Dataphysics OCA 20 optical contact angle tester, with use of the sessile drop method. The method is based on measurement of the equilibrium contact angle the value of which is determined by the surface tensions of solid, liquid and vapour phases, described by the Young equation (Eq. 1):

$$0 = \gamma_{SL} - \gamma_{SV} - \gamma \cos\theta \qquad (1)$$

where θ is the equilibrium contact angle, γ is the surface tension between the given phases, S is solid, L is liquid and V is vapour. The disperse and polar components of the solid materials were calculated with the Wu equations (Eqs. 2 and 3) in the knowledge of the surface tensions of polar and apolar test liquids (water and diiodomethane). The liquids were dropped onto the surface of comprimates 10 mm diameter prepared with a Specac hydraulic press (Specac Inc, UK) at a pressure of 4 tons.

$$(1+\cos\theta)\gamma_1 = ((\gamma_1^d\gamma_s^d)/(\gamma_1^d + \gamma_s^d) + ((\gamma_1^p\gamma_s^p)/(\gamma_1^p + \gamma_s^p)) \quad (2)$$

$$(1+\cos\theta)\gamma_2 = ((\gamma_2^d\gamma_s^d)/(\gamma_2^d + \gamma_s^d) + ((\gamma_2^p\gamma_s^p)/(\gamma_2^p + \gamma_s^p)) \quad (3)$$

where γ^d is the disperse and γ^p is the polar component of the surface tension, γ_1 is the surface tension of the first, and γ_2 is the surface tension of the second test liquid, and γ_s is the surface tension of the solid material.

The plasticity of materials and mixtures was determined with a computer-connected Korsch EK0 eccentric tablet press, instrumented with strain gauges on both punches and a displacement transducer (Micropulse, BTL5-A11-M0050-P-532, Balluff, Germany) on the upper punch. The strain gauges were calibrated with a Wazau HM-HN-30kN-D cell (Kaliber Ltd., Hungary). The transducer distance accuracy was checked by using five measuring pieces of accurately known thickness (1.0, 2.0, 5.0, 7.5 and 10.0 mm) under zero load (Mitutoyo, Japan). The materials were filled into the die and compressed manually (to ensure similar conditions for the well and poorly compressible materials) in the compression force range from 1 to 30 kN. The plasticity was calculated from the results of force displacement measurements with the Stamm-Mathis equation (Eq. 4):

$$Pl = E2 / (E2 + E3) \quad (4)$$

where *E2* and *E3* are the given areas of the force-displacement curve.

4.2.2. Preparation of the samples

Binary mixtures of the excipients were prepared in five different amounts, based on an extended experimental design. The mixtures were lubricated by the addition of 1% of magnesium stearate (Table 1).

The powders were mixed with a Turbula mixer (Willy A. Bachofen Maschienenfabrik, Switzerland) (8 min + 2 min after the addition of the lubricant, at 50 rpm).

The Korsch EK0 (E. Korsch Maschienenfabrik, Germany) eccentric and a Ronchi AM8S (Officine Meccanice F.lli Ronchi, Italy) rotary tablet press mounted with strain gauges were applied for tablet compression, with flat single punches 8 mm in diameter, with a 1 mm wide and 0.2 mm deep bell-shaped bisecting line on the upper punch in the case of the eccentric press. The lower punch of the rotary press is mounted with a 1 mm wide and 0.2 mm deep semicircular bisecting line. The air temperature was 22-25 °C at a relative

humidity of 57-65%. The tablet mass was 0.18 g and the compression rate was 36 tablets/min.

The applied compression force was 5, 10 or 15 kN, based on an experimental design model.

Table 1. Compositions of powder mixtures

Sample	Vivapur 102 (g)	Pearlitol SD 200 (g)	Tablettose (g)	Drotaverine HCl (g)	Magnesium stearate (g)
S1	90	10	-	-	1
S2	70	30	-	-	1
S3	50	50	-	-	1
S4	30	70	-	-	1
S5	10	90	-	-	1
S6	90	-	10	-	1
S7	70	-	30	-	1
S8	50	-	50	-	1
S9	30	-	70	-	1
S10	10	-	90	-	1
S11	85,5	9,5	-	5	1
S12	81	9	-	10	1
S13	76,5	8,5	-	15	1
S14	67,5	7,5	-	25	2

4.2.3. Postcompressional tests

The hardness of the resulting tablets was measured with a Heberlein tablet hardness tester (Heberlein & Co. AG, Switzerland).

For measurement of the force required to break the tablets into halves, a laboratory-constructed hardness tester was utilized (Fig. 6), with three-bend tablet hardness testing. The tablet must be centred under the breaking item, which moves vertically down. The load is detected with a computer-connected measuring cell, which is placed under the sample holder table.

The true density of tablets was determined with a Quantachrome helium stereopycnometer (Quantachrome GmbH., Germany). The porosity was calculated via the following equation (Eq. 5):

$$\phi = 1-(\rho_{apparent}/\rho_{true}) \qquad (5)$$

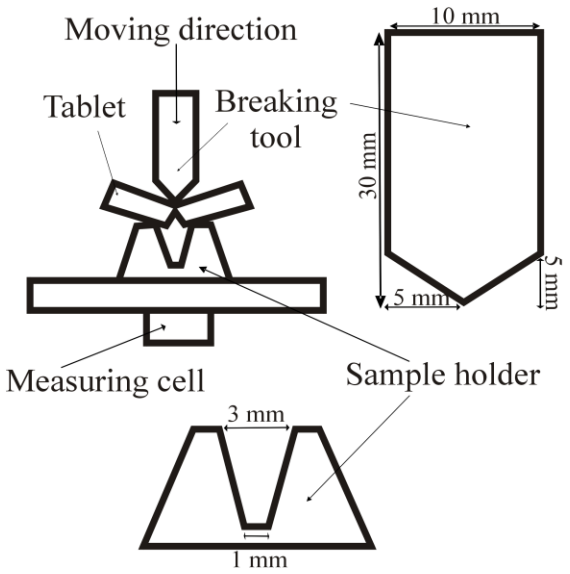

Figure 6. Schematic figure of the tablet hardness tester

The structures of the tablets were analysed with a SkyScan 1172 high-resolution micro CT apparatus (SkyScan Co., Belgium). A schematic figure of a micro CT apparatus is displayed in Fig. 7.

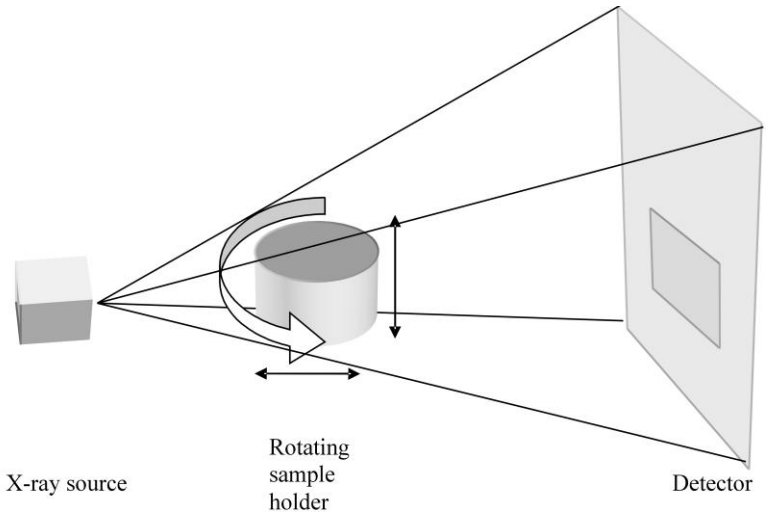

Figure 7. Schematic figure of the X-ray microtomograph

In this study, the X-ray source was set to 89 keV and 112 μA. All tablets were scanned throughout the whole 360° rotation range in 0.15° steps. The total duration of scanning was approximately 3 hours. The radiographs were then reconstructed with a standard cone-beam reconstruction program (NRecon) into 16-bit jpg pictures, each of 3120 x 3120 pixels.

The grey-scale intensities and optical densities in the regions of interests were determined with the ImageJ image-analysing software (National Institute of Health, USA).

4.2.4. Neural network modelling and statistical evaluation

The results were analysed with the Neural Network module of the StatSoft Statistica 6.1 software (StatSoft Inc., Tulsa, Oklahoma, USA). Fifteen experimental data sets were acquired, based on an extended experimental design. The data on 20 tablets were recorded with each setting, which resulted in a 300-member data matrix. 150 cases were selected to teach the ANNs. The 150 cases were divided randomly into training, selection and test sets, containing 100, 25 and 25 cases respectively. The selection set was dedicated to the internal validation of the prediction performance during the training, while the test set was for internal validation after the training. 50 other cases were used for the external validation of the prediction performances of the different ANNs.

The amounts of the two materials and the compression force were used as input variables; and parameters describing the compression process (elastic recovery, lubrication, plasticity, etc.) and postcompressional parameters (tablet hardness, true density and breaking into halves) were investigated as outputs. All parameters were handled as regression problems. In classification problems, the training cases must represent the original distribution of the samples, but in our case the distribution of the results of subdivision was not normal, and the different range widths of the classes of acceptance caused fatal problems in the predictions, handled as a classification problem.

The prediction performances of the different models were compared with the non-parametric Kruskal-Wallis test, with the use of post-hoc comparisons. Use of the non-parametric test was necessary because of the small number, and unknown distribution of the studied samples. The statistical analysis was performed with the StatSoft Statistica 8 software.

5. Results and discussion

5.1. Selection of the optimum ANN model

In the first step of the study, Samples 1 to 5 were compressed with the eccentric press at 3 compression forces. Parameters which describe the compression process (elastic recovery, plasticity, friction work and lubrication coefficient) were recorded in the case of each compressed tablet. The changes in these parameters and some postcompressional properties, such as hardness, density or tendency to accurate halving, were studied with ANNs. The observed vs. predicted correlation coefficients were used to select the best type and structure of the possible ANNs.

As already mentioned in the Literature survey (Section 3), a linear model was used as reference. The average observed vs. the predicted correlation coefficient (based on external validation results) was <0.5, which suggests the poor learning ability of these ANNs. The result of the Kruskal-Wallis test showed that the prediction performance of the GRNN was statistically the same ($p>0.05$) as that of the linear model. The software offers a possibility to reduce the number of radial neurons, and build a new network with retention of the other settings of the GRNN. The performance did not improve on reduction of the number of radial neurons from 100 to 15, the number corresponding to the number of experimental data sets, which resulted in a simpler network structure. Change of the assignment of the radial neurons from random sampling to K-means clustering did not lead to an improvement either.

In contrast, the RBF networks furnished statistically significant better prediction results. The average values of the observed vs. the predicted correlation coefficients were higher and the standard deviations (SDs) were smaller than in the number of cases discussed above. The number of neurons was set to the same value as the outputs. The statistical analysis did not reveal any significant differences between the results acquired with the different settings of the RBF ANN, but the average correlation coefficient for the different parameters (Fig. 8) reached a value of 0.8 only when K-means sampling was used for radial assignment and the K-nearest neighbours value for radial spread was set to 10. As discussed above, the determination of the optimum structure of MLPs is more difficult than for other ANNs. In the present study, one hidden layer was used, and the number of hidden neurons was varied between 5 and 12, corresponding with all the above-discussed recommendations. Five algorithms (standard back-propagation, quick-propagation, Delta-

bar-Delta, conjugate gradient descent and quasi-Newton) were tested to teach the ANNs. The maximum number of learning cycles (epochs) was set to 10000 during training, which stopped when the error of the selection set increased by 0.001 in a 10-epoch window. These settings seemed to be the most appropriate to prevent the networks from over-fitting. Networks taught with the conjugate gradient descent and quasi-Newton algorithms alone displayed poor prediction ability.

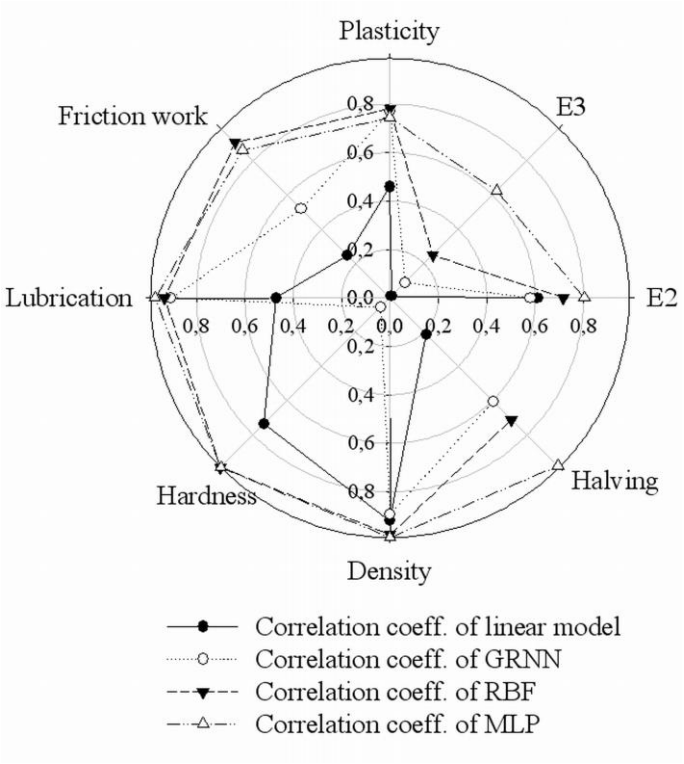

Figure 8. Observed vs. predicted correlations

The other algorithms yielded significantly better results, with no significant difference between them. However, because of the smaller SD and faster convergence, the use of quick-propagation or Delta-bar-Delta is recommended. Similarly, no significant difference was observed on change of the number of hidden neurons, but there was a tendency to need a higher learning rate as the neuron number was increased. Overall, the MLP models afforded statistically the same results as the RBF networks, but the best correlation coefficient (R^2=0.87) was achieved with an MLP with 12 hidden neurons taught with the Delta-bar-Delta algorithm, at a learning rate of 0.01. Further, this model provided the most uniform achievement as regards the prediction of different parameters (Fig. 8). For these reasons, this model was used in the further investigations.

Despite the good correlations, the usefulness of the developed model is strongly limited, because of the poor descriptive power of the selected input parameters. The lack of the

appropriate characteristics of the applied materials and the inappropriate description of the compression process caused the dramatic decrease in the accuracy of the predictions when we mixed other materials with the mixtures or compressed them on different tablet presses.

5.2. Characterization of the compression presses

It is well known from the literature that eccentric presses cause higher loads on the compressed materials than do rotary ones. The next step of the study was a deeper investigation and comparison of the compression mechanism on eccentric and rotary tablet presses. The primary aim of this work was to find and quantify the differences between the characteristic parameters of the different tablet presses, which have significant effects on the properties of the tablets. We used the models of Walker, Heckel and Kawakita to describe the powder densification, and sought relationships with the halving properties of the tablets. The study also focused on the mixtures of microcrystalline cellulose and spray-dried mannitol, as indicated in Table 1. The results of the preformulation tests for these materials and their mixtures are presented in Table 2.

Table 2. Preformulation results on materials and mixtures

Parameter	Vivapur 102	S1	S2	S3	S4	S5	Pearlitol SD 200
Flow time (s)	4.9	4.5	4.2	4.3	3.6	3.1	3.1
Angle of repose (°)	31.7	30.1	28.8	26.7	24.8	23.5	22.8
Bulk density (g/cm^3)	0.39	0.46	0.53	0.65	0.76	0.83	0.73
Hausner factor	1.37	1.24	1.25	1.19	1.15	1.07	1.12
Carr index (%)	26.76	19.34	20.27	15.67	12.67	6.27	10.40
Compactibility	0.03	0.02	0.02	0.02	0.01	0.01	0.01
Cohesiveness	2.93	1.99	1.89	1.68	0.59	0.31	0.92

The anisometric particles of Vivapur 102 (Fig. 3) exhibited poor flow properties during powder rheological tests and this resulted in lower bulk density values. The rearrangement of the particles was irregular, but took place quickly in response to tapping, giving rise to an exponential-type rearrangement profile (R^2=0.9438). The results with Pearlitol indicated that this material can greatly improve the poorer properties of Vivapur. It displays excellent flow properties, and the isometric particles (Fig. 4) demonstrate linear rearrangement behaviour (R^2=0.9428). The properties of the different powder mixtures

varied between the end-points of the two component materials. An increasing quantity of Pearlitol improved the compactibility of the powder, but the cohesiveness decreased, which resulted in lower inter-particulate binding forces. This may be due to a lower number of contact points between the isometric particles. These parameters were calculated from Eq. 6, described by Kawakita et al. [170]:

$$N/C = [N/a + 1/ab] \qquad (6)$$

where N is the number of taps applied for powder densification, while a and $1/b$ are constants referring to the compressibility and cohesiveness, respectively. C is the volume reduction, which can be calculated via the following equation:

$$C = [(V_0 - V)/V_0] \qquad (7)$$

where V_0 is the initial volume of the powder bed, and V is the current volume of the powder after a given number of taps.

Equation 6 is a modification of Eq. 8, which was proposed by Kawakita and Lüdde in 1971 [110] to describe powder densification behaviour during compression:

$$P/C = [P/a + 1/ab] \qquad (8)$$

where P is the applied pressure and C is calculated according to Eq. 7, where V is now the volume of the powder bed at the applied pressure.

We determined the Kawakita constants from the data on samples compressed at 5, 10 or 15 kN, based on the same experimental design as previously, plotted according to the out-of-the-die method. The values of constant a decreased on elevation of the Pearlitol quantity, as an indication of the better rearrangement of the particles during compression, which corresponds to the preformulation data (Table 3). The values of constant a are very similar for the two tablet machines, suggesting that it depends only on the properties of the compressed materials. In contrast, the values of $1/b$, which varied characteristically with the composition in the preformulation tests, displayed a minimum at a mass ratio of 50:50. This means that at this ratio the lowest energy is needed to reduce the volume of the powder to half of the original.

Table 3. Parameters of the different equations calculated from linear regression analysis

Sample	Heckel			Kawakita		Walker	
Eccentric press	*Py*	D_a	D_b	*a*	*1/b*	*W*	*L*
1	217.391	0.775	0.506	0.732	6.907	6.409	15.549
2	196.078	0.782	0.489	0.709	6.088	5.468	17.517
3	217.391	0.775	0.465	0.697	6.267	5.363	18.447
4	256.410	0.785	0.450	0.689	6.863	5.877	17.016
5	312.500	0.779	0.417	0.665	7.649	6.218	15.176
Rotary press							
1	232.558	0.618	0.348	0.727	15.834	14.098	6.534
2	212.766	0.615	0.322	0.701	15.685	13.776	7.116
3	263.158	0.633	0.323	0.687	10.546	9.596	10.364
4	270.270	0.657	0.322	0.691	19.531	14.164	7.035
5	277.778	0.665	0.303	0.671	17.872	14.394	6.278

This may be due to the better utilization of the transmitted energy, which can result from the lower adhesion and friction of the particles on the die wall. This reduces the loss of the energy during the process, and thus a greater proportion of the demanded energy is assigned to the volume reduction. Overall, less energy investment is needed at this ratio for a given volume reduction. This effect corresponds with the results of other calculations discussed below.

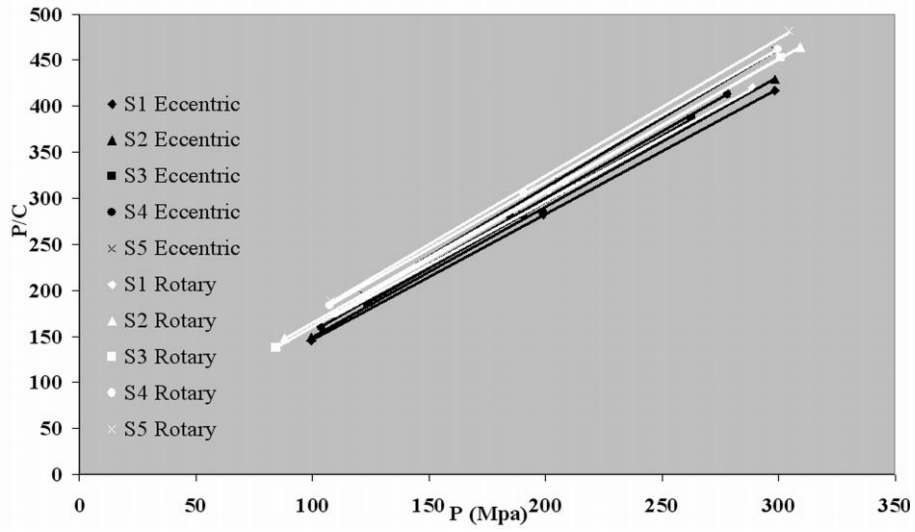

Figure 9. Kawakita-Lüdde plot based on out-of-the-die calculations

Figure 9 reveals that the intercepts of the plots obtained with the two machines are different: the calculated *1/b* values are 2-3-fold higher for the rotary press.

This suggests that the shorter compression time and the simultaneous action of the two punches results in a lower volume reduction for rotary presses at a given compression pressure. With the rotary press, a local minimum can also be observed in factor *1/b* at the ratio 10:90. The possible explanation of this phenomenon may be that the different compression mechanism of the rotary press results in a better rearrangement of the particles at this ratio than with the eccentric press.

Optimum points are also observed in the results calculated from the Walker equations:

$$\log P = - L V + C_1 \qquad (9)$$

$$100 V = -W \log P + C \qquad (10)$$

where P is the applied pressure, V is the relative volume, calculated as V'/V_0, *i.e.* the ratio of the volume at the applied pressure and the initial volume of the powder bed, and C and C_1 are constants. The coefficient L is the pressing modulus, which can be calculated from Eq. 9. It likewise exhibits a maximum at a ratio of 50:50 (Table 3), reflecting the smallest volume reduction at a given pressure at this ratio. This may also be due to the better utilization of the transmitted energy: even at low energy investment, strong bonding are forming between the particles. This is supported by the small value of the coefficient W at this ratio (Table 3), which shows the percentage volume reduction when the pressure changes on a logarithmic scale.

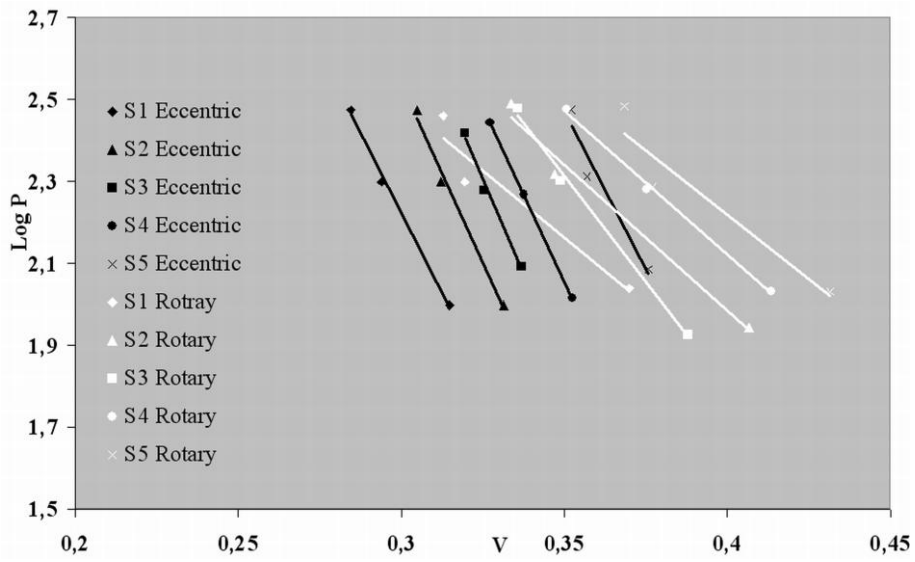

Figure 10. Walker plot based on Eq. 9

Thus, increase of the compression force causes only a minor further volume reduction, because almost the largest possible bonding forces have developed already at lower

compression forces. A difference can be seen in the slopes of the Walker plots relating to the eccentric and rotary presses (Figs 10 and 11).

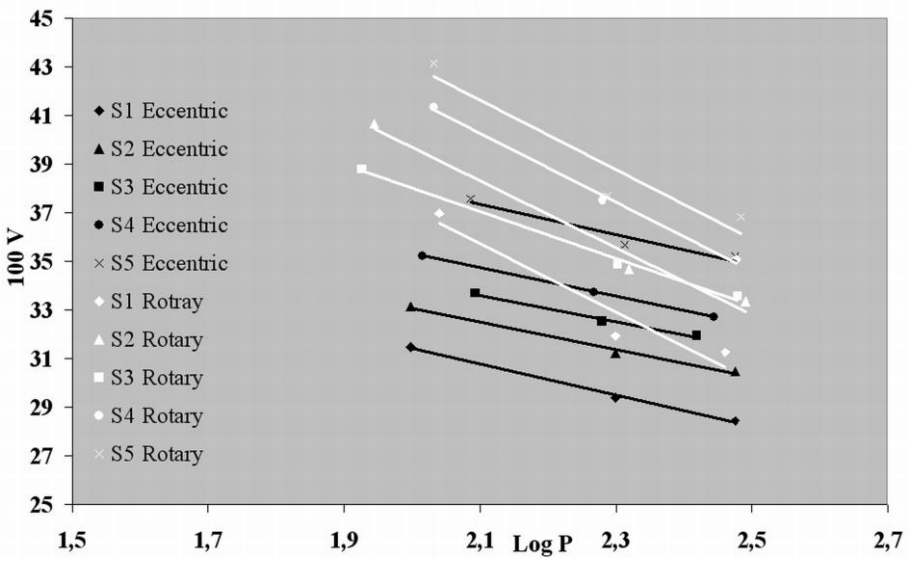

Figure 11. Walker plot based on Eq. 10.

We also used the equation developed by Heckel to acquire more information concerning the powder densification (Fig. 12):

$$\ln(1/1-D) = KP + A \qquad (11)$$

where D is the relative density of the tablet (calculated as the ratio of the apparent density of the tablet and the true density of the powder) at pressure P, while K and A are constants. The reciprocal of constant K is the mean yield pressure (Py). Constant A gives the densification of the powder due to the initial rearrangement of the powder bed (D_a) according to the following equation:

$$D_a = 1 - e^{-A} \qquad (12).$$

With the application of D_a, the densification due to the fragmentation of particles (D_b) can be calculated:

$$D_b = D_a - D_0 \qquad (13)$$

where D_0, related to the initial die filling, is defined as the apparent density of the powder bed at zero pressure.

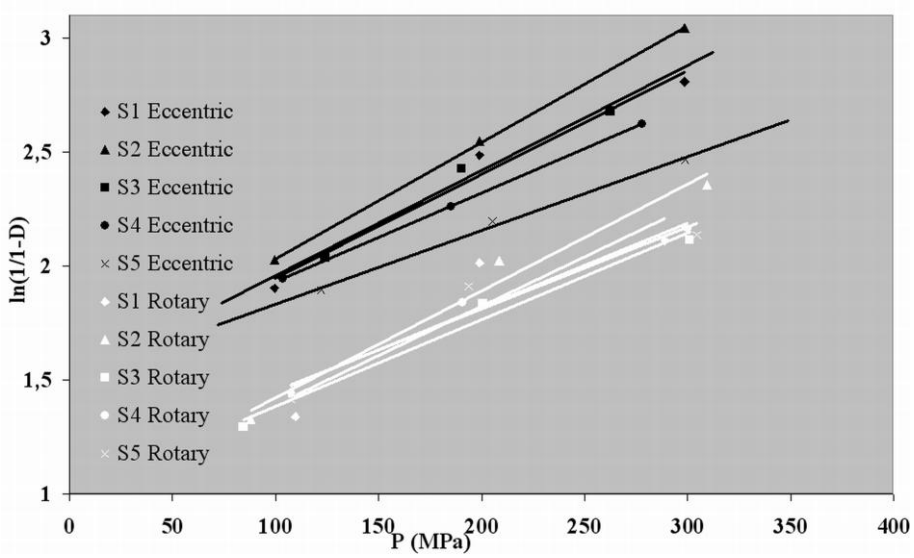

Figure 12. Out-of-the-die Heckel plots

As compared with the other methods, Heckel analysis does not give such unanimous results (Table 3). The mean yield pressure does not display a characteristic change; the differences between the machines are clear. The larger values of D_a and D_b demonstrate that a greater proportion of the particle densification is due to the initial rearrangement and particle fragmentation in the eccentric press. The differences in initial rearrangement and fragmentation may result from the differences in the method of die filling and the compression cycle. The parameters discussed above all influence the postcompressional properties of tablets. Table 4 demonstrates that the tensile strength is almost two times higher for the tablets formed with the eccentric press. It can be seen that the tensile strength decreases with increasing amount of Pearlitol, the small adhesion and cohesion forces and the fewer contact points between the particles greatly reducing the tablet hardness. This parameter is probably the most important factor influencing the breaking. A strong relationship can be observed between the tensile strength of the tablets and the halving properties (Table 5). The results suggest that a tensile strength at about 3.00 MPa is required for acceptable halving on an eccentric press, and even higher values are necessary on a rotary press.

Table 4. Tensile strengths of the tablets (MPa)

Sample	Compression pressure (MPa)		
Eccentric press	100	200	300
1	3.626	5.702	6.038
2	2.384	3.759	4.642
3	1.952	2.670	3.385
4	1.168	2.020	2.861
5	1.231	2.056	2.919
Rotary press			
1	1.280	3.576	3.807
2	0.941	2.508	3.269
3	0.591	1.748	2.456
4	0.605	1.511	2.275
5	0.537	1.803	2.595

These results indicate that the differences in compression mechanism and time cause considerable differences in the proportion of particle fragmentation and the strength of bonding.

Table 5. Amounts of well-halved tablets

Sample	Compression pressure (MPa)		
Eccentric press	100	200	300
1	50%	90%	100%
2	50%	100%	60%
3	60%	100%	80%
4	50%	80%	70%
5	30%	80%	90%
Rotary press			
1	10%	30%	40%
2	0%	10%	40%
3	0%	10%	30%
4	0%	0%	0%
5	0%	0%	10%

The tablet hardness connected with the properties of materials is strongly related to the breaking properties of the tablets. Postcompressional examination of the halving of the

scored tablets is very important, because it is necessary to verify it in the common technical documentation.

The axial stress acting on the bisecting line gives rise to elastic stresses in the tablets, resulting in different degrees of deformation, depending on the properties, deformability and bonding of the tablets. In this case, elastic deformation is advantageous. The change in the deformation can be measured through the application of strain gauges. When the elasticity predominates, the force-time curve rises with increasing axial stress and collapses at the moment of breaking of the tablet (Fig. 13a).

The tablets break well when the masses of the two halves are closely similar. A 50±5% tolerance limit was chosen in this study. The breaking result depends mainly on the hardness of the tablets and was better at higher tensile strength. However, it is additionally influenced by the internal structure of the tablets. When the tablet hardness is low, or internal structural defects exist, the breaking surface crumbles or the tablets break into more than one piece. The new breaking surfaces are associated with extra stress that does not act on the bisecting line. This type of breaking often proceeds through several steps, which are seen in the curves as extra peaks (Fig. 13b).

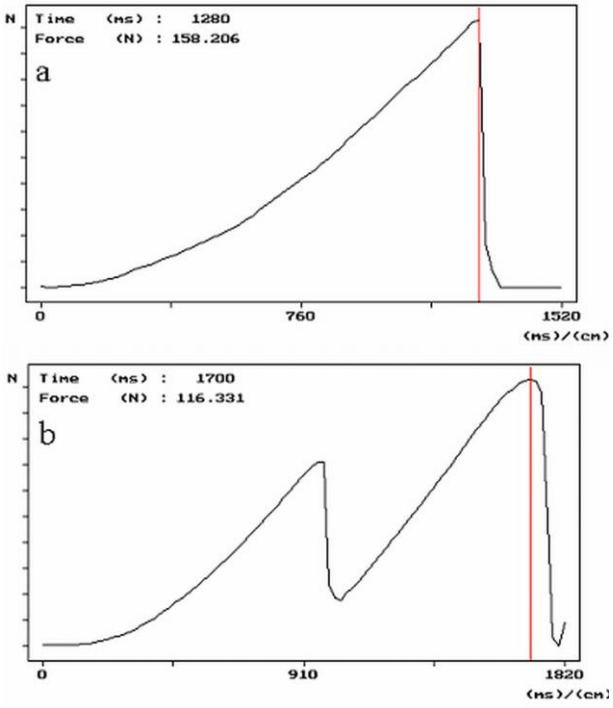

Figure 13. Breaking curves of a well-halved (a) and a not-well-broken tablet (b)

When the structure of the tablet is free from defects, a lower tensile strength may be sufficient for good breaking, as in the case of sample 3. The results allow the conclusion that the tablet hardness must be relatively high for good halving. However, when the

internal structure of the tablets is free from defects, as is presumable in the case of sample 3, a lower hardness may be sufficient. Nevertheless, the application of a higher compression force on a rotary machine is needed to equal the better results on tablets compressed on eccentric machines. No structural defects are formed during compression when the powder is well compressible and undergoes low adhesion to the die wall, and the bonding between the particles is formed quickly. The models of Walker and Kawakita describe these processes better than the Heckel model and furnish a better prediction of the halving properties. The results obtained with the Heckel equation should be utilized with caution.

5.3. Investigation of the tablet texture

To support the above-mentioned consequences and to clarify the reasons for the differences in mechanical behaviour of tablets prepared with different tablet presses, the texture of some of the compressed tablets was studied by X-ray microtomography.

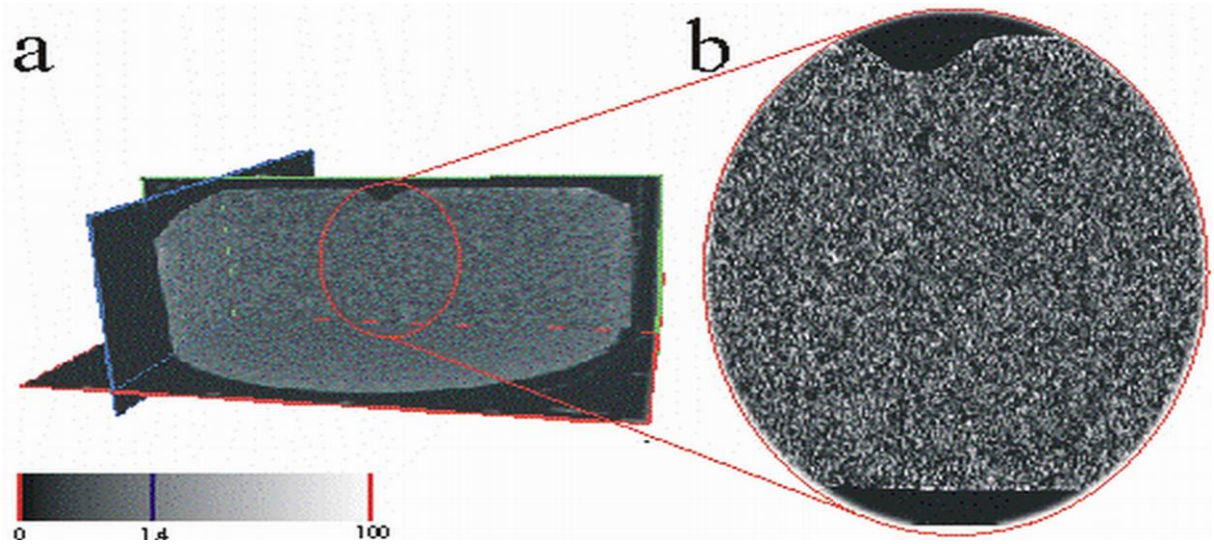

Figure 14. Density distribution in Tablet A (eccentric press, 5 kN)

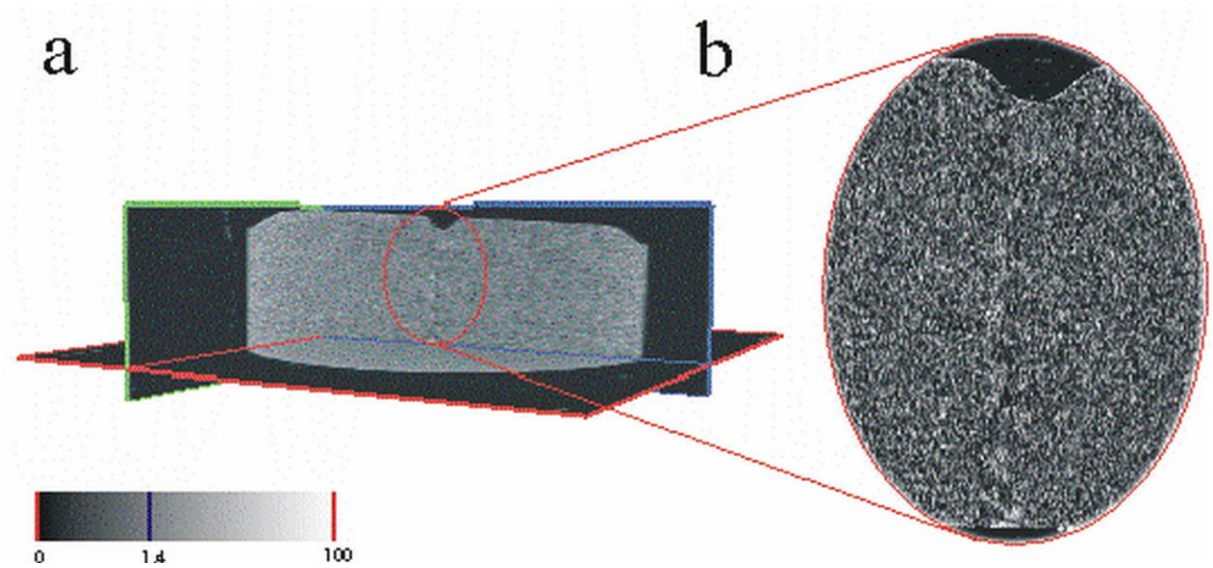

Figure 15. Density distribution in Tablet B (eccentric press, 15 kN)

Tablets of Sample 3 compressed with compression forces of 5 (Tablet A) and 15 kN (Tablet B) on an eccentric, and with 15 kN (Tablet C) on a rotary tablet press, were submitted for this investigation. Among these tablets, Tablet A showed acceptable halving, while Tablets B and C failed the test (see Table 5). The X-ray spectrometric pictures of Tablets A-C are presented in Figs 14-16, respectively.

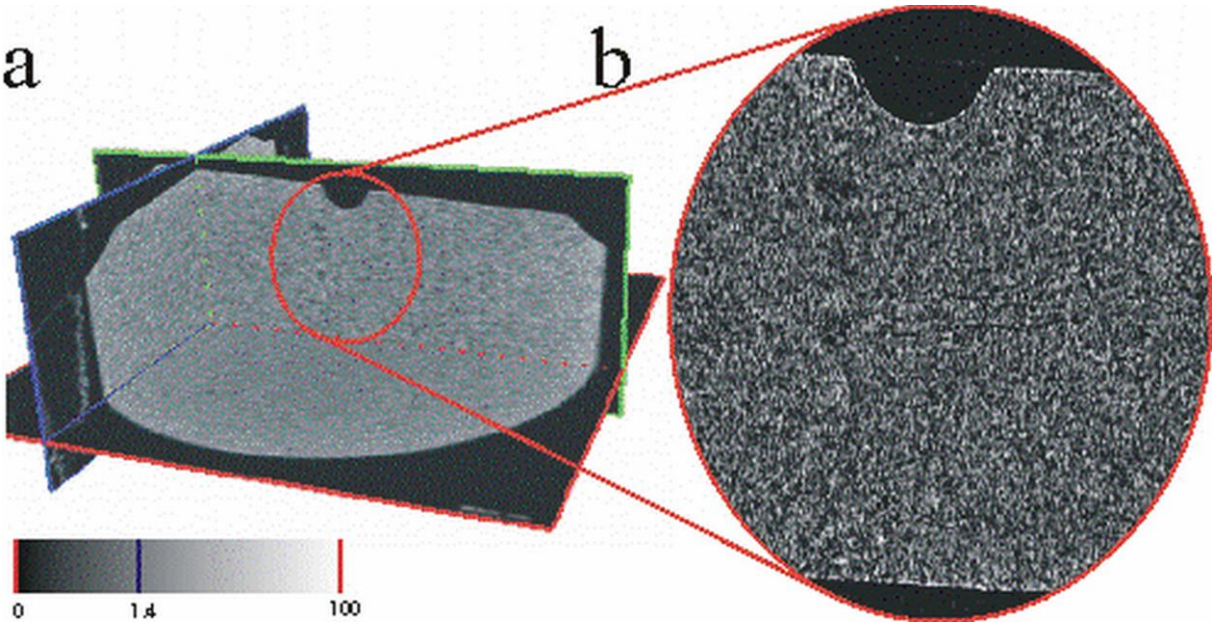

Figure 16. Density distribution in Tablet C (rotary press, 15 kN)

It is clearly visible that, despite the differences in the physicochemical parameters (Table 6), the tablets appear to have essentially similar structures. Their density increases from the centre to the edges, which is a result of the radial movement of the particles.

Table 6. Properties of the tablets

Sample	Tablet A	Tablet B	Tablet C
Press	Eccentric	Eccentric	Rotary
Compression force (kN)	5	15	15
Thickness (mm)	2.9682	2.7776	2.8386
Diameter (mm)	7.9334	7.9278	8.0420
True density (g/cm^3)	1.5202	1.5129	1.4658
Apparent density (g/cm^3)	1.2321	1.3253	1.2655
Porosity	0.189	0.124	0.137
Radial hardness (N)	72.20	118.0	88.0
Axial hardness (N)	57.72	81.89	9.50

The grey-scale intensity data (Table 7) of the different regions of interest (Fig. 17) indicate that the density gradient increases with increasing compression force. In general, it can be stated that, because of the friction on the die wall, the edge region is 1.1 to 1.4 times denser than the centre region of the tablets.

Table 7. Grey-scale intensities in the different regions of interest

Area	Mean	SD	Min	Max
Tablet A				
1a	75.533	41.961	0	255
2a	62.945	41.371	0	247
3a	62.339	42.593	0	255
4a	62.048	43.252	0	255
5a	74.969	45.250	0	255
6a	54.206	41.071	0	213
Tablet B				
1b	78.150	38.716	0	255
2b	64.946	37.563	0	247
3b	66.949	38.655	0	244
4b	69.361	37.165	0	234
5b	88.662	37.915	0	255
6b	59.013	37.569	0	196
Tablet C				
1c	81.121	36.108	0	255
2c	65.639	35.684	0	224
3c	63.665	36.737	0	252
4c	64.276	38.083	0	248
5c	79.358	38.319	0	255
6c	58.851	36.562	0	218

Moreover, because of the effects discussed above, a low-density pore (Fig. 17, regions 6a, 6b and 6c) is formed in the centre of the tablets, which exerts a significant effect on the breaking.

However, in spite of these similarities, the microstructures of the samples reveal important differences. Tablet A, which has the highest porosity, exhibits poor breaking properties, despite the particles being rearranged along vertical lines of force, i.e. the rich pore network allows breaking in many ways, which usually results in a rough breaking surface susceptible to crumbling. This is to be seen in Fig. 18a, where the mean grey-scale intensities of 256 pixel^2 areas are displayed, with the marking of the possible ways of breaking.

The structure of Tablet B (Fig. 15) is much less porous, and there are more considerable differences in the density distribution. Similarly as for Tablet A, the low-density area visible under the score line (Fig. 15b) is of greater importance because of the lower porosity. This area associated with the vertically rearranged particles ensures that the breaking force will pass through the tablet vertically, resulting in a breaking surface perpendicular to the action (Fig. 18b).

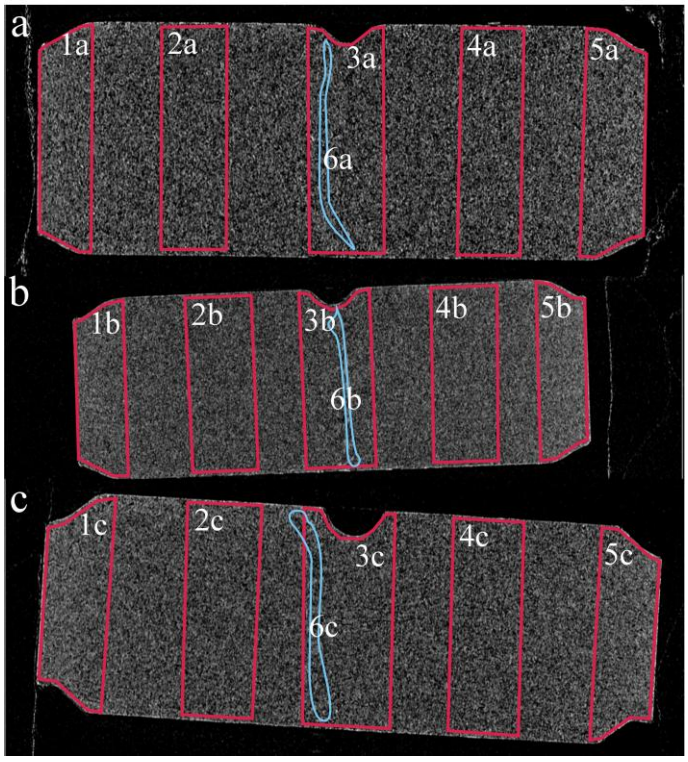

Figure 17. Regions of interest in the different tablets (Tablet A (a), Tablet B (b) and Tablet C (c))

In the case of the tablets prepared with the rotary press, the main problem was the breaking into unequal parts. The previous part of the study suggested that a possible reason is the fact that rotary presses cause only half the stress on the powder bed relative to eccentric presses. However, the porosity of the tablet is unexpectedly not so much higher as

compared with that of Tablet B. The structure reveals that the direction of the lines of forces has become deformed, probably because of the bidirectional compression force. This results in an oblique pore structure, which is clearly indicated by the mean grey intensities of the cross-sectional data (Fig. 18c). Moreover, the score line is more hollow and this makes the low-density area wider. These structural properties lead the breaking force away from the score line and give rise to breaking into unequal halves.

The oblique force lines are probably due to the tilting of the punches during the compression [116]. As this phenomenon can not be observed with eccentric presses, the type of the applied tablet press could be more important than previously expected. Nevertheless, according to Cespi et al., tilting is greater at higher compression forces, which

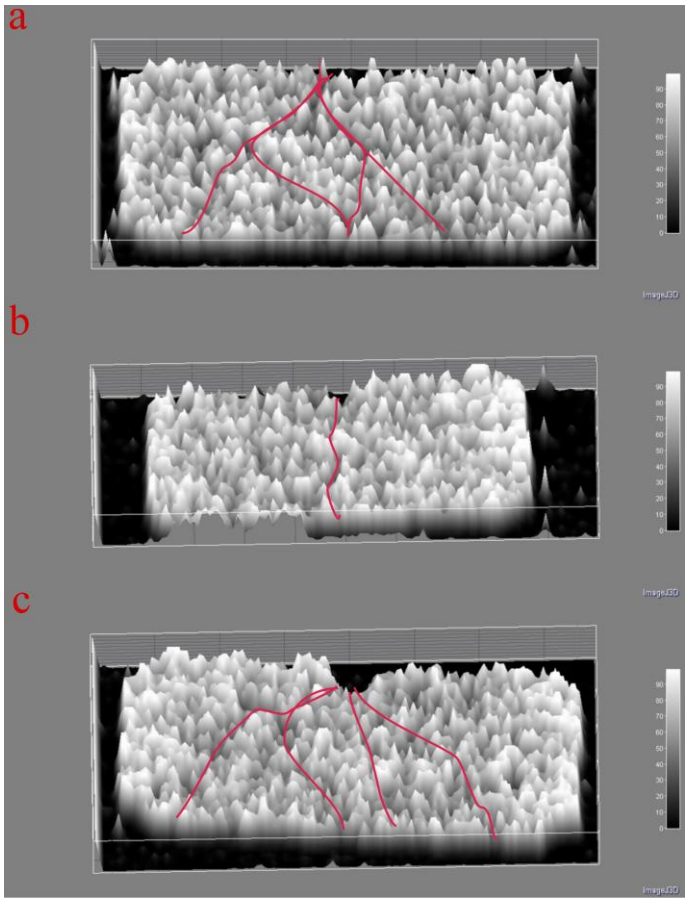

Figure 18. Grey-scale intensities and possible breaking directions in the cross-sections of Tablet A (a), Tablet B (b) and Tablet C (c).

could necessitate the search for a new optimum point at lower compression forces. The new optimum point presumes the application of a modified composition. For this modification it must be known how the change in composition will change the behaviour

of the mixture. This necessitates an exact characterization of the physicochemical properties.

5.4. Physicochemical characterization of the materials

It was mentioned in the previous parts of this thesis that the structural defects caused by the extensive friction or elastic recovery after compression have a significant influence to the breaking properties of the scored tablets. This makes prediction of the probable behaviour of the chosen mixtures necessary.

Prediction of the probable behaviour of mixtures from the properties of the individual materials is a very complex problem, where numerous factors should be taken into account. The relationships are rarely linear, because of the interactions of the different factors. In the present study, many unexpected phenomena were observed in the behaviour of the mixtures. The surface and structural characteristics of mixtures are essentially determined by the properties of the materials, but the particle size and shape (as parameters which strongly influence the result of mixing) should also be taken into account. Another important problem that the plasticity of the materials is not constant, but depends on the applied compression force. A decreasing value of the plasticity indicates the increasing resistance of the materials against the increasing load. The different slopes of the plasticity-compression force functions make prediction of the properties of mixtures difficult. The most important physicochemical properties of the raw materials are displayed in Table 8.

Table 8. Physicochemical properties of the materials

Material	γ_{TOT} (J/m^2)	γ^d (J/m^2)	γ^p (J/m^2)	Critical plasticity (%)	Particle size (μm)	Flow time (s)
Drotaverine HCl	80.24	35.76	44.28	98	30	n/m*
Vivapur 102	76.95	30.98	46.96	95	80	n/m*
Pearlitol SD200	72.07	29.89	42.18	93	60	8,8
Tablettose 70	82.62	36.42	47.21	93	200	10,1
Magnesium stearate	31.53	4.65	26.88	-	-	-

* not measurable

Here, the critical plasticity means the plasticity of the given material extrapolated to zero load. Materials with higher surface free energy show high adhesion to the stainless steel parts of the tablet presses. This will influence both the filling of the die and the friction during the ejection of the tablet. The high adhesion will hinder the free flow of the

materials, as in the case of Drotaverine. However, this property is also related to particle size and shape. As mentioned above, the free flow of Vivapur is hindered by the anisometric particle shape, and not by the high surface free energy. Meanwhile, Tablettose displays excellent flow properties because of the agglomeration. The decreased specific surface area results in a decreased tendency to adhesion. The unagglomerated α-lactose monohydrate which has a particle size of ~30 μm, is highly adhesive and shows no flow properties. Nevertheless, the agglomerates of Tablettose are susceptible to breaking during compression, the specific surface increases and this results in high friction and adhesion during the ejection of Tablettose-containing tablets. The strength of the adhesion between the different materials can be characterized by the value of the work of adhesion, which can be calculated with the following equation (Eq. 14):

$$W_a = \frac{\gamma_1^d \gamma_2^d}{\gamma_1^d + \gamma_2^d} + \frac{\gamma_1^p \gamma_2^p}{\gamma_1^p + \gamma_2^p} \qquad (14)$$

where γ^d is the dispersive and γ^p is the polar component of the surface free energy, γ_1 is the surface energy of the first, and γ_2 is the surface energy of the second material. When the work of adhesion is compared with the cohesive energy between the particles of the material, the spreading coefficient can be calculated (Eq. 15):

$$S_{12} = \frac{\gamma_1^d \gamma_2^d}{\gamma_1^d + \gamma_2^d} + \frac{\gamma_1^p \gamma_2^p}{\gamma_1^p + \gamma_2^p} - \frac{\gamma_1}{2} \qquad (15)$$

where γ_1 is the total surface free energy of the first material. When the value of the spreading coefficient is positive, the spreading of the first material on the surface of the second one is advantageous, and the higher value, the better spreading (Table 9). This leads one step closer to an understanding of the mixture properties. It is advantageous that materials with lower surface free energy will spread on the surface of materials with higher surface free energies and decrease their adhesive behaviour. However, as mentioned above, this relationship is not linear: the particle size of the materials must be taken into account. Materials with smaller particles will predominate on the surface, which is why the surface energy is involved with greater weight (Fig 19).

Table 9. Work of adhesion and spreading coefficients

Material 1	Material 2	Work of adhesion (mJ/m^2)	Spreading coefficient
Vivapur 102	Drotaverine	156.60	2.71
Pearlitol SD 200	Drotaverine	151.53	7.39
Tablettose	Drotaverine	163.52	-3.67
Magnesium stearate	Drotaverine	83.37	20.31
Pearlitol SD 200	Vivapur 102	148.83	4.68
Tablettose	Vivapur 102	160.11	-7.13
Magnesium stearate	Vivapur 102	84.01	10.95
Magnesium stearate	Pearlitol SD 200	81.77	18.71
Magnesium stearate	Tablettose	85.01	21.95
Drotaverine	Steel	98.92	-61.16
Vivapur 102	Steel	99.88	54.02
Pearlitol SD 200	Steel	96.68	-47.46
Tablettose	Steel	101.27	-65.97
Magnesium stearate	Steel	71.92	8.86

It is clearly visible that the Drotaverine, which has the smallest particles in these mixtures, has a dominating effect in the mixtures above 50 m/m%, which causes serious problems during the tabletting of mixtures with high Drotaverine content. Nevertheless, these problems can be corrected by the addition of lubricants. It can be seen from the data in Table 9 that magnesium stearate has a very low surface free energy, and its spreading is advantageous, even on the surface of other pharmaceuticals or stainless steel.

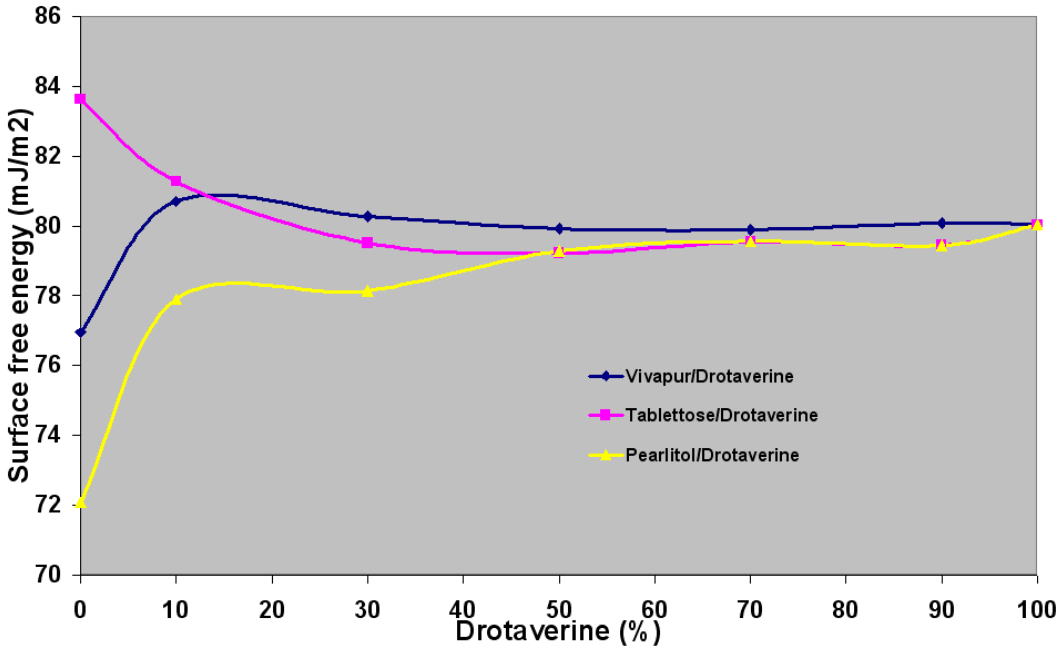

Figure 19. Change in surface free energy in binary mixtures of materials

It forms a film between the mixture and the die wall, and so decreases the friction. However, it should be used carefully, because it wears off, and can dramatically decrease the plasticity of other materials (Fig. 20). Furthermore, in higher concentrations it can modify the pressure relationship of this parameter, and turn the function into a power curve. This means a greater decrease in plasticity at lower compression forces (Fig. 20d), which will influence the postcompressional characteristics of the tablets.

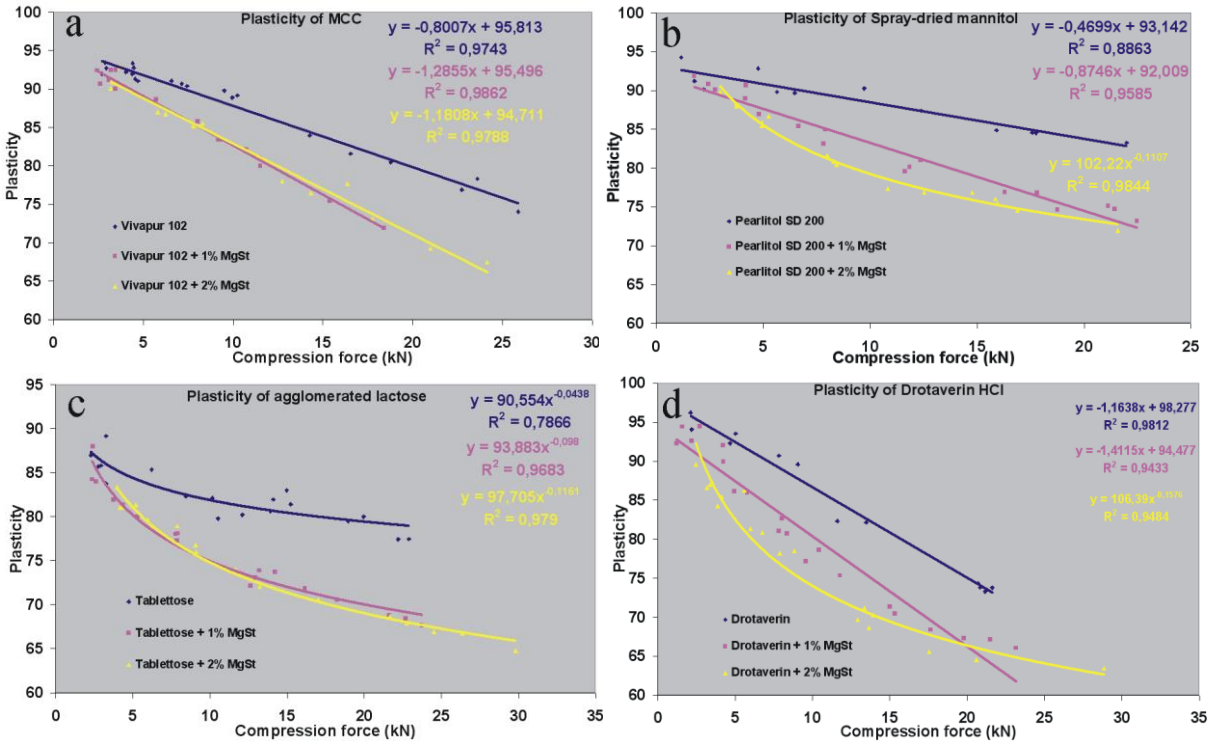

Figure 20. Plasticity of the Vivapur 102 (a), Pearlitol SD 200 (b), Tablettose (c) and Drotaverine (d), pure (blue) and with the addition of 1% (pink) or 2% (yellow) of magnesium stearate.

The postcompressional characteristics can be well predicted in the knowledge of the surface free energy and plasticity of the applied materials. Comparison of the hardness-compression force curves of the comprimates prepared from the pure materials reveal clearly the relationships (Fig. 21). The surface properties are of greater importance at lower compression forces. Materials with higher surface energy such as Drotaverine or Tablettose, can not be compressed at low compression forces, because the adhesion to the punches is greater than the interparticulate binding forces, and the tablets show strong lamination and capping. These problems can not be observed for materials with smaller surface free energy. At higher compression forces, the role of plasticity would be more

important. The hardness of the tablets exhibits a linear increment with increasing compression force when the plasticity of the compressed material shows no or only a minimal compression force dependence, as for Pearlitol SD 200 (Figs 20b and 21). In contrast, materials with a higher compression force dependence demonstrate a non-linear increment in tablet hardness. In extreme cases, such as in the case of Drotaverine, the hardness of the tablets can decrease above a given compression force, because of the extremely high elastic recovery, and the breaking up of the interparticulate bonding.

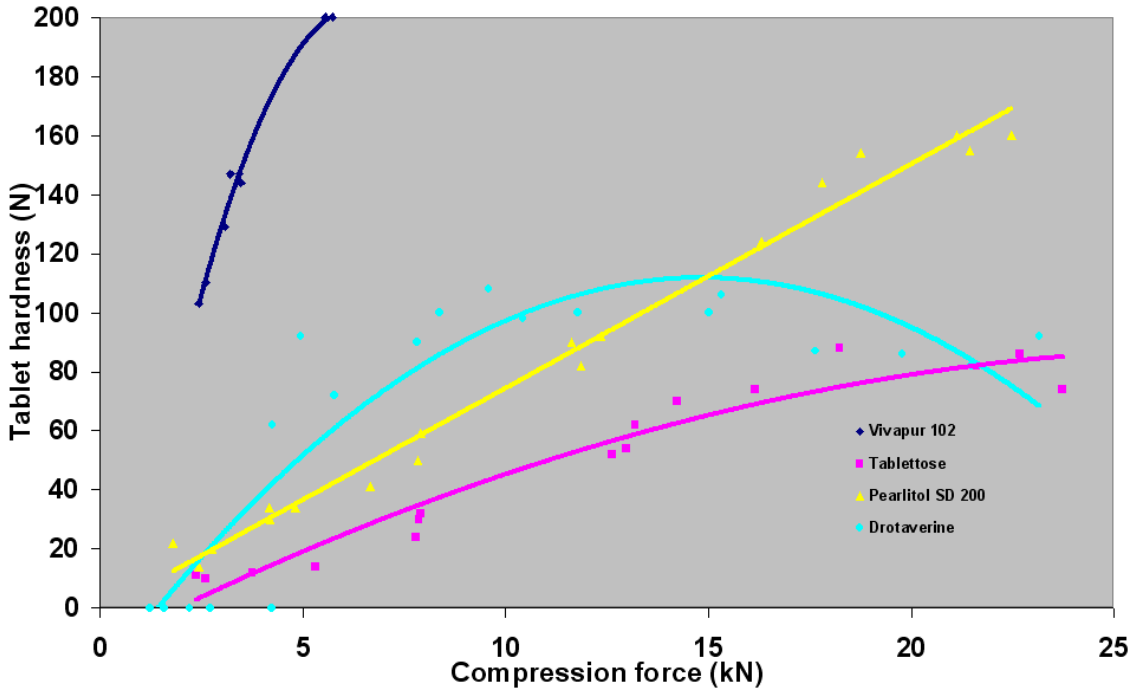

Figure 21. Postcompressional hardness characteristics of Vivapur 102 (dark-blue), Pearlitol SD 200 (yellow), Tablettose (purple) and Drotaverine (light-blue)

Nevertheless, prediction of the behaviour of mixtures is very complex; in such a case, the differences in particle size, the mixing effects, and the adhesion between the different materials should also be taken into account. However, when these characteristics are known for the mixtures, the probable hardness (one the most important optimization parameters for scored tablets) will be predictable.

5.5. Development of the new neural model

Based on the results of the above-mentioned studies, a new neural model was developed. The results suggested that besides the applied compression force, the time of compression and the type of tablet press are also important parameters. For characterization of the applied materials, the surface free energy, the polarity index, and the slope and intercept of the plasticity function should be appropriate parameters. Because of the difficulties in the modelling of the behaviour of complex systems, the properties of the compressed mixtures were used for the training of the new model.

All of the above-mentioned parameters were used as input variables; the output variables were the tensile strength and the breakability of the tablets. The data on Samples 8, 11 and 12 and a few randomly selected data were used for the external testing of the prediction ability of the developed network. On the basis of the results in the first part of the study, an MLP network was used with n+m+1 hidden neurons. Delta-bar-Delta was used as the training algorithm. The minimum error level was reached in less than 100 training epochs. However, the external validation tests showed very poor predictive force. The system made no differentiation between tablets prepared at different compression forces; only the change between samples was visible. The results did not improve either for different training algorithms or for the changes in the complexity of the system. This is probably due to the high proportion of the material-characterizing parameters among the input variables, which made a reduction of these parameters in the original data set necessary. The pruning of input data was impossible during the training of the network, which showed that the omission of information from the model results in a decrease in performance. The application of less information in such a complex model should be avoided, so combination of the different parameters appeared be more advantageous. The surface free energy and polarity index of the materials were replaced with the calculated adhesion force against stainless steel, while the slope and intercept of the plasticity function were replaced by the calculated plasticity value corresponding to the applied compression force.

After the training with the modified data set, the prediction performance of the system increased significantly ($p<0.05$). However, both the Delta-bar-Delta and the quick-propagation algorithm converged too quickly with the previously applied stopping conditions. The changes of the minimum improvement in the selection set from 0.001 to 0.01 and the window from 10 to 100 epochs have brought some improvement but not significantly so. Further improvement could be achieved when the training algorithm was

changed to back-propagation, which in this case provided greater accuracy at the expense of slower convergence. In the case of the best model, a second training phase was used with a gradient-based quasi-Newton algorithm.

The results of the internal testing demonstrated appropriate observed vs. predicted correlation coefficients (R^2=0.874 for tensile strength and R^2=0.899 for breakability). However, the external testing of the prediction performance yielded much poorer results. There was no correlation between the observed vs. predicted tensile strength. (Fig. 22).

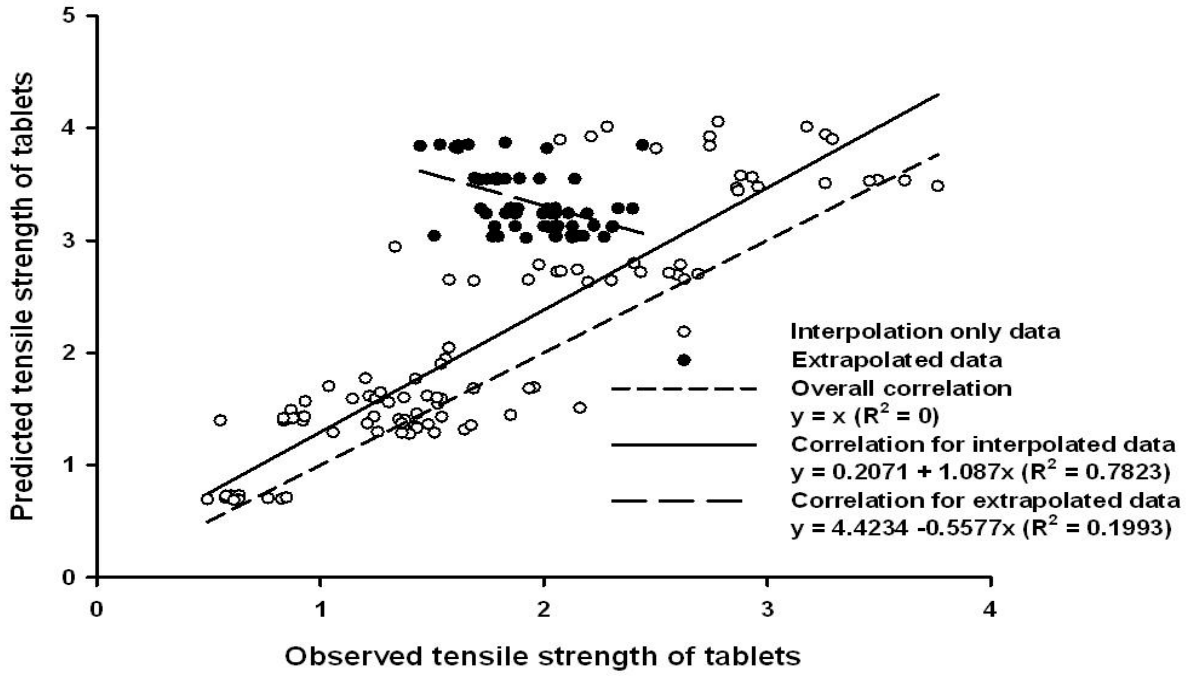

Figure 22. Observed vs. predicted correlation of tensile strength

Nevertheless, when only those data were investigated which were within the limits of the training data set, and required no extrapolation, the correlation coefficients increased significantly (R^2=0.7823). The extrapolated data were considerably overestimated and displayed negative correlation. Furthermore, it is clearly visible that (because of the learning mechanism) the predicted values did not follow the natural deviation in the observed tensile strength. The predicted values deviated slightly around the average values. If this disturbing effect of the deviation is taken into account, the values of the correlation can be further improved (Fig. 23). In the case of the breakability, the external testing also showed poorer results than the internal testing. The halving properties were usually overestimated in the case of lower values, and slightly underestimated for higher ones (Fig. 24).

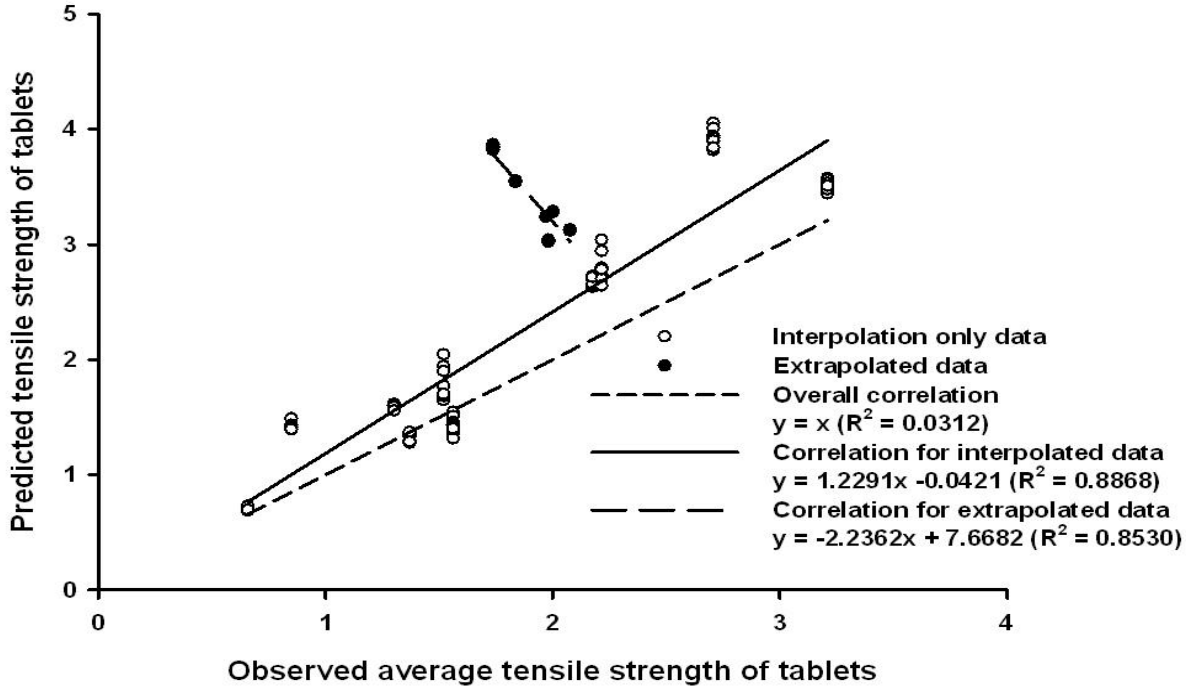

Figure 23. Observed average vs. predicted correlations of tensile strength

However, when these deformations are taken into account appropriate screening can be carried out for the potentially well-breakable compositions, despite the poorer correlations.

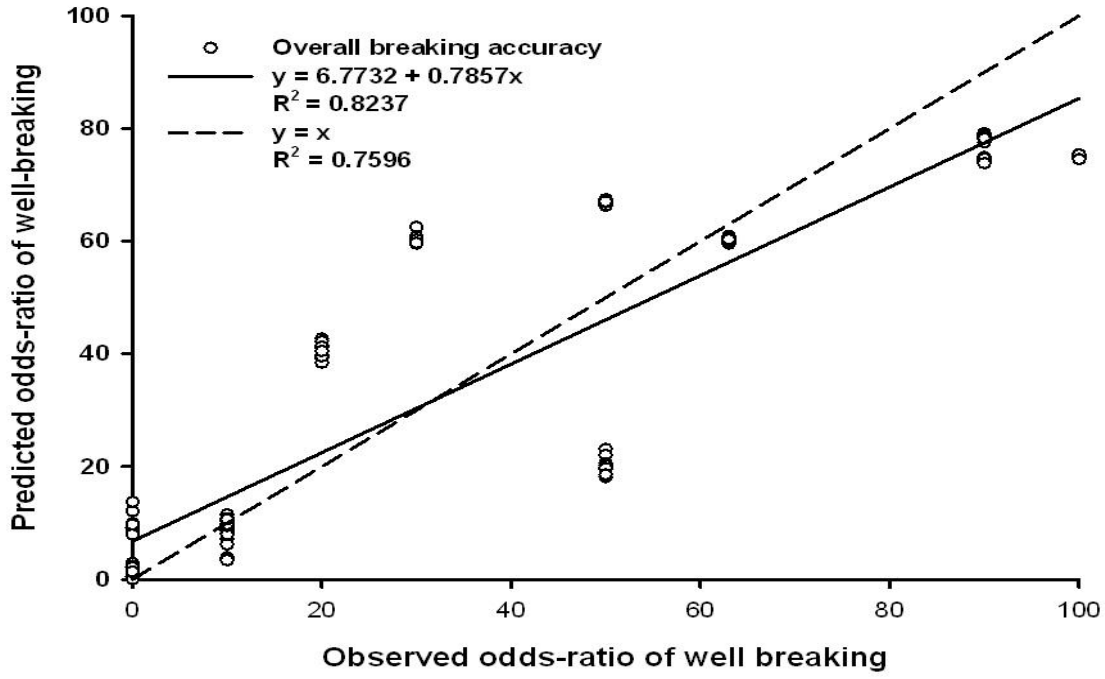

Figure 24: Observed vs. predicted correlation of the breakability

The developed ANN seems to be an appropriate model for prediction of the postcompressional properties of scored tablets, even despite the poorer correlations. The

difference between the prediction accuracy of the interpolated and extrapolated data suggests that these problems can be easily solved by increasing and widening of the training data set. However, this requires a large number of further experiments.

6. Summary

The primary aim of the study was the in silico modelling of the compression of scored tablets, for prediction of the postcompressional properties, and especially the subdivision of the products with the help of ANNs.

Major conclusions:

- The *artificial neural network* is a useful modelling technique in pharmaceutical research and development. The *Multilayer Perceptron* seems to be the best type of neural network because of its high flexibility.
- *Gradient-based algorithms* show an inappropriate learning performance as compared with *back-propagation-based algorithms*, but the combination of the two types could result in a significant improvement in the predicted data. Improved back-propagation algorithms, such as quick-propagation or Delta-bar-Delta, displays faster convergence to the minimum error, but the faster working sometimes results in less accuracy.
- Care must be taken as concerns the selection of the data for the input data set: unbalanced data can cause serious problems in the functioning of the neural networks, which can lead to inappropriate predictions.
- Numerous *physicochemical properties* of the applied materials and operational parameters of the tablet press must be taken into account for the development of a universally functioning neural network.
- The *adhesion and friction* to the die wall, and the *elastic recovery* are perhaps the most important physical phenomena in respect of the postcompressional properties of the tablets. The *adhesion work* influences both the flow properties/die filling and the friction work during the ejection of the tablet. This parameter could be calculated from the *surface free energy* of the materials or mixtures. However, prediction of the surface energy of the powder mixtures from the parameters of the mixed components is a very complex problem. Besides the adhesion force and the spreading coefficient, the size and shape of the particles have significantly influence the arrangement in the mixture, which will determine the

overall behaviour during compression. The exact description of these relationships requires further investigations.

- The *plasticity* of the different materials shows a certain dependency on the compression force. If this dependence is considerable, the hardness-compression force functions will be curved, and the prediction of the postcompressional properties will be more difficult.
- The applied *compression force* probably has the most significant effect on the postcomprompressional properties of the tablets. However, the effective load has other components, such as the *time of compression*, as suggested by the results of the mathematical models of compression.
- The *type of the tablet press* is also of appreciable importance not only because of the compression time differences, but the direction of action exert a significant influence on the rearrangement of the particles and the lines of the forces. These effects could be investigated well by means of *computer microtomography*.

Practical usefulness

- The *in silico modelling* of the production processes is of ever greater importance in the pharmaceutical industry. The increasing time and costs of the development of a new drug, and the increasing strictness of the drug authorities, necessitates the deep planning and the use of cost saving methods.
- The *ICH Q8 guideline* [171] requires the demonstration of "an enhanced knowledge of product performance over a range of material attributes, manufacturing process options and process parameters", which can be supported with the developed neural model.
- Furthermore, this model is *able to predict* the probable postcompressional properties of scored tablets, from preformulation data on the applied powder mixtures, which is a useful tool in the reduction of the number of required experiments.
- The applied mathematical models facilitate an understanding of the *differences between eccentric and rotary presses*, which simplifies data transfer between the different tablet presses. The understanding of the structural differences between the tablets with various properties can lead to a significant improvement in the breaking accuracy and reliability of the marketed products.
- The recognition of the *importance of the surface properties* of materials in the field of direct compression contributes to the description of the behaviour of the materials

during compression, and to predictability of the postcompressional tablet properties. However, an exact description as to how the properties of the components determine the properties of a binary or higher order mixture requires further investigations.

7. References

1. J. Barra, F. Lescure, F. Falson-Rieg, E. Doelker *Pharm. Res.* 15 (1998) 1727-1736
2. F. Ndindayino, D. Henrist, F. Kiekens, C. Vervaet, J.P. Remon *Int. J. Pharm.* 189 (1999) 113–124
3. N. Rasenack, B. W. Müller *Int. J. Pharm.* 244 (2002) 45–57
4. J. S. Kaerger, S. Edge, R. Price *Eur. J. Pharm. Sci.* 22 (2004) 173–179
5. C. Sun, D. J.W. Grant *Int. J. Pharm.* 215 (2001) 221–228
6. E. N. Hiestand *Eur. J. Pharm. Biopharm.* 44 (1997) 229-242
7. F. Podczeck, J. M. Newton, M. B. James *Int. J. Pharm.* 145 (1996) 221-229
8. M.S. Anuar, B.J. Briscoe *Powder Technol.* 195 (2009) 96–104
9. M.G. Vachon, D. Chulia *Int. J. Pharm.* 177 (1999) 183–200
10. G. F. Palmieri, E. Joiris, G. Bonacucina, M. Cespi, A. Mercuri *Int. J. Pharm.* 298 (2005) 164–175
11. B. De Spiegeleer, L. Van Vooren, T. Thonissen, P. Joye, B. Cornelissen, G. Lammens G. Slegers *J. Food Drug Anal*.,13 (2005) 22-29
12. K. C. van der Steen, H. W. Frijlink, C. Maarten, A. Schipper, D. M. Barends *AAPS PharmSciTech*, 11 (2010) 126-132
13. K.R. Drakea, J.M. Newton, S. Mokhtary-Saghafi, P.N. Davies *Eur. J. Pharm. Sci.* 30 (2007) 273–279
14. J. Noviasky, V. Lo, D. D. Luft, *MSI* 55 (2006) 707-708
15. E. van Santen, D.M. Barends, H.W. Frijlink *Eur. J. Pharm. Biopharm.* 53 (2002) 139–145
16. N. Rodenhuis, P. A. G. M. dee Smet, D. M. Barends *Eur. J. Pharm. Sci.* 21 (2004) 305–308
17. N. Rodenhuis, P. A. G. M. de Smet, D. M. Barends *Pharm World Sci* 25 (2003) 173–176
18. L. van Hooren, B. de Spiegeleer, T. Thoisen, P. Joye, J. van Durme, G. Slegers, *J. Pharm. Pharmaceut. Sci.* 5 (2002) 190-198

19. J. L. Marriott, R. L. Nation *Aust. Prescr.* 25 (2002) 133–135
20. R. Quinzler, S. P. W. Schmitt, M. Pritsch, J. Kaltschmidt, W. E Haefeli *BMC Med. Inf. Dec. Making* 9 (2009) doi:10.1186/1472-6947-9-30
21. J. Bachynsky, C. Wiens, K. Melnychuk *Pharmacoeconomics* 5 (2002) 339-346
22. E. Vranić, A. Uzunović *Bosn. J. Basic Med. Sci.* 7 (2007) 328-334
23. S. W. Hill, A. S. Varker, K. Karlage, P. B. Myrdal *J Manag Care Pharm.* 15 (2009) 253-261
24. A. Stockis, S. de Bruyn, X. Deroubaix, B. Jeanbaptiste, E. Lebacq Jr., F. Nollevaux, G. Polid, D. Acerbi *Eur.J. Pharm. Biopharm.* 53 (2002) 49–56
25. Ph. Eur. 6.
26. W.A. Ritschel, A. Bauer-Brandl *Die Tablette* Editio Cantor Verlag (2002)
27. N. Sandler, D. Wilson *J. Pharm. Sci.-US* doi: 10.1002/jps.21884
28. K. Terada, E. Yonemochi, *Solid State Ionics* 172 (2004) 459–462
29. E. N. Hiestand *J. Pharm. Sci.-US* 55 (1966) 1325-1344
30. T. H. Muster, C. A. Prestridge *J. Pharm. Sci-US* 91 (2002) 1432-1444
31. Y. H. Kiang, H. G. Shi, D. J. Mathre, W. Xu, D. Zhang, S. Panmai *Int. J. Pharm.* 280 (2004) 17–26
32. R. Dingreville, J. Qu, M. Cherkaoui *J. Mech. Phys. Solids* 53 (2005) 1827–1854
33. I. Nikolakakis, J. M. Newton, S. Malamataris *Eur. J. Pharm. Sci.* 17 (2002) 229–238
34. X. Pepin, S. Blanchon, G. Couarraze *J.Pharm. Sci.-US* 90 (2001) 332-339
35. F. Thielmann, M. Naderi, M. A. Ansari, F. Stepanek *Powder Technol.* 181 (2008) 160–168
36. Zs. Tüske, G. Regdon Jr., I. Erős, S. Srčič, K. Pintye-Hódi *Powder Technol.* 155 (2005) 139–144
37. O. Planinšek, R. Pišek, A Trojak, S. Srčič *Int. J. Pharm.* 207 (2000) 77–88
38. L. A. Felton, J. W. McGinity *Eur. J. Pharm. Biopharm.* 47 (1999) 3–14
39. J. Bajdik, M. Marciello, C. Caramella, A. Domján, K. Süvegh, T. Marek, K. Pintye-Hódi *J. Pharm. Biomed. Anal.* 49 (2009) 655–659
40. H. Olsson, A. Adolfsson, C. Nyström *Int. J. Pharm.* 143 (1996) 233-245
41. V. Swaminathan, J. Cobb, I. Saracovan *Int. J. Pharm.* 312 (2006) 158–165
42. Y. Kuno, M. Kojima, H, Nakagami, E, Yonemochi, K. Terada *Eur. J. Pharm. Biopharm.* 69 (2008) 986–992

43. J. C. Feeley, P. York, B. S. Sumby, H. Dicks *J. Mater. Sci.* 37 (2002) 217–222
44. Q. Zhou, B. Armstrong, I. Larson, P. J. Stewart, D. A.V. Morton *J. Pharm. Sci.-US* doi: 10.1002/jps.21885
45. J. Bajdik, K. Pintye-Hódi, O. Planinšek, G. Regdon Jr., R. Dreu, S. Srčič, István Erős *Int. J. Pharm.* 269 (2004) 393–401
46. S. W. Hardler, D. A. Zuck, J. A. Wood *J. Pharm. Sci.-US* 59 (1970) 1787-1792
47. W.C. Liao, J. L. Zatz *J. Pharm. Sci.-US* 68 (1979) 488-494
48. S. Baumgartner, o. Planinšek, S. Srčič, J. Kristl *Eur. J. Pharm. Sci.* 27 (2006) 375–383
49. P. Singh, S. J.Desai, A. P. Simonelli, W. I. Higuchi *J. of Pharm. Sci.-US* 57 (1968) 217-226
50. M. Rillosi, G. Buckton *Int. J. Pharm.* 117 (1995) 75-84
51. G. Zografi S. S. Tam *J. Pharm. Sci.-US* 65 (1976) 1145-1149
52. X. Pepin, S. Blanchon, G. Couarraze *PSTT* 2 (1999) 111-118
53. T. H. Muster, C. A. Prestidge *Int. J. Pharm.* 234 (2002) 43–54
54. T. H. Muster *Int. J. Pharm.* 282 (2004) 189–191
55. J.W. Dove, G. Buckton, C. Doherty *Int. J. Pharm.* 138 (1996) 199-206
56. N. M. Ahfata, G. Buckton, R. Burrows, M. D. Ticehurst *Eur.J. Pharm. Sci.* 9 (2000) 271–276
57. O. Planinšek, A. Trojak, Stane Srčič *Int. J. Pharm.* 221 (2001) 211–217
58. I. M. Grimsey, J. C. Feeley, P. York *J. Pharm. Sci.-US* 91 (2002) 571-583
59. G. Buckton, H. Gill *Adv. Drug Deliver. Rev.* 59 (2007) 1474–1479
60. M.D. Ticehurst , P. York , R.C. Rowe, S.K. Dwivedi *Int. J. Pharm.* 141 (1996) 93 99
61. O. Planišek, G. Buckton *J. Pharm. Sci.-US* 92 (2003) 1286-1294
62. M. J. Telko, A. J. Hickey *J. Pharm. Sci.-US* 96 (2007) 2647-2654
63. J. C. Hooton, C. S. German, M. C. Davies, C. J. Roberts *Eur. J. Pharm. Sci.* 28 (2006) 315–324
64. A. Saxena, J. Kendrick, I. Grimsey, L. Mackin *Int. J. Pharm.* 343 (2007) 173–180
65. A. Saxena, J. Kendrick, I.M. Grimesey, R. Roberts, P. York *J. Pharm. Sci.-US* doi: 10.1002/jps.21864

66. I. Bravo-Osuna, C. Ferrero, M.R. Jiménez-Castellanos *Eur. J. Pharm. Biopharm.* 66 (2007) 63–72
67. J. T. Carstensen *Solid Pharmaceutics: Mechanical Properties and Rate Phenomena* Academic Pres Inc. (1980) 173-214
68. O. Antikainen, J. Yliruusi *Int. J. Pharm.* 252 (2003) 253–261
69. C. Pontiera, M. Viana, E. Champion, D. Bernache-Assollant, D. Chulia *Eur. J. Pharm. Biopharm.* 51 (2001) 249-257
70. T. Suzuki, H. Nakagami *Eur. J. Pharm. Biopharm.* 47 (1999) 225–230
71. F. Ndindayino, D. Henrist, F. Kiekens, G. Van den Mooter, C. Vervaet, J.P. Remon *Int. J. Pharm.* 235 (2002) 149–157
72. N. Rasenack, B. W. Müller *Int. J. Pharm.* 244 (2002) 45–57
73. C. Sun, D. J. W. *Grant J. Pharm. Sci.-US* 90 (2001) 569-579
74. C. Sun, D. J. W. Grant *Pharm. Res.* 18 (2001) 274-280
75. Y. Feng, D. J. W. Grant *Pharm. Res.* 23 (2006) 1608-1616
76. Y. Feng, D. J. W. Grant, C. C. Sun *J. Pharm. Sci.-US* 96 (2007) 3324-3333
77. B. van Veen, G.K. Bolhuis, Y.S. Wu, K. Zuurman, H.W. Frijlink *Eur. J. Pharm. Biopharm* 59 (2005) 133–138
78. S. Patel, A. M. Kaushal, A. K. Bansal Eur. *J. Pharm. Biopharm.* 69 (2008) 1067-1076
79. Zs. Sáska, J. Dredán, E. Balogh, O. Luhn, G. Shafir, I. Antal *Powder Technol.* 201 (2010) 123-129
80. J. T. Fell, J. M. Newton *J. Pharm. Sci.-US* 59 (1970) 688-691
81. J. M. Newton, I. Haririan, F. Podczeck *Eur. J. Pharm. Biopharm.* 49 (2000) 59-64
82. P. N. Davies, H. E.C. Worthington, F. Podczeck, J. M. Newton Eur. J. Pharm. Biopharm. 67 (2007) 268–276
83. T. Çomoglu *J. Fac. Pharm. Ankara* 36 (2007) 123-133
84. R.W. Heckel *Trans. Metall. Soc. AIME* 221 (1961a) 671-675
85. R.W. Heckel *Trans. Metall. Soc. AIME* 221 (1961b) 1001-1008
86. C. Ferrero, N. Mufioz, M.V. Velasco, A. Mufioz-Ruiz, R. Jiménez-Castellanos *Int. J. Pharm.* 147 (1997) 11 21
87. M. de la Luz Reus Medina, V. Kumar *J. Pharm. Sci.-US* 96 (2007) 408-420
88. V. Busignies, P. Tchoreloff, B. Leclerc, M. Besnard, G. Couarraze *Eur. J. Pharm. Biopharm.* 58 (2004) 569–576
89. L. Yang, G. Venkatesh, R. Fassihi *Int. J. Pharm.* 152 (1997) 45-52

90. T. Kuny, H. Leuenberger *Int. J. Pharm.* 260 (2003) 137–147
91. P. Di Martino, E. Joiris, S. Martelli *Il Farmaco* 59 (2004) 747–758
92. P. M. Belda, J. B. Mielck *Eur. J. Pharm. Biopharm.* 60 (2005) 133–145
93. C. Ferrero, M.R. Jiménez-Castellanos *Int. J. Pharm.* 248 (2002) 157-171
94. P. Di Martino, M. Scoppa, E. Joiris, G.. F. Palmieri a, C. Andres, Y. Pourcelot, S. Martelli *Int. J. Pharm.* 213 (2001) 209–221
95. P. M. Belda, J. B. Mielck *Eur. J. Pharm. Biopharm.* 48 (1999) 157-170
96. A. Michrafy, M. S. Kadiri, J. A. Doods *Trans IChemE* 81 (2003) 946-952
97. M. Kuentz, H. Leuenberger *J. Pharm. Sci.-US* 88 (1999) 174-179
98. S. F. Yap, M. J. Adams, J. P. K. Seville, Z. Zang *Powder Technol.* 185 (2008) 1-10
99. R. Panelli, F. A. Filho *Powder Technol* 114 (2001) 255–261
100. J.M. Sonnergaard *Eur. J. Pharm. Sci.* 11 (2000) 307–315
101. P.J. Denny *Powder Technol.* 127 (2002) 162– 172
102. J.M. Sonnergaard *Int. J. Pharm.* 193 (1999) 63-71
103. A. Hassanpour, M. Ghadiri *Powder Technol.* 141 (2004) 251– 261
104. C. C. SUN *J. Pharm. Sci.-US* 94 (2005) 2061-2068
105. M. Viana, P. Jouannin, C. Pontier, D. Chulia *Talanta* 57 (2002) 583–593
106. C. C. SUN *J. Pharm. Sci.-US* 94 (2005) 2132-2134
107. M. Krumme, Lothar Schwabe, Karl-Heinz Fromming *Eur. J. Pharm. Biopharm.* 49 (2000) 275-286
108. J. Zhao, H.M. Burt, R.A. Miller *Int. J. Pharm.* 317 (2006) 109–113
109. E.E. Walker *Trans. Faraday Soc*. 19 (1923) 73-82
110. K. Kawakita, K.H. Lüdde. *Powder Technol*. 4 (1971) 61-68
111. R. Pitchumani, O. Zhupanska, G. M. H. Meesters, B. Scarlett *Powder Technol.* 144 (2004) 56–64
112. Frauke Fichtner, A. Rasmuson, G. Alderborn Int. *J. Pharm.* 292 (2005) 211–225
113. P. C. Schmidt, M. Leitritz *Eur. J. Pharm. Biopharm.* 44 (1997) 303-313
114. C. K. Tye, C. C. Sun, G. E. Amidon *J. Pharm. Sci.-US* 94 (2005) 465-472
115. K. M. Picker *Eur. J. Pharm. Biopharm.* 50 (2000) 293-300
116. M. Cespi, M. Misci-Falzi, G. Bonacucina, S. Ronchi, G. F. Palmieri *J. Pharm. Sci.-US* 97 (2008) 1277-1284
117. F. Kiekens, A. Debunne, C. Vervaet, L. Baert, F. Vanhoutte, I. Van Assche, F. Menard, J. P. Remon *Eur. J. Pharm. Sci.* 22 (2004) 117–126

118. J. M. Newton, I. Haririan, F. Podczeck *Powder Technol* 107 (2000) 79–83
119. X. Fu, M. Dutt, A. C. Bentham, B. C. Hancock, R. E. Cameron, J. A. Elliott *Powder Technol* 167 (2006) 134–140
120. C. Y. Wu, T. O. M. Ruddy, A.C. Bentham, B.C. Hancock, S.M. Best, J.A. Elliott *Powder Technol.* 152 (2005) 107–117
121. R. Al-Raousha, K. A. Alshibli *Physica A* 361 (2006) 441–456
122. I.C. Sinka, S.F. Burch, J.H. Tweed, J.C. Cunningham *Int. J. Pharm.* 271 (2004) 215–224
123. R. A. Ketcham, G. J. Iturrino *J. Hydrol.* 302 (2005) 92–106
124. X. Jia, R. A.Williams *Dissolution Technologies* (2006) 11-19
125. R. Al-Raoush *Physica A* 377 (2007) 545–558
126. F. Stepanek, A. Loo, T. S. Lim *J. Pharm. Sci.-US* 95 (2006) 1614-1625
127. L. Salvo, P. Cloetens, E. Maire, S. Zabler, J.J. Blandin, J.Y. Buffiere, W. Ludwig, E. Boller, D. Bellet, C. Josserond *Nucl. Instrum. Meth. B* 200 (2003) 273–286
128. K. E. Thompson, C. S. Willson, W. Zhang *Powder Technol.* 163 (2006) 169–182
129. J. C. Fiala *J. Microscopy* 218 (2005) 52–61
130. J. Vlassenbroeck, M. Dierick, B. Masschaele, V. Cnudde, L. Van Hoorebeke, P. Jacobs *Nucl. Instrum. Meth. A* 580 (2007) 442–445
131. B. C. Hancock, M. P.Mullarney *Pharm. Technol.* (2005) 92-100
132. Q. Shao, R. C. Rowe, P. York *Eur. J. Pharm. Sci.* 28 (2006) 394–404
133. J. Bourquin, H. Schmidli, P. Hoogevest, H. Leuenberger *Pharm. Dev. Technol.* 2 (1997) 111–121
134. J. Bourquin, H. Schmidli, P.V. Hoogevest, H. Leuenberger *Pharm. Dev. Tech.* 2 (1997) 95–109
135. J. Bourquin, H. Schmidli, P.V. Hoogevest, H. Leuenberger *Eur. J. Pharm. Sci.* 6 (1998)287–300.
136. J. Bourquin, H. Schmidli, P. Hoogevest, H. Leuenberger *Eur. J. Pharm. Sci.* 7 (1998) 5–16
137. J. Bourquin, H. Schmidli, P. Hoogevest, H. Leuenberger *Eur. J. Pharm. Sci.* 7 (1998) 17–28
138. A.P. Plumb, R.C. Rowe, P. York, C. Doherty *Eur. J. Pharm. Sci.* 16 (2002) 281–288

139. A.P. Plumb, R.C. Rowe, P. York, M. Brown *Eur. J. Pharm. Sci.* 25 (2005) 395–405
140. S. Inghelbrecht, J. P. Remon, P. Fernandes de Aguiar, B. Walczak, D. L. Massart, F. Van De Velde, P. De Baets, H. Vermeersch, P. De Backer *Int. J. Pharm.* 148 (1997) 103-115
141. S. Watano, Y. Sato, K. Miyanami *Powder Technol.* 90 (1997) 153-159
142. M. Türkoglu, H. Varol, M. Celikok *Eur. J. Pharm. Biopharm.* 57 (2004) 279–286
143. H. Sunada, Y. Bi *Powder Technol.* 122 (2002) 188–198
144. A. P. Plumb, R. C. Rowe, P. York, C. Doherty *Eur. J. Phar. Sci.* 16 (2002) 281–288
145. H. Hruschka, M. Natter *Eur. J. Oper. Res.* 114 (1999) 346-353
146. N. Qu, X. Li, Y. Dou, H. Mi, Y. Guo, Y. Ren *Eur. J. Pharm. Sci.* 31 (2007) 156–164
147. Y. Sun, Y. Peng, Y. Chen, A. J. Shukla *Adv. Drug Deliv. Rev.* 55 (2003) 1201–1215
148. S. Ibrić, M. Jovanović, Z. Djurić, J. Parojčić, S. D. Petrović, L. Solomun, B. Stupar *AAPS PharmSciTech* 4 (2003) Article 9 (http://www.pharmscitech.org)
149. J. Takahara, K. Takayama, T. Nagai *J. Control. Release* 49 (1997) 11–20
150. Y. Chen, T. W. McCall, A. R. Baichwal, M. C. Meyer *J. Control. Release* 59 (1999) 33–41
151. S. Surini, H. Akiyama, M. Morishita, T. Nagaia, Kozo Takayama *J. Control. Release* 90 (2003) 291–301
152. J. Parojčić, S. Ibrić, Z. Djurić, M. Jovanović, O. I. Corrigan *Eur. J. Pharm. Sci.* 30 (2007) 264–272
153. L. Du, L. Wu, J. Lu, W. Guo, Q. Meng, C. Jiang, S. Sheng, L. Teng *Chem. Res. Chinese U.* 5 (2007) 518-523
154. Y. Dou, H. Mi, L. Zhao, Y. Ren, Y. Ren *Spectrochim. Acta A* 65 (2006) 79–83
155. G. H. Golub *Numer. Math.* 7 (1965) 206–216
156. T.F. Chan *ACM T. Math. Software* (1982) 872−883.
157. H. Hruschka, M. Natter *Eur. J. Oper. Res.* 114 (1999)346−353
158. L. Feng, W. Hong *Neural Comput & Applic* 18 (2009) 377–380
159. D.F. Specht *IEEE T. Neural. Networ.* 2 (1991) 568−576

160. G. Yazici, Ö. Polat, T. Yildirim *MCIAI 2006 LNAI* 4293 (2006) 348−356
161. T. Kohonen, P. Lehtiö, J. Rovamo, J. Hyvärinen, K. Bry, L. Vainio *Neuroscience* 2 (1977) 1065−1076
162. D. Rumelhart, G. Hinton, R. Williams *Nature* 323 (1986) 533–536
163. A. Ghaffari, H. Abdollahi, M.R. Khoshayand, I. Soltani Bozchalooi, A. Dadgar, M. Rafiee-Tehrani *Int. J. Pharm.* 327 (2006) 126–138
164. G. Yu, Y. Zhao, Z. Wei *Appl. Math. Comput* 187 (2007) 636−643
165. S. Xu, L. Chen *ICITA* (2008) 683-686 ISBN: 978-0-9803267-2-7
166. Y. Sun, Y. Peng, Y. Chen, A. J. Shukla *Adv. Drug. Deliver. Rev.* 55 (2003) 1201–1215
167. Y. Bai, H. Zhang, Y. Hao *Chaos, Solitons and Fractals* 15 (2009) 69-77
168. K. Takayama, M. Fujikawa, Y. Obata, M. Morishita *Adv. Drug Deliver. Rev.* 55 (2003) 1217–1231
169. J.I. Wells *Pharmaceutical Preformulation: The physicochemical properties of drug substances.* Ellis Horwood Ltd. (1988) 209−211
170. K. Kawakita, K., I. Hattori, M. Kishigami. *J. Powder Bulk Solids Technol*. 1 (1977) 3-8
171. ICH Q8 – Guidance for Industy http://www.fda.gov/downloads/RegulatoryInformation/Guidances/ucm128029.pdf

Acknowledgements

I am very grateful to my supervisor

Prof. Dr. Klára Pintye-Hódi

for her support. I greatly appreciate her continuous help during the preparation of my thesis and providing the excellent facilities for this study. I owe my warm gratitude to her for her criticism, encouragement and numerous discussions during my Ph.D. work.

I express my grateful thanks to **Sanofi-Aventis scholarship** to the kind support of my Ph.D. studies.

I would like to thank

Prof. Dr. Piroska Szabó-Révész and **Prof. Dr. István Erős**

present and former Head of the Ph.D. programme of Pharmaceutical Technology for providing me with the possibility to complete my work under their guidance.

My warmest thanks to **Prof. Dr. Piroska Szabó-Révész** present Head of the Department of Pharmaceutical Technology, for her invaluable advice.

I express my grateful thanks to

Prof. Dr. Stane Srčič

Head of the Department of Pharmaceutical Technology, University of Ljubljana, for providing the possibility for me to carry out scientific research in his department. I owe him my thanks for his advice and instructions.

I express my kindest thanks to all my co-authors, especially to

Péter Kása jr.

for their collaboration in this work.

I thank all members of the department for their help and friendship.

I owe my thanks to my family and my friends for their support, encouragement and understanding attitude during these years.

ANNEX

Related articles

I

PHARMACEUTICAL TECHNOLOGY

Modeling of Subdivision of Scored Tablets with the Application of Artificial Neural Networks

T. SOVÁNY, P. KÁSA, K. PINTYE-HÓDI

Department of Pharmaceutical Technology, University of Szeged, Eötvös u. 6. H-6721 Szeged, Hungary

Received 24 February 2009; revised 6 May 2009; accepted 15 May 2009

Published online 30 June 2009 in Wiley InterScience (www.interscience.wiley.com). DOI 10.1002/jps.21853

ABSTRACT: The subdivision of scored tablets is an important problem for the exact individual therapy of patients. The recent guidelines of the EU require verification of the equal mass of the tablet halves, but this problem has previously never been investigated in papers published on the production technological aspects. Our aim was therefore to study the effects of the physicochemical properties of the raw materials and the effects of the compression process on the breaking parameters of the tablets. Artificial neural networks (ANNs) were applied for data analysis and modeling, which are very useful optimizing systems. The abilities of four different types of ANNs to predict the parameters of the compression process and the tablets were compared. The radial basis function and multilayer perceptron ANNs furnished statistically significant better results than linear or generalized regression neural networks. These ANN models revealed that the subdivision of scored tablets is strongly influenced by the production parameters and the compositions of the powder mixtures. © 2009 Wiley-Liss, Inc. and the American Pharmacists Association J Pharm Sci 99:905–915, 2010

Keywords: *in silico* modeling; neural networks; structure property relationships; excipients; physicochemical; compression; powder technology; tableting; scored tablets; subdivision

INTRODUCTION

Tablets, the most common dosage form in the pharmacy, have many advantages. They are easy to use, and the effect can be well regulated, but the individual treatment of patients requires different doses. To solve this problem, companies produce many doses, or apply scored tablets. The good subdivision of scored tablets is an important problem for the pharmaceutical industry. The new EU guidelines prescribe verification of the exactness of breaking into halves. Ph. Eur. 6 too relates to masses of the tablet halves, with the condition that the distribution of the active pharmaceutical ingredient (API) is uniform within the tablet. Subdivision is a multifactorial problem, which depends on the production method and the tablet properties. Compression with eccentric or rotary tablet presses causes differences in the structure or density distribution within the tablets, which influences the breaking properties. The tablet properties can be influenced by the parameters of the punches (shape, height of the bisecting line, etc.) and by the properties of the component materials. We first investigated the effect of the composition on the breaking properties. Tablets compressed industrially contain more than one component. Since the novel preparations contain the active agent only in low

Correspondence to: K. Pintye-Hódi (Telephone: 36-62-545576; Fax: 36-62-545571; E-mail: klara.hodi@pharm.u-szeged.hu)

Journal of Pharmaceutical Sciences, Vol. 99, 905–915 (2010)

doses, the properties of the preparation depend much more on the properties of the excipients. It is important, therefore, to study the behavior of excipient mixtures. The different parameters of the materials, such as the crystal habit, particle size, cohesion and adhesion forces, surface free energy, and moisture content, cause differences in the compressibility and compaction behavior of powders and powder mixtures. The preformulation and production results can be analyzed by means of different mathematical equations or with artificial neural networks (ANNs).

ANNs model the structure and function of the human brain, are able to accommodate to different problems, and hence are able to "learn." In the past decade, many articles have studied their usefulness in pharmaceutical process modeling.[1–7] In general, ANNs are build up from nodes, connected with weights. Two main ANN types can be distinguished. Supervised ANNs have strongly hierarchical structures; the nodes are regulated in layers (Fig. 1). The teaching of supervised ANNs is based on the changing of the weights of the connections, whereas unsupervised ANNs have no hierarchical structure, and the number of neurons is not determined preliminarily. During the training phase, the neurons are regulated into groups, and the information is based not only on the connections between the groups, but also on the distances between the groups, that is, a topological map. In the present study, four different supervised ANNs were compared.

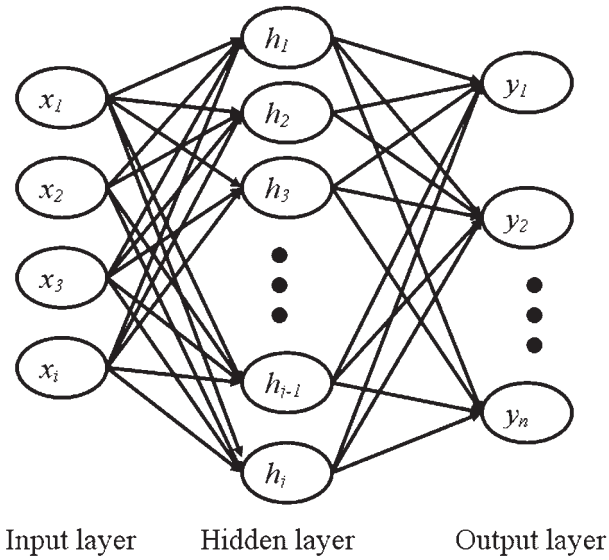

Figure 1. General structure of supervised ANNs.

It is a scientific principle that, if the data give a good fit, then the simplest model should always be chosen. The simplest, one-layer ANN model is the linear. The input and output neurons are directly connected, without hidden neurons. This structure gives an NxM matrix with an Nx1 bias vector. The learning is based on the singular value decomposition (SVD) algorithm.[8,9]

The multilayer ANNs are more advanced. In the radial basis function (RBF) network, the input neurons are connected with the neurons of the radial layer. These neurons are associated with a Gaussian activation function, and carry out the clustering of data *via* sub-sampling or the K-means method.[10] Their number are generally corresponds to the number of output neurons. The processed data are usually subjected to a linear transformation *via* the SVD algorithm.

Bayesian or generalized regression neural network (GRNN), reported by Specht,[11] are similar to the RBF, but there are also some differences. The GRNN has two hidden layers. The radial layer has the same function as in the RBF network, but the number of neurons usually corresponds to the number of training cases. The second layer is the pattern layer, which calculates the weighted sum of the vectors from the radial neurons.[12] The number of neurons in the pattern layer is always the number of outputs +1. The drawback of such ANNs is that extrapolation is not possible because of the Gaussian activation.

In contrast, the multilayer perceptron (MLP), which is based on the one-layer perceptron model of Kohonen et al.,[13] and which was evaluated by Rumelhart et al.,[14] is probably the most popular type of ANNs, as it is freely variable. It can handle one or more hidden layers with linear, hyperbolic tangent or logistic activation functions. Thanks to its popularity numerous learning algorithms (back-propagation, conjugate gradient descent, quasi-Newton, etc.) have been developed for the MLP.[15,16] Its high variability allows the MLP to offer probably the most powerful models, but finding the optimal structure of the ANN is somewhat difficult. It is generally considered that one layer is sufficient for the modeling of most problems. A number of recommendations are available in the literature for determination of the number of hidden neurons. The Kolomorogov theorem specifies that the optimal number of hidden neurons is the number of inputs +1.

Another recommendation is that the number of hidden neurons is half of the sum of the numbers of input and output neurons. Other equations have been developed by Jadid et al. and by Carpenter for determination of the maximal number of hidden neurons,[17] but the number is still usually determined *via* trials.

METHODS AND MATERIALS

The tablets were made from microcrystalline cellulose (MCC; Vivapur 102, J. Rettenmaier & Söhne, Rosenberg, Germany) and spray-dried mannitol (SDM; Pearlitol SD 200, Roquette Pharma, Lestrem, France) in different mass proportions (Tab. 1). 1% of magnesium stearate (Ph. Eur.) was added to promote lubrication of the tablets.

The particle size distribution of the powders was examined with a Laborlux S light microscope and a Quantimet 500 MC image-analyzing system (Leica Cambridge Ltd., Cambridge, UK), based on measurement of 1000 particles. A scanning electron microscope (Hitachi 2400 S, Tokyo, Japan) was used to study the morphological properties of crystals, and a Polaron sputter apparatus (Polaron Equipment Ltd., Greenhill, UK) was applied to induce electric conductivity on the surface of the samples.

The flow properties (flow time, angle of repose and bulk density) of the materials and powder mixtures were determined with a PharmaTest PTG 1 (Pharma Test Apparatebau GmbH, Hainburg, Germany), using metal funnel, with orifices 10 and 15 mm in-diameter.

The compaction behavior of the powders was measured with an Engelsmann Stampfvolumeter (JRS Pharma, Rosenberg, Germany).

Powder mixtures were mixed with a Turbula mixer (Willy A. Bachofen Maschinenfabrik, Basel, Switzerland) for 8 min + 2 min after the addition of the lubricant, with 50 rpm.

Table 1. Powder Mixtures

Sample	Vivapur 102 (g)	Pearlitol SD 200 (g)	Magnesium Stearate (g)
S1	90	10	1
S2	70	30	1
S3	50	50	1
S4	30	70	1
S5	10	90	1

A Korsch EK0 eccentric tablet machine (E. Korsch Maschinenfabrik, Berlin, Germany) mounted with strain gauges and a displacement transducer was applied to compress the powder mixtures with flat punches, 8 mm in diameter, with a bell shaped bisecting line 1 mm wide and 0.2 mm deep on the upper punch.. The air temperature was 22–25°C at a relative humidity of 57–65%. The tablet mass was 0.18 g and the compression rate was 36 tablets/min.

The hardness of the tablets was measured with a Heberlein tablet hardness tester (Heberlein & Co. AG, Switzerland), and the breaking force required to break the tablets in half was determined with a laboratory-constructed apparatus (Fig. 2), with tool, three-bend tablet hardness testing. The tablet is centered under the breaking tool, which moves vertically down. The load is detected with a computer-connected measuring cell placed under the sample holder.

The results were analyzed with the Neural Network module of StatSoft Statistica 6.1 software (StatSoft, Inc., Tulsa, OK). Fifteen experimental data sets were acquired, based on an extended experimental design. The data on 20 tablets were recorded with each settings, which resulted in a 300-member data matrix. One hundred fifty cases were selected to teach the ANNs. The 150 cases were divided randomly to training, selection and test sets, containing 100, 25, and 25 cases respectively. Selection set is dedicated for the internal validation of the prediction performance during the training, meanwhile test set is for internal validation after the training. Fifty other cases were used for the external validation of the prediction performances of the different ANNs.

The amounts of the two materials and the compression force were used as input variables; and parameters describing the compression process (elastic recovery, lubrication, plasticity, etc.) and postcompression parameters (tablet hardness, true density and breaking into halves) were investigated as outputs. All parameters were handled as regression problems. In classification problems the training cases must represent the original distribution of the samples, but in our case the distribution of the results of subdivision was not normal, and the different range width of the classes of acceptance caused fatal problems in the predictions, handled it as classification problem.

The prediction performance of the different models was compared with the nonparametric

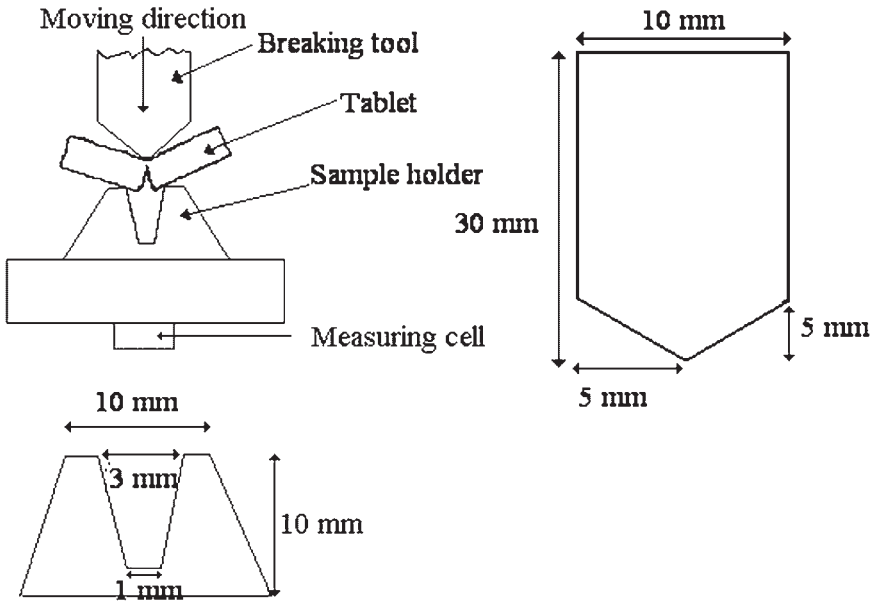

Figure 2. Schematic outline of the self-developed hardness tester.

Kruskal–Wallis test, with the use of post-hoc comparisons. The statistical analysis was performed with StatSoft Statistica 8 software.

RESULTS AND DISCUSSION

Preformulation Results

The aim of the present work was to study how the physicochemical properties of binary powder mixtures determine the mechanical strength and subdivision of scored tablets. Two widely used pharmaceutical excipients, a grade of MCC, widely used as a dry binder in direct compression, and a filler material SDM was chosen, with well characterized properties. The anisometric particles of the MCC had a mean length of 75 μm, and some aggregates were observable. This small particle size is associated with a large surface area and high cohesivity, which results in poor flow properties (Tab. 2). Especially the results measured with a metal funnel, with a 10-mm orifice but also those with a 15-mm orifice were acceptable, but not excellent.[18] In contrast, spray dried mannitol (SDM) (which is composed of isometric particles with a mean particle size of 63 μm, containing holes resulting from the spray-drying production method), exhibits good flow properties even with the 10-mm diameter orifice. The isometric particles result in a better arrangement, and a much higher bulk density than for MCC.

The behavior of these two materials also differed during compaction. The testing of the rearrangement of the particles was based on the bulk and tapped densities. The particles of MCC display an exponential rearrangement profile[19] during the compression phase (Tab. 3). This means that the rearrangement in the die is

Table 2. Flow Properties of Materials

Orifice Diameter (mm)	Time (s)	Angle (°)	Weight (g)	Volume (mL)	Density (g/mL)
Vivapur102					
10	n.m.	n.m.	n.m.	n.m.	n.m.
15	4.9 (±0.58)[a]	31.7 (±0.50)	31.6 (±1.46)	80.9 (±0.29)	0.391 (±0.0046)
Pearlitol SD 200					
10	8.8 (±0.60)	27.0 (±1.57)	40.1 (±4.54)	67.0 (±0.5)	0.601 (±0.0373)
15	3.1 (±0.06)	22.8 (±0.26)	40.0 (±0.70)	55.0 (±0.44)	0.727 (±0.0012)

n.m., not measurable.
[a](±SD).

Table 3. Compaction Properties of Bulk Materials

Compaction Behavior	Vivapur 102	Pearlitol SD 200
Hausner factor	1.37	1.12
Carr index	26.76	10.40
Compactibility	34.86	117.27
Cohesiveness	2.93	0.92
Rearrangement	Exponential	Linear

initially fast, but the resistance then increases. Hence, the cohesiveness between the particles is high. In contrast, SDM has a linear rearrangement profile, which means that the rearrangement of the particles during compression is constant. This is associated with low cohesiveness, which results in low binding forces between the particles.

The properties of the powder mixtures changed appreciably on variation of the composition. At 90:10 SDM/MCC, the lubricated powder mixture exhibits better properties than those of unlubricated SDM (Fig. 3). The outstanding compactibility of this mixture might be due to the very uniform arrangement of the isometric particles.

ANN Analysis

In the first step, the data were modeled *via* the linear ANN as reference. The average observed versus the predicted correlation coefficient (based on external validation results) was <0.5, which suggests the poor learning ability of this ANN. The result of the Kruskal–Wallis test showed, that the prediction performance of the GRNN was statistically the same ($p > 0.05$) as those of the linear model. The software offers a possibility to reduce the number of radial neurons, and build a new network with the retaining of the other settings of the GRNN. The performance did not improve on reduction of the number of radial neurons from 100 to 15, the number corresponding to the number of experimental data sets, which resulted in a simpler network structure. Change of the assignment of the radial neurons from random sampling to K-means clustering did not lead to an improvement either.

In contrast, the RBF networks furnished statistically significant better prediction results. The average values of the observed versus the predicted correlation coefficients were higher and the SDs were smaller than in the number of cases discussed above. The number of neurons was set to the same value as the outputs. The statistical analysis did not reveal any significant differences between the results acquired with different settings of the RBF ANN, but the average correlation coefficient reached a value of 0.8 only when K-means sampling was used for radial assignment and the K-nearest neighbors value for radial spread was set to 10.

As discussed above, the determination of the optimal structure of MLPs is more difficult than for other ANNs. In the present study, one hidden layer was used, and the number of hidden neurons was varied between 5 and 12, corresponding with all the above discussed recommendations. Five algorithms (standard back-propagation, quick-propagation, Delta-bar-Delta, conjugate gradient descent and quasi-Newton) were tested to teach

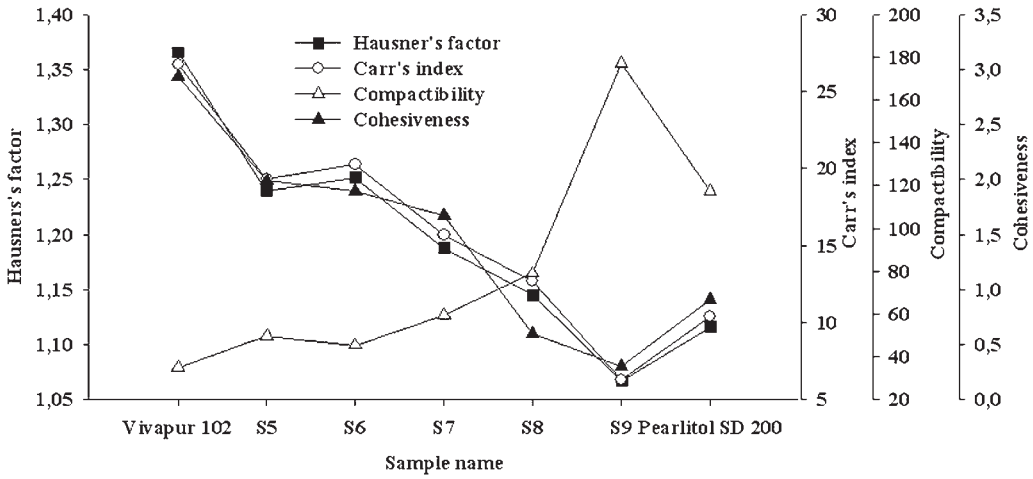

Figure 3. Flowing and compaction properties of powder mixtures.

the ANNs. The maximal number of learning cycles (epochs) was set to 10,000 during training, which stopped when the error of the selection set increased by 0.001 in a 10 epochs window. These settings seemed to be the most appropriate to prevent the networks from over-fitting. Networks taught with the conjugate gradient descent and quasi-Newton algorithms alone, displayed poor prediction ability. The other algorithms yielded significantly better results, with no significant difference between them. However, because of the smaller SD and faster convergence, the use of quick-propagation or Delta-bar-Delta is recommended. Similarly, no significant difference was observed on change of the number of hidden neurons, but there was a tendency to need for a higher learning rate as the neuron number was increased. Overall the MLP models afforded statistically the same results as the RBF networks, but the best correlation coefficient ($R^2 = 0.87$) was achieved with a MLP with 12 hidden neuron taught with the Delta-bar-Delta algorithm, at a learning rate of 0.01. Furthermore, this model provided the most uniform achievement as regards the prediction of different parameters (Fig. 4). For these reasons, this model was used in the further investigations.

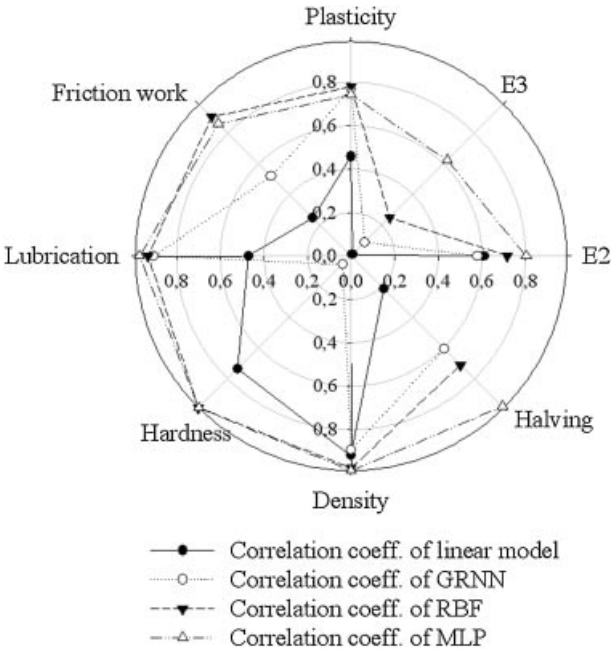

Figure 4. Prediction ability of ANNs based on observed versus predicted correlation coefficients.

Compression Process

We modeled the results of the calculated parameters for the whole concentration range with the help of ANNs. The results of the compression process indicated that all the powder mixtures were well compressible. As revealed by the preformulation data, SDM improved the properties of the powder mixtures during the compression: the plasticity increased, and the elastic recovery decreased at a higher SDM quantity (Fig. 5a and b). At above 50%, however, the effect of SDM decreased, because the positive effects of MCC were no longer manifested. The lubrication coefficient was above 0.8 for all samples and compression forces. Thus, 1% magnesium stearate was sufficient for the lubrication of the powder mixtures (Fig. 5c). It was also observed, that the tablet hardness and the density decreased (Fig. 5e and f). One possible explanation of this may be that the regular shape and low moisture content of SDM lead to very low cohesiveness, which impairs the interparticulate binding forces within the tablet.

Subdivision of Tablets

The postcompression testing of the subdivision of scored tablets is very important. Our study has shown that the tablet hardness, and hence the interparticulate binding forces, greatly influence the subdivision. Depending on the applied compression force and the compositions of the tablets, the breaking into halves can change considerably (Fig. 6). The tablets break well when they do not crumble, but divide into halves with closely the same mass. We accepted a $50 \pm 5\%$ tolerance range, because of the small mass of the tablets.

The stronger the interparticulate bonding and the elastic behavior of tablets after compression, the better the breaking into halves. The best breaking properties were displayed with 90% MCC, at a compression force of 15 kN. At this composition, the similarity of the masses of the tablet halves was within the tolerance limits (Tab. 4a). However, the hardness of these tablets was >200 N, which makes it difficult to break these tablets by hand. For practical reasons, a tablet hardness of ~100 N is optimal. Figure 7a depicts the breaking curve of a well-halved tablet. It can be seen that the loading causes stress in the tablet, with elastic deformation and a clean break at the limit value. After the breaking of the tablet, the curve collapses sharply. A high quantity of

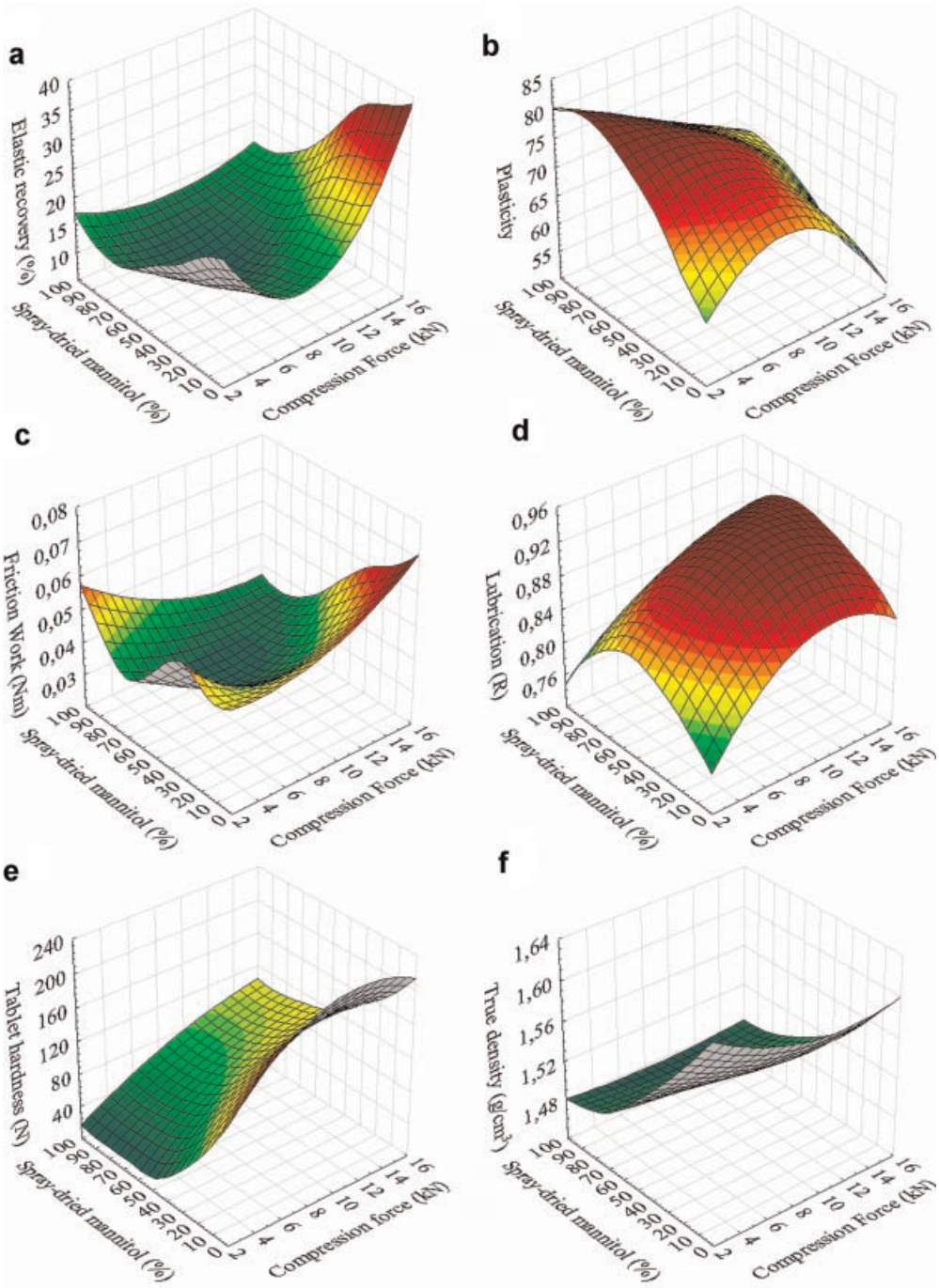

Figure 5. Response surfaces of the tableting parameters (elastic recovery (a), plasticity (b), lubrication (c), friction work (d), tablet hardness (e), and true density (f)) as functions of the amount of SDM and the compression force.

SDM and a high compression force make the structure of the tablets rigid; the elastic properties decrease, and hence the deformation in response to the breaking force causes breaking in several steps. In this case, decrease of the compression force strongly decreases the tablet hardness, which leads to crumbling of the tablet halves. Furthermore, at low hardness, tablets can break into more than two pieces, with the result of some extra forces acting not on the bisecting line. These

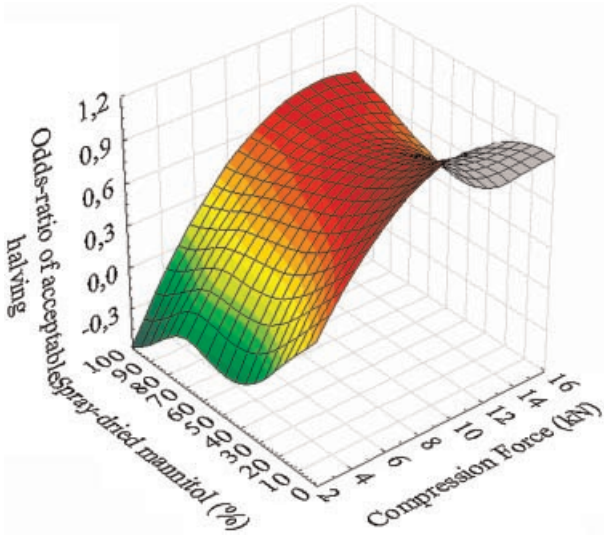

Figure 6. Response surface for the subdivision of tablets.

forces appear in the breaking curve as secondary peaks, as displayed in Figure 7b. In these cases, the similarity of the masses of the tablet halves is often outside the limits, or the loss of mass is so high that the result is unacceptable (Tab. 4b and c). Examination of the compression process demonstrated (Fig. 5c and d) that the friction work and the lubrication were associated with the best performance at 50 mass% of SDM, and a compression force of 10 kN. The structure of these tablets also results in good breaking properties, and the lower tablet hardness suggests that they would be useful in practice.

CONCLUSIONS

The present study related to the subdivision of directly compressed binary powder mixtures. It is

Table 4. Results of Subdivision of Tablets With Different Compositions

Tablet Number	% of Tablet Mass: First Half	% of Tablet Mass: Second Half	% Loss of Tablet Mass
a: Vivapur 102 90%, Pearlitol SD 200 10% 15 kN			
1	54.14	45.86	0.00
2	51.09	48.96	−0.06
3	52.53	47.50	−0.03
4	52.51	47.27	0.22
5	53.11	46.67	0.22
6	51.03	48.52	0.45
7	50.20	49.80	0.00
8	50.32	49.59	0.08
9	51.70	48.30	0.00
10	55.60	44.18	0.23
Mean	52.22	47.67	0.11
SD	1.72	1.75	0.16

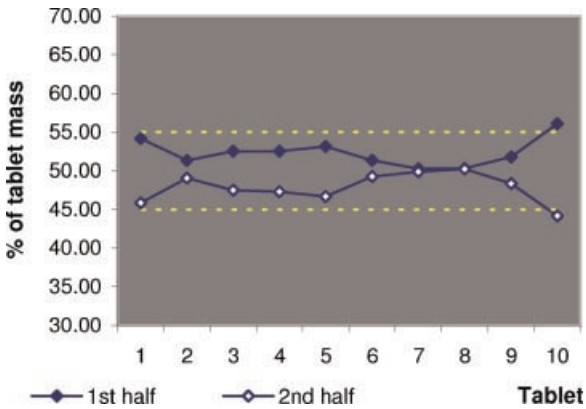

(*Continued*)

 DOI 10.1002/jps

Table 4. (*Continued*)

Tablet Number	% of Tablet Mass: First Half	% of Tablet Mass: Second Half	% Loss of Tablet Mass
b: Vivapur 102 30%, Pearlitol SD 200 70% 15 kN			
1	56.25	43.69	0.06
2	55.65	44.32	0.03
3	59.19	40.56	0.25
4	58.28	41.53	0.19
5	51.27	48.18	0.55
6	54.35	45.46	0.19
7	56.79	43.05	0.17
8	55.98	43.93	0.08
9	53.20	46.82	−0.03
10	50.96	49.07	−0.03
Mean	55.19	44.66	0.15
SD	2.75	2.75	0.17

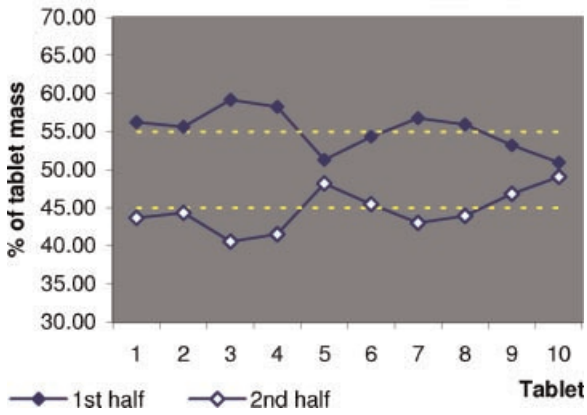

c: Vivapur 102 10%, Pearlitol SD 200 90% 15 kN			
1	52.38	47.29	0.33
2	52.65	31.20	16.15
3	51.22	34.57	14.21
4	56.02	43.81	0.17
5	46.11	38.87	15.02
6	52.02	32.74	15.24
7	55.60	43.91	0.50
8	49.23	33.59	17.18
9	56.06	33.42	10.52
10	68.25	30.40	1.35
Mean	53.95	36.98	9.07
SD	5.92	6.05	7.50

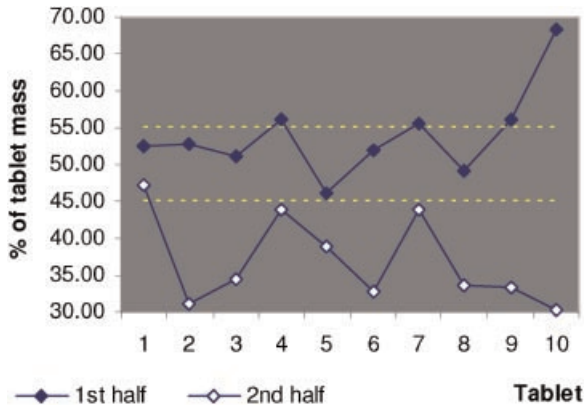

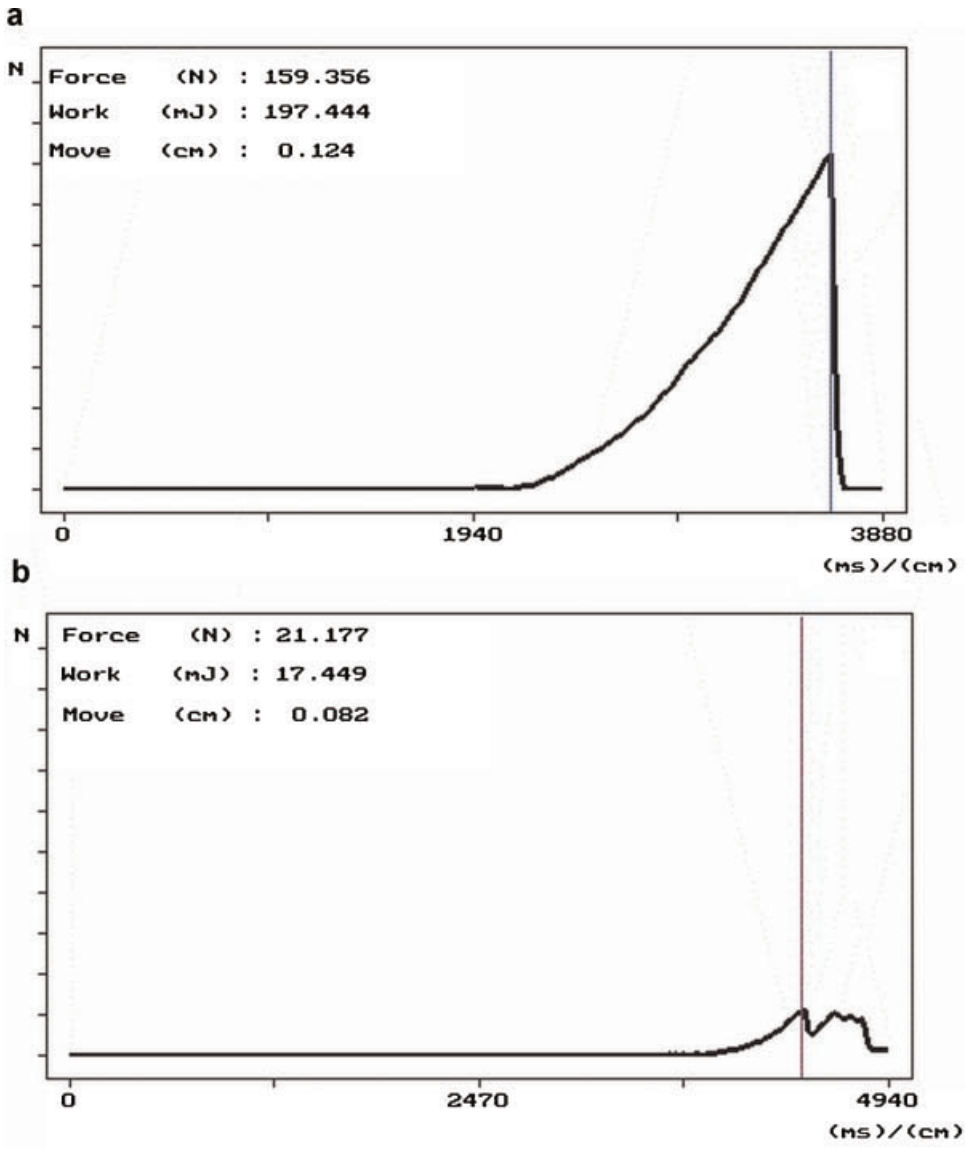

Figure 7. Breaking curve of a well-halved (a), and a not well-broken (b) tablet.

very important to study which parameters can influence the breaking properties of tablets, because the novel guidelines of the EU require verification of the equal masses of the tablet halves. The observations and the results of analysis indicated that the subdivision of tablets is greatly influenced by the properties of the raw materials. In a comparison of the different ANNs, the linear and GRNN models exhibited an inadequate prediction performance, whereas the predictions of the RBF and MLP models were suitable for the analysis of the compression and postcompression parameters. The results of these models demonstrated that mixtures containing $<50\%$ SDM compressed at >10 kN are suitable for the production of scored tablets. However, further investigations are required to clarify how many API can be added to these mixtures without dramatic changes in the main parameters.

ACKNOWLEDGMENTS

This work was supported by a Sanofi-Aventis scholarship.

REFERENCES

1. Bourquin J, Schmidli H, Hoogevest P, Leuenberger H. 1997. Application of artificial neural networks (ANNs) in the development of solid dosage forms. Pharm Dev Technol 2:111–121.

2. Bourquin J, Schmidli H, Hoogevest PV, Leuenberger H. 1997. Basic concepts of artificial neural networks (ANN) modeling in the application to pharmaceutical development. Pharm Dev Tech 2:95–109.
3. Bourquin J, Schmidli H, Hoogevest PV, Leuenberger H. 1998. Comparison of artificial neural networks (ANN) with classical modeling techniques using different experimental designs and data from a galenical study on a solid dosage form. Eur J Pharm Sci 6:287–300.
4. Bourquin J, Schmidli H, Hoogevest P, Leuenberger H. 1998. Advantages of artificial neural networks (ANNs) as alternative modeling technique for data sets showing non-linear relationships using data from a galenical study on a solid dosage form. Eur J Pharm Sci 7:5–16.
5. Bourquin J, Schmidli H, Hoogevest P, Leuenberger H. 1998. Pitfalls of artificial neural networks (ANNs) modeling technique for data sets containing outlier measurements using a study on mixture properties of a direct compressed dosage form. Eur J Pharm Sci 7:17–28.
6. Plumb AP, Rowe RC, York P, Doherty C. 2002. The effect of experimental design on the modeling of a tablet coating formulation using artificial neural networks. Eur J Pharm Sci 16:281–288.
7. Plumb AP, Rowe RC, York P, Brown M. 2005. Optimisation of the predictive ability of artificial neural network (ANN) models: A comparison of three ANN programs and four classes of training algorithm. Eur J Pharm Sci 25:395–405.
8. Golub GH. 1965. Numerical methods for solving least squares problems. Numer Math 7:206–216.
9. Chan TF. 1982. An improved algorithm for computing the singular value decomposition. ACM T Math Software 8:872–883.
10. Hruschka H, Natter M. 1999. Comparing performance of feedforward neural nets and K-means for cluster-based market segmentation. Eur J Oper Res 114:346–353.
11. Specht DF. 1991. A general regression neural network IEEE T. Neural Netw 2:568–576.
12. Yazici G, Polat Ö, Yildirim T. 2006. Genetic optimizations for Radial Basis Function and General Regression Neural Networks. MCIAI 2006, LNAI 4293, 348–356.
13. Kohonen T, Lehtiö P, Rovamo J, Hyvärinen J, Bry K, Vainio L. 1977. A principle of neural associative memory. Neuroscience 2:1065–1076.
14. Rumelhart D, Hinton G, Williams R. 1986. Learning representations by backpropagation errors. Nature 323:533–536.
15. Ghaffari A, Abdollahi H, Khoshayand MR, Soltani Bozchalooi I, Dadgar A, Rafiee-Tehrani M. 2006. Performance comparison of neural network training algorithms in modeling of bimodal drug delivery. Int J Pharm 327:126–138.
16. Yu G, Zhao Y, Wei Z. 2007. A descent nonlinear conjugate gradient method for large-scale unconstrained optimization. Appl Math Comput 187:636–643.
17. Sun Y, Peng Y, Chen Y, Shukla AJ. 2003. Application of artificial neural networks in the design of controlled release drug delivery systems. Adv Drug Deliver Rev 55:1201–1215.
18. Wells JI. 1988. Pharmaceutical Preformulation: The physicochemical properties of drug substances. Ellis Horwood Ltd. Chichester, pp. 209–211.
19. Carstensen JT. 1980. Solid pharmaceutics: mechanical properties and rate phenomena. Academic Press, Inc. New York, pp. 188–190.

II

AAPS PharmSciTech, Vol. 10, No. 2, June 2009 (© 2009)
DOI: 10.1208/s12249-009-9225-2

Research Article

Comparison of the Halving of Tablets Prepared with Eccentric and Rotary Tablet Presses

T. Sovány,[1] P. Kása Jr.,[1] and K. Pintye-Hódi[1,2]

Received 17 December 2008; accepted 1 March 2009; published online 21 April 2009

Abstract. The aim of this study was to compare the densification of powder mixtures on eccentric and rotary tablet presses and to establish relationships with the halving properties of the resulting scored tablets. This is an important problem because the recent guidelines of EU require verification of the equal masses of tablet halves. The models of Walker, Heckel, and Kawakita were used to describe the powder densification on the two machines. The calculated parameters revealed that the shorter compression cycle of rotary machines results in poorer densification and lower tablet hardness at a given compression force. This is manifested in poorer halving properties, which are influenced mainly by the hardness. Better densification improves the halving even at lower tablet hardness. This demonstrates that these parameters can be good predictors of tablet halving properties.

KEY WORDS: direct compression; halving; Heckel analysis; Kawakita analysis; Walker analysis.

INTRODUCTION

Tablets are the most common dosage form in medicine. For the individual therapy of patients, it is important to vary the dose. In the pharmaceutical industry, this problem is often solved through the production of scored tablets. A difficult problem associated with the use of such tablets is to ensure their breaking into equal halves. This is a multi-factorial problem, the solution of which must be verified in accordance with the EU guidelines.

Numerous parameters can influence the structure of tablets, and this in turn exerts effects on the breaking. The properties of the compressed materials, the shape of the punches, and the type of the tablet press, for instance, all influence the halving properties. Powder densification is not achieved in a uniform manner with the different tablet presses: With eccentric machines, only the upper punch is active during the compression, whereas with rotary presses, both punches penetrate in the die, and the compression time is shorter as compared with eccentric presses. For both types of machines, the measurement of axial forces is relatively easy through the application of strain gauges; however, the determination of the displacement is easier with eccentric machines because it is influenced only by the movement of the upper punch. The productivity of eccentric machines is much less than that of rotary machines, so they are not use in industrial production. However, the deformation and densification properties of materials can be studied very well with these presses, and it is therefore very important to establish relationships between the densification performances of the machines and to predict the behavior of materials on rotary presses.

In the past century, many different models have been proposed with which to describe the densification of materials during compression. The first model was developed by Walker (1), whose analysis is based on the reduction in volume of the powder bed as a function of the logarithm of the applied compression force.

The model devised by Heckel (2,3) is based on the theory that there is a linear relationship between the behavior of materials and the compression force during the compaction and thus between the densification and the pressure. Despite some critical observations (4), this model is probably the most widely used in pharmaceutical technology (5–8), often in comparison with other models (9–12), such as the Kawakita equation, developed 10 years later (13,14). In this latter model, the volume reduction at the applied pressure is described as a function of the pressure. In most of the publications, the data measured in the die are used in the calculations. Busignies *et al.* (15) studied the compaction behavior of granular lactoses, comparing the results of the Heckel equation measured with in-the-die method with those calculated from the properties of the ejected tablets, i.e., with the out-of-the-die method. In our study, we have also used this latter model to compare the densification on eccentric and rotary presses, for which Palmieri *et al.* (16) applied the in-the-die-method.

MATERIALS AND METHODS

Binary mixtures of microcrystalline cellulose (Vivapur 102, J. Rettenmeier & Söhne, Germany) and spray-dried mannitol (Pearlitol SD 200, Roquette Pharma, France),

[1] Department of Pharmaceutical Technology, University of Szeged, Eötvös str. 6, Szeged, 6720, Hungary.
[2] To whom correspondence should be addressed. (e-mail: klara.hodi@pharm.u-szeged.hu)

lubricated by the addition of 1% of magnesium stearate (Ph. Eur.), were compressed (Table I).

The powders were mixed with a Turbula mixer (Willy A. Bachofen Maschienenfabrik, Switzerland; 8 min+2 min after the addition of the magnesium stearate, 50 rpm).

The flow properties of the materials and mixtures were determined with a PharmaTest PTG-1 powder rheological tester (Pharma Test Appartebau, Germany).

The compaction behavior of the materials was tested with an Engelsmann stampfvolumeter (JRS Pharma, Germany).

A Korsch EK0 (E. Korsch Maschienenfabrik, Germany) eccentric and a Ronchi AM8S (Officine Meccanice F.lli Ronchi, Italy) rotary tablet press mounted with strain gauges and an eccentric press with a displacement transducer of the upper punch were applied for tablet compression, with flat single punches 8 mm in diameter and with a bisecting line.

The hardness of the resulting tablets was measured with a Heberlein tablet hardness tester (Heberlein & Co. AG, Switzerland).

For measurement of the force required to break the tablets into halves, a laboratory-constructed hardness tester was utilized (Fig. 1), using three-bend tablet hardness testing. The tablet must be centered under the breaking item, which moves vertically down. The load is detected with a computer-connected measuring cell, which is placed under the sample holder.

The true densities of powders and tablets were determined with a Quantachrome helium stereopycnometer (Quantachrome GmbH., Germany).

RESULTS

The primary aim of this work was to study the densification behavior of binary powder mixtures of two widely used pharmaceutical excipients on eccentric and rotary tablet presses. We used the models of Walker, Heckel, and Kawakita to describe the powder densification and sought relationships with the halving properties of the tablets. The dry binder microcrystalline cellulose Vivapur 102 and the filler material spray-dried mannitol (Pearlitol SD 200) were mixed in different ratios, as indicated in Table I. The results of the preformulation tests for these materials and their mixtures are presented in Table II. The anisometric particles of Vivapur 102 (Fig. 2) exhibited poor flow properties during powder rheological tests, and this resulted in lower bulk density values. The rearrangement of the particles was irregular but took place quickly in response to tapping, giving rise to an exponential-type rearrangement profile. The results with Pearlitol indicated that this material can greatly improve the poorer properties of Vivapur. It displays excellent flow properties, and the isometric particles (Fig. 3) demonstrate

Table I. Compositions of Powder Mixtures

Sample[a]	Vivapur 102 (%)	Pearlitol SD 200 (%)
1	90	10
2	70	30
3	50	50
4	30	70
5	10	90

[a] The mixtures were lubricated by the addition of 1% Mg-stearate

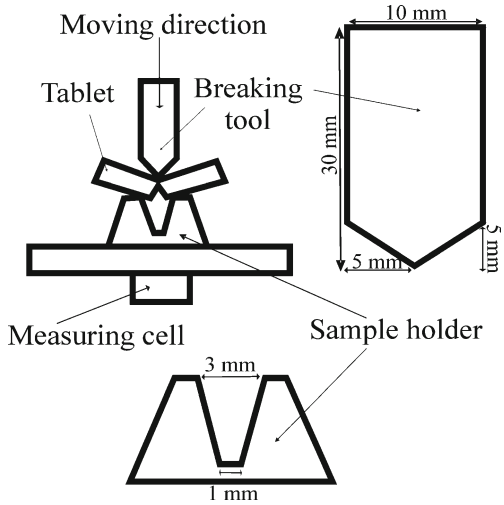

Fig. 1. Schematic figure of laboratory constructed tablet hardness tester

linear rearrangement behavior. The properties of the different powder mixtures varied between the end points of the two component materials. An increasing quantity of Pearlitol improved the compactibility of the powder, but the cohesiveness decreased, which resulted in lower inter-particulate binding forces. This may be due to a lower number of contact points between the isometric particles. These parameters were calculated from Eq. 1, described by Kawakita *et al.* (17):

$$N/C=[N/a+1/ab] \tag{1}$$

where N is the number of taps applied for powder densification, while a and $1/b$ are constants referring to the compressibility and cohesiveness, respectively. C is the volume reduction, which can be calculated via the following equation:

$$C = [(V_0 - V)/V_0] \tag{2}$$

where V_0 is the initial volume of the powder bed, and V is the current volume of the powder after a given number of taps.

Equation 1 is a modification of Eq. 3, which was proposed by Kawakita and Lüdde in 1971 to describe powder densification behavior during compression:

$$P/C = [P/a + 1/ab] \tag{3}$$

where P is the applied pressure and C is calculated according to Eq. 2, where V is now the volume of the powder bed at the applied pressure.

We determined the Kawakita constants from the data on samples compressed at 5, 10, or 15 kN, plotted according to the out-of-the-die method. The values of constant a decreased on elevation of the Pearlitol quantity, as an indication of the better rearrangement of the particles during compression, which corresponds to the preformulation data (Table III). The values of the constant a are very similar for the two tablet machines, suggesting that it depends only on the properties of the materials. In contrast, the values of $1/b$, which varied characteristically with the composition in the preformulation tests, displayed a minimum at a mass ratio of 50:50. This means that, at this ratio, the lowest energy is needed to reduce the volume of the powder to half of the original. This may be due to the better utilization of the

Table II. Preformulation Results on Materials and Mixtures

Parameter	Vivapur 102	1	2	3	4	5	Pearlitol SD 200
Flow time (s)	4.9	4.5	4.2	4.3	3.6	3.1	3.1
Angle of repose (deg)	31.7	30.1	28.8	26.7	24.8	23.5	22.8
Bulk density (g/cm^3)	0.39	0.46	0.53	0.65	0.76	0.83	0.73
Hausner factor	1.37	1.24	1.25	1.19	1.15	1.07	1.12
Carr index (%)	26.76	19.34	20.27	15.67	12.67	6.27	10.40
Compactibility	0.03	0.02	0.02	0.02	0.01	0.01	0.01
Cohesiveness	2.93	1.99	1.89	1.68	0.59	0.31	0.92

transmitted energy, which can be a result of the lower adhesion and friction of the particles on the die wall. This reduces the loss of the energy during the process, so a bigger proportion of the demanded energy is assigned to the volume reduction. Overall, the less energy investment is needed at this ratio to given volume reduction. This effect is corresponding with the results of other calculations discussed below. Figure 4 reveals that the intercepts of the plots obtained with the two machines are different: the calculated *1/b* values are two- to threefold higher for the rotary press. This suggests that the shorter compression time and the simultaneous action of the two punches result in a lower volume reduction for rotary presses at a given compression pressure. With the rotary press, a local minimum can be observed in factor *1/b* also at ratio 10:90. A possible explanation of this phenomenon can be that the different compression mechanism of the rotary press results to a better rearrangement of particles at this ratio as on eccentric press.

Optimum points are also observed in the results calculated from the Walker equations:

$$\log P = -LV + C_1 \tag{4}$$

$$100V = -W \log P + C \tag{5}$$

where P is the applied pressure, V is the relative volume, calculated as V'/V_0, *i.e.*, the ratio of the volume at the applied pressure and the initial volume of the powder bed, and C and C_1 are constants. The coefficient L is the pressing modulus, which can be calculated from Eq. 4. It likewise exhibits a maximum at a ratio of 50:50 (Table III), reflecting the smallest volume reduction at a given pressure at this ratio. This also may be due to the better utilization of the transmitted energy. As a result of the already low-energy investment, strong bonds are formed between the particles. This is supported by the small value of the coefficient W at this ratio (Table III), which shows the percentage volume reduction when the pressure changes on a logarithmic scale. Thus, the increase of the compression force causes only a minor further volume reduction because almost the biggest possible bonding forces have developed already at lower ones. A difference can be seen in the slopes of the Walker plots relating to the eccentric and rotary presses (Figs. 5 and 6).

We also used the equation developed by Heckel to acquire more information concerning the powder densification (Fig. 7):

$$\ln (1/1 - D) = KP + A \tag{6}$$

where D is the relative density of the tablet (calculated as the ratio of the apparent density of the tablet and the true density of the powder) at pressure P, while K and A are constants. The reciprocal of constant K is the mean yield pressure (P_y). Constant A gives the densification of the powder due to the

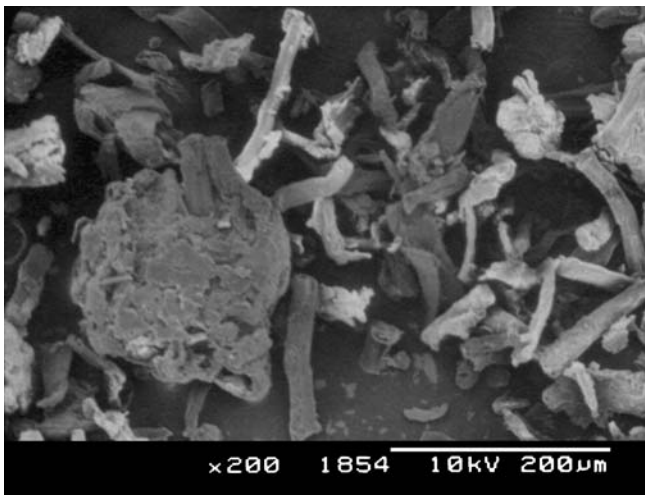

Fig. 2. SEM picture of Vivapur 102

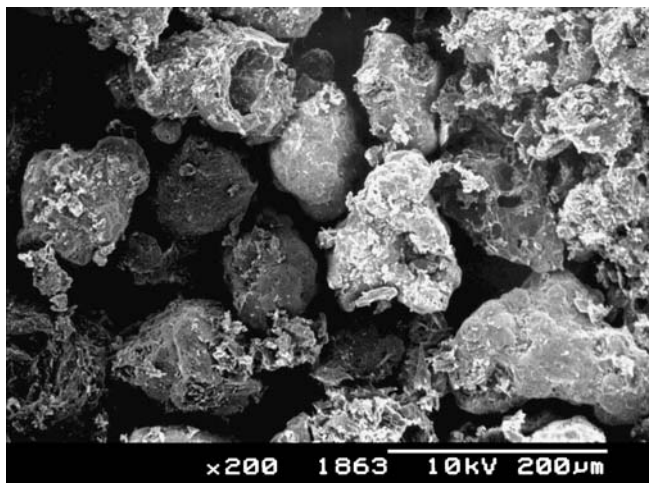

Fig. 3. SEM picture of Pearlitol SD 200

Table III. Parameters of the Different Equations Calculated from Linear Regression Analysis

	Heckel			Kawakita		Walker	
Sample	P_y	D_a	D_b	a	$1/b$	W	L
Eccentric press							
1	217.391	0.775	0.506	0.732	6.907	6.409	15.549
2	196.078	0.782	0.489	0.709	6.088	5.468	17.517
3	217.391	0.775	0.465	0.697	6.267	5.363	18.447
4	256.410	0.785	0.450	0.689	6.863	5.877	17.016
5	312.500	0.779	0.417	0.665	7.649	6.218	15.176
Rotary press							
1	232.558	0.618	0.348	0.727	15.834	14.098	6.534
2	212.766	0.615	0.322	0.701	15.685	13.776	7.116
3	263.158	0.633	0.323	0.687	10.546	9.596	10.364
4	270.270	0.657	0.322	0.691	19.531	14.164	7.035
5	277.778	0.665	0.303	0.671	17.872	14.394	6.278

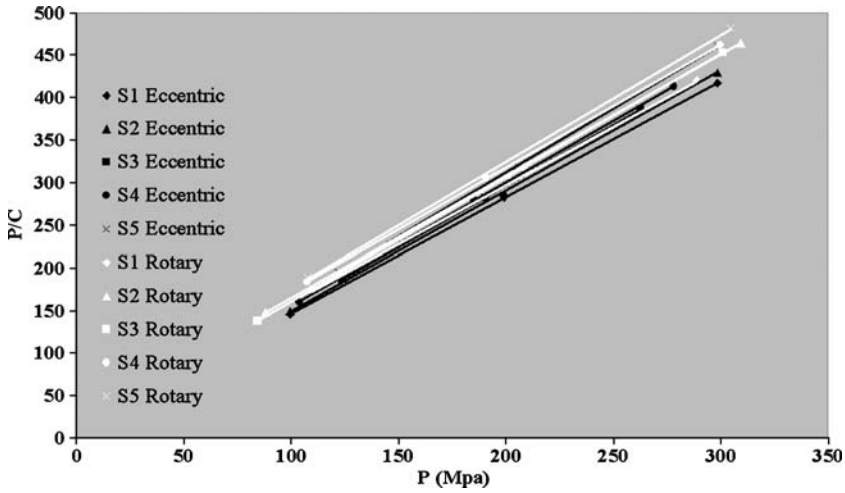

Fig. 4. Kawakita plot calculated with the out-of-the-die method

Table IV. Tensile Strengths of the Tablets (MPa)

	Compression pressure (MPa)		
Sample	100	200	300
Eccentric press			
1	3.626	5.702	6.038
2	2.384	3.759	4.642
3	1.952	2.670	3.385
4	1.168	2.020	2.861
5	1.231	2.056	2.919
Rotary press			
1	1.280	3.576	3.807
2	0.941	2.508	3.269
3	0.591	1.748	2.456
4	0.605	1.511	2.275
5	0.537	1.803	2.595

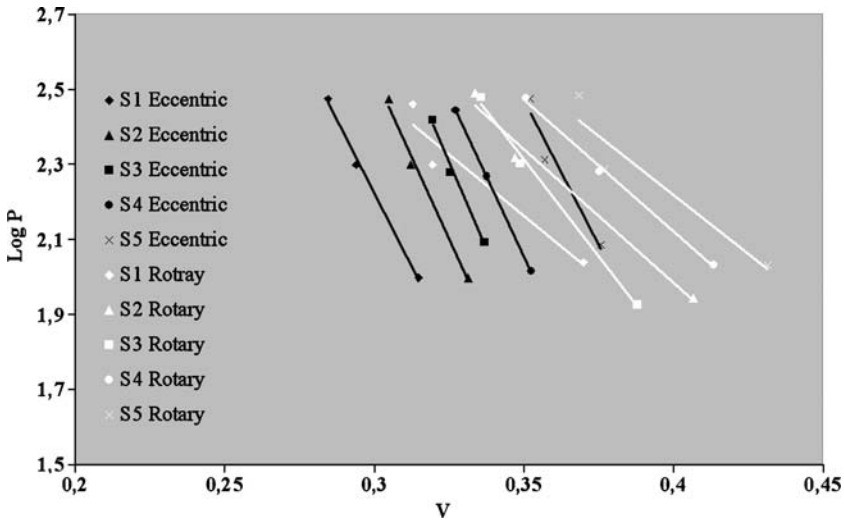

Fig. 5. Walker plot based on Eq. 4

initial rearrangement of the powder bed (D_a) according to the following equation:

$$D_a = 1 - e^{-A} \tag{7}$$

With the application of D_a, the densification due to the fragmentation of particles (D_b) can be calculated:

$$D_b = D_a - D_0 \tag{8}$$

where D_0, related to the initial die filling, is defined as the apparent density of the powder bed at zero pressure.

As compared with the other methods, Heckel analysis does not give such unanimous results (Table III). The mean yield pressure does not display a characteristic change; the differences between the machines are clear. The larger values of D_a and D_b demonstrate that a greater proportion of the particle densification is due to the initial rearrangement and particle fragmentation in the eccentric press. The differences in initial rearrangement and fragmentation may result from the differences in the method of die filling and the compression cycle.

The parameters discussed above all influence the post-compressional properties of tablets. Table IV demonstrates that the tensile strength is almost two times higher for the tablets formed with the eccentric press. It can be seen that the tensile strength decreases with increasing amount of Pearlitol, the small adhesion and cohesion forces and the fewer contact points between the particles greatly reducing the tablet hardness. This parameter is probably the most important influencing factor of the breaking. A strong relationship can be observed between tensile strength of tablets and halving properties (Table V). The results suggest that tensile strength at about 3.00 MPa is required to the acceptable halving on eccentric press, and even higher values are necessary on rotary one.

DISCUSSION

The primary aim of this study was to establish relationships between powder densification on different tablet presses and the halving properties of the resulting tablets. The calculations with the equations suggest that the longer

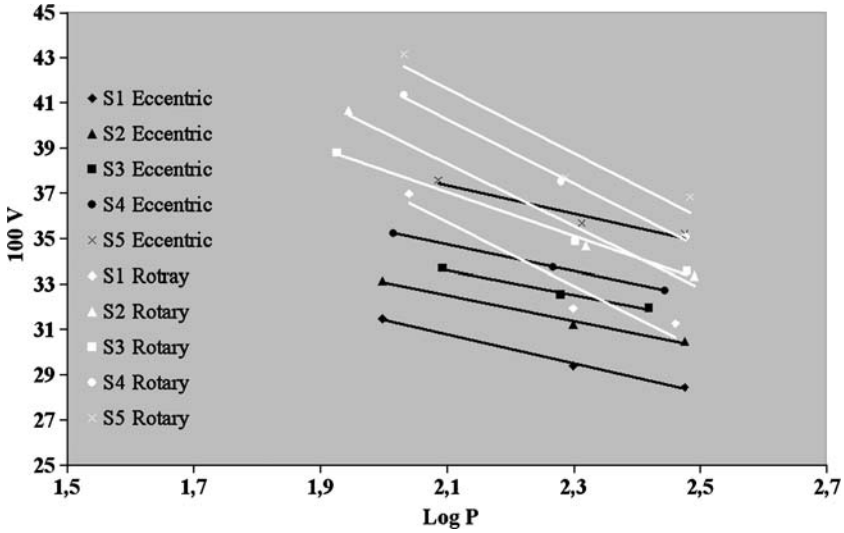

Fig. 6. Walker plot based on Eq. 5

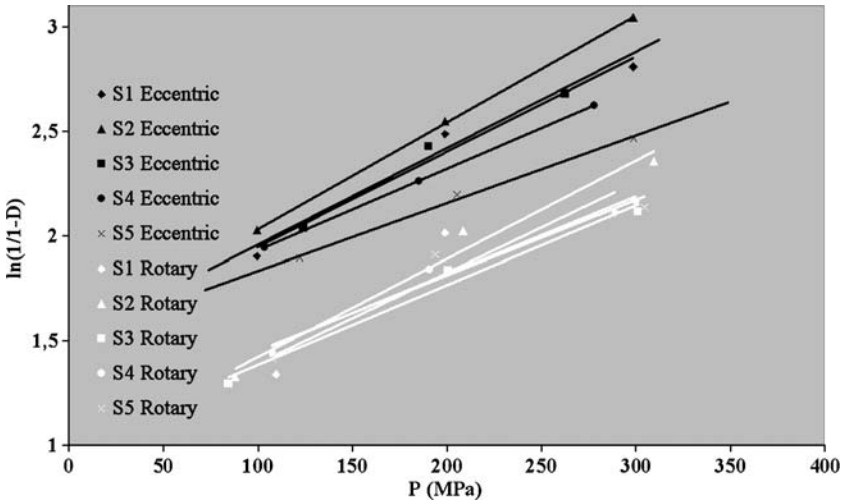

Fig. 7. Heckel plot based on the out-of-the-die method

time of compression causes a two- to threefold higher stress on use of the eccentric machine at the same compression force. This causes a greater proportion of particle fragmentation, but the bonding between particles becomes much stronger, resulting to greater hardness.

The tablet hardness and the properties of the materials are strongly related to the breaking properties of the tablets. Postcompressional examination of the halving of the scored tablets is very important because it is necessary to verify it in the pharmaceutical file. The axial stress acting on the bisecting line gives rise to elastic stresses in the tablets, resulting in different degrees of deformation, depending on the properties, deformability, and bonding of the tablets. In this case, elastic deformation is advantageous. The change in the deformation can be measured through the application of strain gauges. When the elasticity predominates, the force–time curve rises with increasing axial stress and collapses at the moment of breaking of the tablet (Fig. 8a). The tablets break well when the masses of the two halves are closely similar. We chose a 50±5% tolerance limit in this study. The breaking result depends mainly on the hardness of the tablets and was better at higher tensile strength. However, it is additionally influenced by the internal structure of the tablets.

Table V. Amounts of Well-halved Tablets

	Compression pressure (MPa)		
Sample	100	200	300
Eccentric press			
1	50%	90%	100%
2	50%	100%	60%
3	60%	100%	80%
4	50%	80%	70%
5	30%	80%	90%
Rotary press			
1	10%	30%	40%
2	0%	10%	40%
3	0%	10%	30%
4	0%	0%	0%
5	0%	0%	10%

When the tablet hardness is low or internal structural defects exist, the breaking surface crumbles or the tablets break into more than one piece. The new breaking surfaces are associated with extra stress that does not act on the bisecting line. This type of breaking often proceeds through several steps, which are seen in the curves as extra peaks (Fig. 8b). When the structure of the tablet is free from defects, a lower tensile strength may be sufficient for good breaking, as in the case of sample 3. The results allow the conclusion that the tablet hardness must be relatively high for good halving. However, when the internal structure of the tablets is free from defects, a lower hardness may be sufficient. Nevertheless, the application of a higher compression force on a rotary

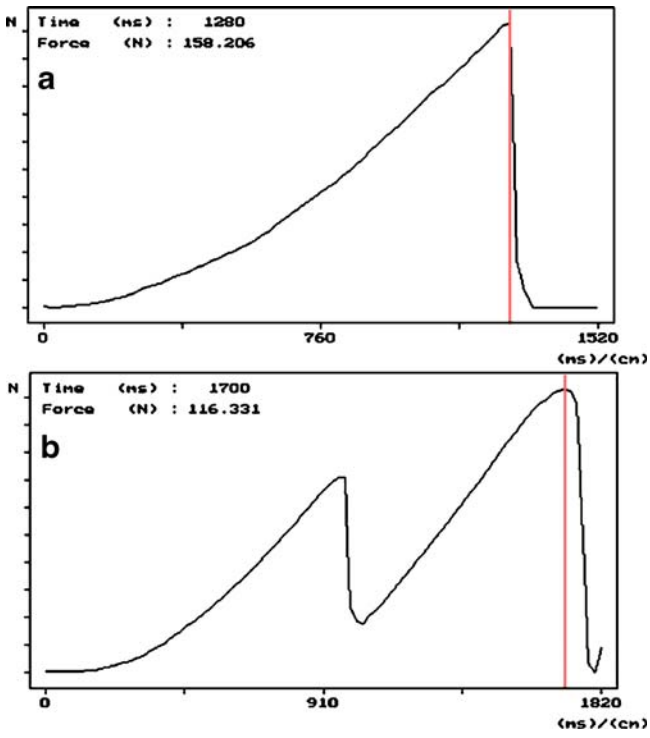

Fig. 8. Breaking curves of a well-halved (**a**) and a not-well-broken tablet (**b**)

machine is needed to equal the better results on tablets compressed on eccentric machines. No structural defects are formed during compression when the powder is well compressed and undergoes low adhesion to the die wall, and the bonding between the particles is formed quickly. The models of Walker and Kawakita describe these processes better than the Heckel model and furnish a better prediction of the halving properties. The results obtained with the Heckel equation should be utilized with caution.

CONCLUSIONS

Overall, it can be stated that the properties and the densification behavior of the powders strongly influence the halving properties of scored tablets. The relationships between the densification behavior of powders and the applied compression force can be characterized well with the use of the equations of Heckel, Walker, and Kawakita. They also can give useful information to the comparison of the behavior of materials on different tablet presses. Comparing these results, with the properties of compressed tablets, conclusions can be drawn about the probable halving properties.

ACKNOWLEDGMENT

The work was supported by a Sanofi-Aventis scholarship.

REFERENCES

1. Walker EE. The properties of powder. Part VI. The compressibility of powders. Trans Faraday Soc 1923;19:73–82.
2. Heckel RW. Density–pressure relationships in powder compaction. Trans Metall Soc AIME 1961;221:671–5.
3. Heckel RW. An Analysis of powder compaction phenomena. Trans Metall Soc AIME 1961;221:1001–8.
4. Sonnergaard JM. A critical evaluation of Heckel equation. Int J Pharm 1999;193:63–71.
5. Ilkka J, Paronen P. Prediction of the compression behaviour of powder mixtures by the Heckel equation. Int J Pharm 1993;94:181–7.
6. Kuentz M, Leuenberger H. A new model for the hardness of a compacted particle system, applied to tablets of pharmaceutical polymers. Powder Techol 2000;111:145–53.
7. Kuny T, Leuenberger H. Compression behaviour of the enzyme β-galactosidase and its mixture with microcrystalline cellulose. Int J Pharm 2003;260:137–47.
8. Rees JE, Grant DJ. Influence of elastic deformation of particles on Heckel analysis. Pharm Dev Technol 2001;6:193–7.
9. Patel S, Kaushal AM, Bansal AK. Effect of the particle size and compression force on compaction behavior and derived mathematical parameters of compressibility. Pharm Res 2006;24:111–24.
10. Sonnegaard JM. Impact of particle density and initial volume on mathematical compression models. Eur J Pharm Sci 2000;11:307–15.
11. Patel S, Kaushal AM, Bansal AK. Compaction behavior of roller compacted ibuprofen. Eur J Pharm Biopharm 2008;69:743–9. doi:10.1016/j.ejpb.2008.01.005
12. Denny PJ. Compaction equations: a comparison of the Heckel and Kawakita equations. Powder Technol 2002;127:162–72.
13. Kawakita K, Lüdde KH. Some considerations on powder compaction equations. Powder Technol 1971;4:61–8.
14. Kawakita K, Hattori KI, Kishigami M. Charactheristic constants in Kawakita's powder compression equations. J Powder Bulk Solids Technol 1977;1:3–8.
15. Busignies V, Tchoreloff P, Leclerc B, Besnard M, Couarraze G. Compaction of crystallographic forms of pharmaceutical granular lactoses. I. Compressibility. Eur J Pharm Biopharm 2004;58:569–76.
16. Palmieri GF, Joiris E, Bonacucina G, Cespi M, Mercuri A. Differences between eccentric and rotary tablet machines in the evaluation of powder densification behaviour. Int J Pharm 2005;298:164–75.
17. Yamashiro M, Yuasa Y, Kawakita K. An experimental study on the relationships between compressibility, fluidity and cohesion of powder solids at small tapping numbers. Powder Technol 1983;34:225–31.

III

Research Article

X-RAY Spectrometry

Received: 13 January 2009 Revised: 17 June 2009 Accepted: 2 July 2009 Published online in Wiley Interscience: 11 August 2009

(www.interscience.com) DOI 10.1002/xrs.1205

X-ray computed microtomography for determination of relationships between structure and breaking of scored tablets

T. Sovány,[a] P. Kása Jr,[a] K. Vakli[b] and K. Pintye-Hódi[a]*

This paper reports on the relationship between the structure and halving properties of scored tablets. The results of the density measurements and structure determination by X-ray computed microtomography revealed that this analytical technique is very suitable for the investigation of porous structures and aggregates thanks to its noninvasive character. The results of the analyses show that besides various porosities also big differences exist in the arrangement of the particles inside the comprimates. These basic qualitative differences in the structure of tablets prepared with different tablet presses greatly influence their breaking, and must be taken into consideration during the production of dosage forms. Copyright © 2009 John Wiley & Sons, Ltd.

Introduction

The scored tablet is a widely used solid dosage form which combines the advantages of tablets (e.g. easy administration and stability) with dose flexibility.[1] This is very advantageous, particularly in pediatrics. However, very accurate breaking into halves is required to ensure the safe blood levels of the drug, in accordance with the guidelines of the drug authorities, which prescribe verification of the correct halving of scored tablets.

Such halving is a considerable problem in the pharmaceutical field,[2] but is a poorly studied topic in pharmaceutical technology. The halving properties depend greatly on the composition of the applied powder mixtures and the compression process.[3,4] These factors strongly influence the internal structure of the tablet, which governs its halving.

Two main problems can occur during the halving of tablets: breaking into halves with different masses and loss of mass (Fig. 1). Both problems are strongly linked with the internal structure of the tablets. Porosity and hardness seem to be good indicators of the prospective halving properties, but it is preferred to know the general density and force distribution inside the tablet. These parameters are determined by the material properties (which determine the type and strength of bonding at a given stress) and by the processes that occur during compression (which determine the stress acting on the powder).

The current analytical method for the measurement of tablet porosity is gas adsorption porosimetry. This is a useful, noninvasive method for determination of the skeletal density of the sample, but cannot provide appropriate information concerning the real structure. For hardness determination, the pharmacopeial method or three-bend hardness testing is widely used; these are useful, but destructive methods. Some authors have attempted to determine tablet hardness with spectroscopic methods, but the result depends appreciably on the penetration of the waves into the sample.[5] For samples with a high capping tendency, which usually contain significant structural defects, this method generally overestimates the real hardness of the sample. Hardness measurements can be combined with microscopic methods for study of the tablet or the breaking surface, but this method is also inappropriate for structure determination, because of the potential destruction of the sample.

X-ray computed microtomography (micro CT) is a rapid and noninvasive technique which can demonstrate the particle arrangement inside the tablet, and furnish useful information concerning its structure.[6,7] The theoretical background of this method is that X-rays are attenuated via absorption and/or scattering as they pass through a sample. From such the radiation attenuation, two-dimensional gray-scale projections of the sample can be detected, and the overall combination of these projection furnishes three-dimensional information. By repetition of this while the sample is rotated, the three-dimensional structure can be reconstructed from the data on the two-dimensional shadow images by means of a special algorithm.[7] The density distribution in scored tablets with different shapes was studied earlier and conclusions were drawn as regards the halving.[8] However, the effects of different compaction processes of the two main types of tablet presses on the tablet structure have not been investigated previously. The aim of the present paper, therefore, was thus to acquire information via micro CT on the qualitative differences in structure and density distribution of tablets with a given shape prepared with different tablet presses.

Materials and Methods

The tablets were compressed from a 1 : 1 binary mixture of two widely used pharmaceutical excipients, microcrystalline cellulose (Vivapur 102, J. Rettenmeier & Söhne, Germany) and spray-dried

* *Correspondence to: K. Pintye-Hódi, Department of Pharmaceutical Technology, University of Szeged, Eötvös u. 6., H-6721 Szeged, Hungary. E-mail: klara.hodi@pharm.u-szeged.hu*

a *Department of Pharmaceutical Technology, University of Szeged, H-6720, Eötvös u. 6., Szeged, Hungary*

b *Joó Katalin Analytical Trading and Supporting Ltd. H-2131, Alkotmány u. 7., Göd, Hungary*

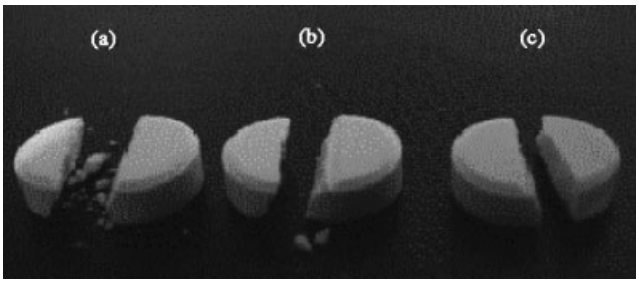

Figure 1. Pictures of a tablet with a crumbled breaking surface (a), a tablet broken into uneven halves (b), and an acceptably well-broken tablet (c).

Figure 2. Tablet hardness tester.

mannitol (Pearlitol SD 200, Roquette Pharma, Italy), lubricated by the addition of 1% magnesium stearate (Ph. Eur.).

A Turbula mixer (Willy A. Bachofen Machienenfabrik, Switzerland) was applied for 8 min to prepare the 1 : 1 powder mixture, and for 2 min after the addition of the lubricant, at 50 rpm.

Round and flat scored tablets with a diameter of 8 mm were compressed on a Korsch EK0 (E. Korsch Machienenfabrik, Germany) eccentric press or a Ronchi AM8S (Officine Meccanice F.lli Ronchi, Italy) rotary tablet press at compression forces of 5 and 15 kN. Eccentric presses are batch-type machines, where only the upper punch is active during the compression phase, with a relatively long compression time. In contrast, rotary presses operate in continuous running, and both punches are active during compression, resulting in a momentary load on the powder bed. The compression force was detected with strain gauges built into the punches. The other parameters were a temperature of 24 °C, an RH of 57%, and a compression speed of 30 tablets/min. Hundred

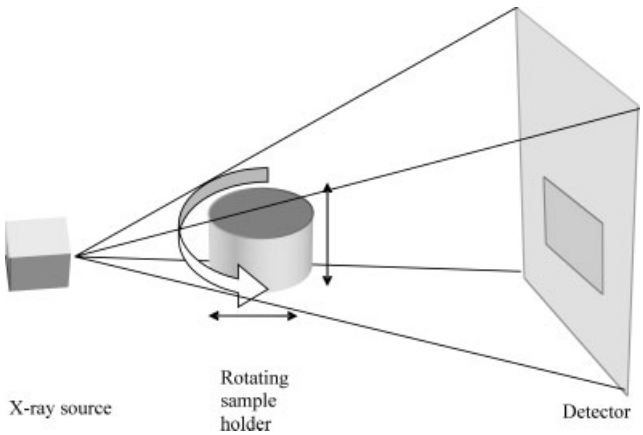

Figure 3. Schematic figure of a micro CT apparatus.

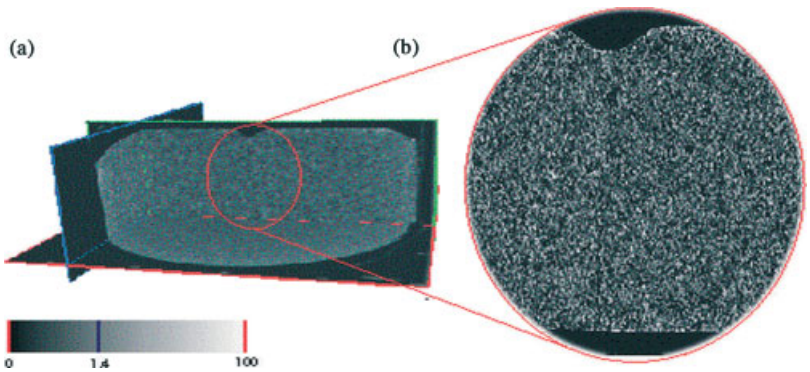

Figure 4. Density distribution in Tablet A (eccentric press, 5 kN).

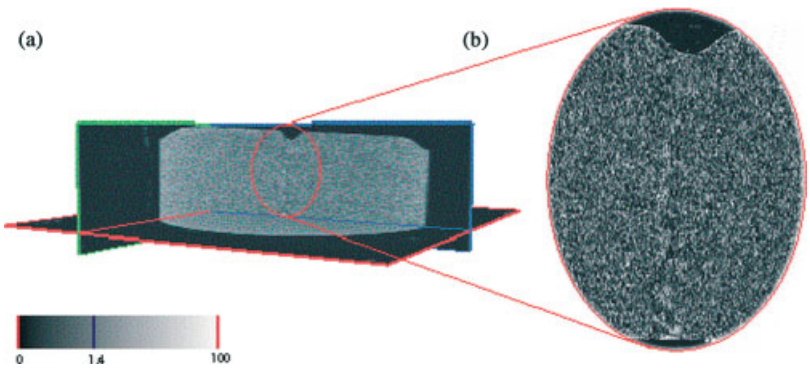

Figure 5. Density distribution in Tablet B (eccentric press, 15 kN).

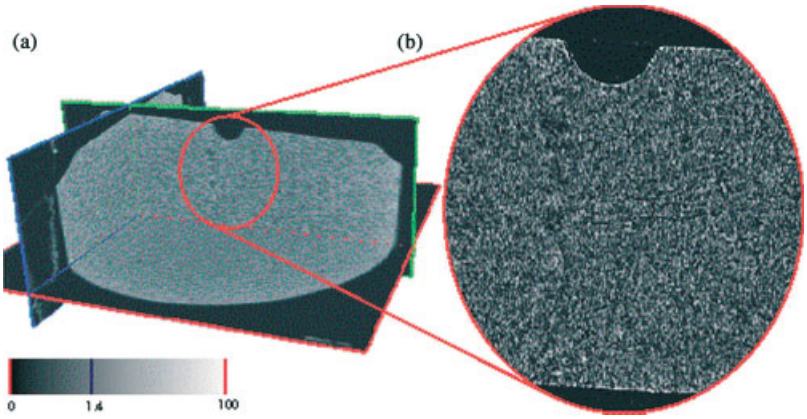

Figure 6. Density distribution in Tablet C (rotary press, 15 kN).

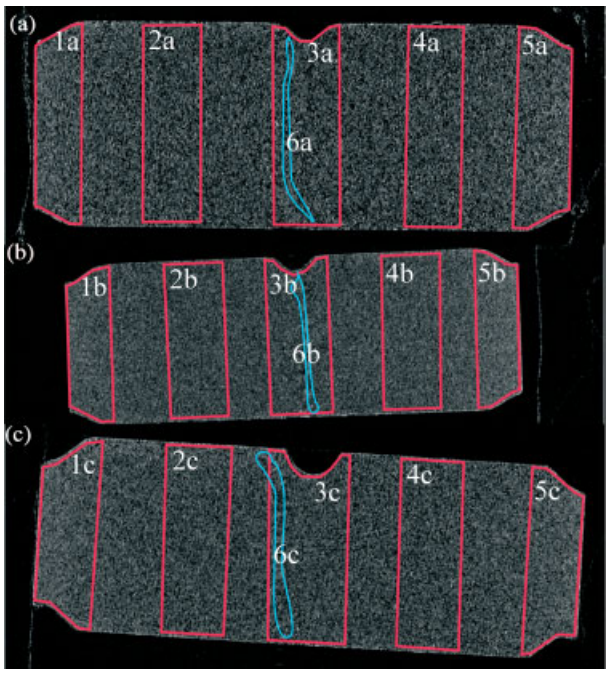

Figure 7. Regions of interest in different tablets (Tablet A (a), Tablet B (b) and Tablet C (c)).

tablets were compressed at each setting, without prelubrication of the die, for modeling of the industrial conditions.

Three-point bend testing was used for measurement of the force required to break the tablets into halves. Measurements were made with a laboratory-constructed tablet hardness tester; the elastic deformation occurring in the tablets was measured with strain gauges (Fig. 2).

The true density of tablets was determined with a Quantachrome helium stereopycnometer (Quantachrome GmbH., Germany). The porosity was calculated via the following equation (Eqn 1):

$$\phi = 1 - (\rho_{\text{apparent}}/\rho_{\text{true}}) \quad (1)$$

The structures of the tablets were analyzed with a SkyScan 1172 high-resolution micro CT apparatus. A schematic figure of a micro CT apparatus is displayed in Fig. 3. In this study, the X-ray source was set to 89 keV and 112 μA. All tablets were scanned in the whole 360° rotation range throughout 0.15° steps. The total duration

Table 1. Properties of the tablets

Sample Press	Tablet A Eccentric	Tablet B Eccentric	Tablet C Rotary
Compression force (kN)	5	15	15
Thickness (mm)	2.968	2.777	2.838
Diameter (mm)	7.933	7.927	8.042
True density (g/cm^3)	1.5202	1.5129	1.4658
Apparent density (g/cm^3)	1.2321	1.3253	1.2655
Porosity	0.189	0.124	0.137
Radial hardness (N)	72.20	118.0	88.0
Axial hardness (N)	57.72	81.89	9.50

Table 2. Gray-scale intensities in different regions of interest

Area	Mean	SD	Min	Max
Tablet A				
1a	75.533	41.961	0	255
2a	62.945	41.371	0	247
3a	62.339	42.593	0	255
4a	62.048	43.252	0	255
5a	74.969	45.250	0	255
6a	54.206	41.071	0	213
Tablet B				
1b	78.150	38.716	0	255
2b	64.946	37.563	0	247
3b	66.949	38.655	0	244
4b	69.361	37.165	0	234
5b	88.662	37.915	0	255
6b	59.013	37.569	0	196
Tablet C				
1c	81.121	36.108	0	255
2c	65.639	35.684	0	224
3c	63.665	36.737	0	252
4c	64.276	38.083	0	248
5c	79.358	38.319	0	255
6c	58.851	36.562	0	218

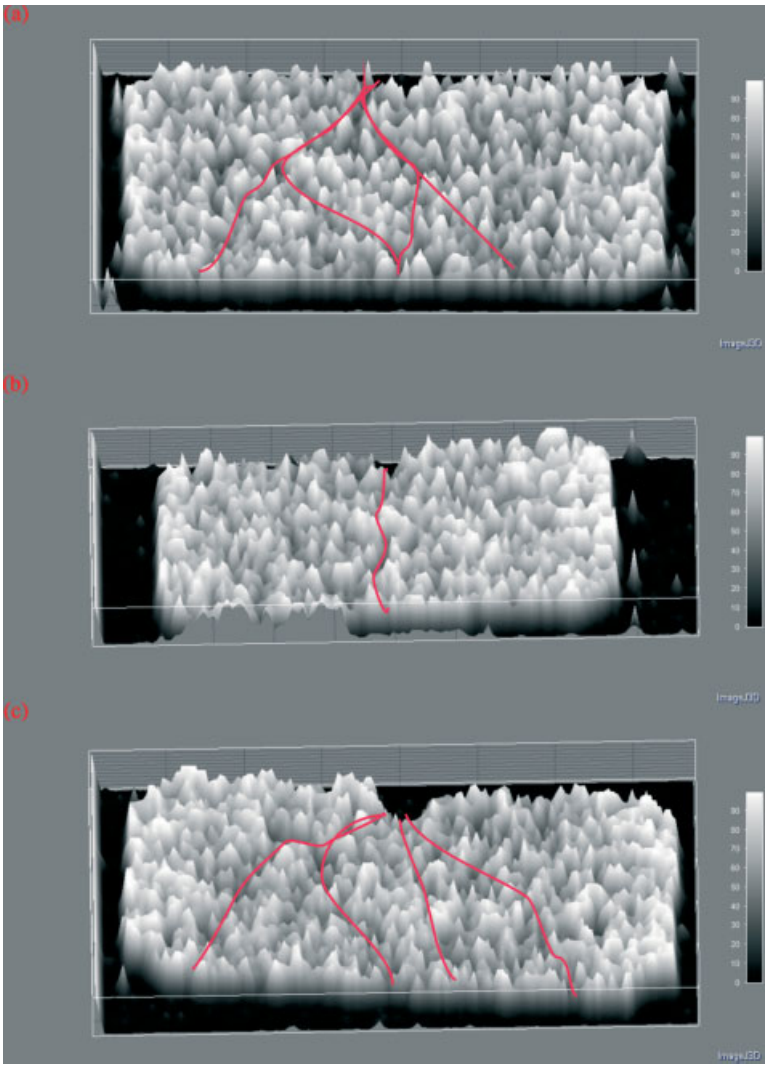

Figure 8. Gray-scale intensities and possible breaking directions in the cross sections of Tablet A (a), Tablet B (b) and Tablet C (c).

of scanning was approximately 3 h. The radiographs were then reconstructed with a standard cone-beam reconstruction program (NRecon) into 16-bit jpg pictures, each of 3120 × 3120 pixels.

The gray-scale intensities and optical densities in the regions of interests were determined with the ImageJ image-analyzing software (National Institute of Health, USA)

Results and Discussion

The aim of the present study was to clarify the reasons for the differences in mechanical behavior of tablets prepared with different tablet presses. The particles show bidirectional movement during compression. Rearrangement proceeds along the axial lines of the transmitted forces, and they provide some movement in the radial direction too, away from the punches. These radial components can result in considerable friction and adhesion to the die wall. A high level of friction can conduce to the formation of structural damage, which changes the mechanical behavior of the tablets. The quantity, duration and direction of the load determine the movement and rearrangement of the particles and cause significant differences in the structures of tablets compressed by different tablet presses. For structural investigation, three samples were selected from the tablets, compressed from the excipient mixture which displayed optimal compressibility in our previous studies.[3,4]

The results of the breaking studies revealed that the tablets prepared with the eccentric press at a compression force of 15 kN (Tablet B) demonstrated acceptable halving properties. However, the tablets compressed from the same material with rotary press under the same conditions (Tablet C) failed this test. These latter results were comparable only with those on the tablets prepared with the eccentric press at a compression force of 5 kN (Tablet A). The X-ray spectrometric pictures of Tablets A–C are presented in Figs 4–6, respectively. It is clearly visible that, despite the differences in the physicochemical parameters (Table 1), the tablets appear to have essentially similar structures. Their density increases from the center to the edges, which is a result of the radial movement of the particles. The gray-scale intensity data (Table 2) of different regions of interest (Fig. 7) indicate that the density gradient increases with increasing compression force. In general, it can be stated that, because of the friction on the die wall, the edge region is 1.1 to 1.4 times denser than the center region of the tablets. Moreover, because of the effects discussed above, a low-density pore (Fig. 7, regions 6a, 6b and 6c) is formed in the center

of the tablets, which exerts a significant effect on the breaking. However, in spite of these similarities, the microstructures of the samples reveal important differences. Tablet A, which has the highest porosity, exhibits poor breaking properties despite the particles being rearranged along vertical lines of force, i.e. the rich pore network allows breaking in many ways, which usually results in a rough breaking surface susceptible to crumbling. This is to be seen in Fig. 8(a), where the mean gray-scale intensities of 256 pixel^2 areas are displayed, with the marking of the possible ways of breaking.

The structure of Tablet B (Fig. 5) is much less porous, and there are more considerable differences in the density distribution. Similarly as for Tablet A, the low-density area visible under the score line (Fig. 5(b)) is of greater importance because of the lower porosity. This area associated with the vertically rearranged particles ensures that the breaking force will pass through the tablet vertically, resulting in a smooth breaking surface (Fig. 8(b)).

In the case of the tablets prepared with the rotary press, the main problem was the breaking into unequal parts. Our previous study suggested that a possible reason is the fact that rotary presses cause only half the stress on the powder bed relative to eccentric presses. However, the porosity of the tablet is unexpectedly not so much higher as compared with that of Tablet B. The structure reveals that the direction of the lines of forces has become deformed, probably because of the bidirectional compression force. This results in an oblique pore structure, which is clearly indicated by the mean gray intensities of the cross-sectional data (Fig. 8(c)). Moreover, the score line is hollower and this makes the low-density area wider. These structural properties lead the breaking force away from the score line and give rise to breaking into unequal halves.

Conclusions

The above results reveal that micro CT is a powerful noninvasive technique for the analysis of the microstructures of pharmaceutical solid dosage forms. They further indicate that the use of an eccentric or a rotary tablet press can give rise to variations in density distribution and have a significant impact on the mechanical properties of tablets, which influences their storage, transport and usage. The knowledge of the differences between the microstructures of scored tablets can help in the development of the production method and point to the optimal shapes of the punches and the score line; this can additionally facilitate data transfer between various tablet presses.

Acknowledgements

We would like to thank the SkyScan Company (B-2550, Kontich, Belgium) for measurements. This work was supported by a Sanofi-Aventis scholarship.

References

[1] N. Rodenhuis, P. A. G. M. De Smet, D. M. Barends, *Eur. J. Pharm. Sci.* **2004**, *21*, 305.
[2] E. van Santena, D. M. Barendsa, H. W. Frijlink, *Eur. J. Pharm. Biopharm.* **2002**, *53*, 139.
[3] T. Sovány, P. Kása jr., K. Pintye-Hódi, *AAPS PharmSciTech* DOI: 10,1208/s12249-009-9225-2.
[4] T. Sovány, P. Kása jr, K. Pintye-Hódi, *J. Pharm. Sci. – US* DOI: 10.1002/jps.21853.
[5] S. Virtanen, O. Antikainen, J. Yliruusi, *Int. J. Pharm.* **2008**, *360*, 40.
[6] D. Traini, G. Loreti, A. S. Jones, P. M. Young, *Microsc. Anal.* **2008**, *111*, 13.
[7] B. C. Hancock, M. P. Mullarney, *Pharm. Technol.* **2005**, *29*, 92.
[8] I. C. Sinka, S. F. Burch, J. H. Tweed, J. C. Cunningham, *Int. J. Pharm.* **2004**, *271*, 215.